uOttawa

L'Université canadienne
Canada's university

FACULTÉ DES ÉTUDES SUPÉRIEURES ET POSTOCTORALES

uOttawa

L'Université canadienne
Canada's university

FACULTY OF GRADUATE AND POSDOCTORAL STUDIES

Cynthia Rose Coffill
AUTEUR DE LA THÈSE / AUTHOR OF THESIS

Ph.D. (Biochemistry)
GRADE / DEGREE

Department of Biochemistry, Microbiology and Immunology
FACULTÉ, ÉCOLE, DÉPARTEMENT / FACULTY, SCHOOL, DEPARTMENT

The Study of Signaling Pathways Controlling Neuronal Apoptosis Inhibitory Protein (NAIP) Expression and Function

TITRE DE LA THÈSE / TITLE OF THESIS

Alexander MacKenzie
DIRECTEUR (DIRECTRICE) DE LA THÈSE / THESIS SUPERVISOR

CO-DIRECTEUR (CO-DIRECTRICE) DE LA THÈSE / THESIS CO-SUPERVISOR

EXAMINATEURS (EXAMINATRICES) DE LA THÈSE / THESIS EXAMINERS

Remy Aubin

Jonathan Lee

Colin Duckett (absent)

Rashmi Kothary

Gary W. Slater
Le Doyen de la Faculté des études supérieures et postdoctorales / Dean of the Faculty of Graduate and Postdoctoral Studies

The Study of Signaling Pathways Controlling Neuronal Apoptosis Inhibitory Protein (NAIP) Expression and Function

A Thesis Submitted to the School of Graduate Studies

University of Ottawa

In Partial Fulfillment of the Requirements for the Degree of Doctor of Philosophy

Department of Biochemistry
Faculty of Medicine

By

Cynthia Rose Coffill

Your file Votre référence
ISBN: 978-0-494-18579-7
Our file Notre référence
ISBN: 978-0-494-18579-7

ABSTRACT

Deletions in the gene for Neuronal Apoptosis Inhibitory Protein (*NAIP*) have been suggested to exacerbate the severity of motor neuron loss in patients with Spinal Muscular Atrophy (SMA). NAIP is the founding mammalian member of the inhibitor of apoptosis (IAP) protein family that is characterized by highly conserved amino-terminal motifs called baculovirus IAP repeats (BIR). Previous *in vitro* and *in vivo* analyses with an adenovirus expressing NAIP but lacking exons 14 and 17 of the full-length cDNA (NAIPΔE14/17) displayed measurable cytoprotection against apoptotic-induced cell death. In the present study, cytoprotective effects were obtained with adeno-*NAIPΔE14/17* alone in the human neuroblastoma SH-SY5Y. Pretreatment of these cells with trophic factors failed to improve the cytoprotection mediated by NAIP. Similarly, the anti-apoptotic effect of NAIP was observed in HeLa cells transiently transfected with constructs expressing full-length *NAIP* and *NAIPΔE14/17.* To further investigate NAIP's cellular role, human HeLa and rat PC12 stable cell lines were developed by integrating a tetracycline-dependent transcription factor construct that was able to selectively regulate a second DNA construct containing full-length NAIP. Doxorubicin, etoposide and TNFα were used to test the cytoprotectiveness of NAIP. Surprisingly, cells overexpressing the full-length NAIP protein did not display increased survival, as determined by a WST-1 metabolism assay, suggesting that long-term exposure to an IAP may result in cellular compensatory mechanism.

In an effort to delineate the signal transduction pathways that modulate the genes encoding murine *Naip*, the neuroblastoma cell line, neuro-2a was exposed to a number of

signaling pathway specific inhibitors and activators. Cyclic AMP analogs, db-cAMP and 8-Br-cAMP both increased the *Naip* transcript, as did the plant isoflavone, genistein. Serum starvation was also found to increase *Naip* levels. We show that sodium butyrate (NaB), a broad-spectrum activator of many signaling pathways, increased the *Naip* mRNA levels of by 3-fold. By focusing on the NaB induction, it appears that *Naip* can be modulated by more than one signaling pathway as inhibition of JAK2 in the presence of NaB resulted in a significant and additive increase in the *Naip* transcript. In combination with various kinase inhibitors, the NaB-induced up-regulation was found not be dependent on the ERK, p38 or PKA pathways. A broad based kinase inhibitor, H-7 down-regulated *Naip* and also attenuated the NaB-induced up-regulation of *Naip*. Our data suggest that the *Naip* gene can be induced by NaB through the H-7 sensitive PKC or PKG but not PKA-pathways.

To examine whether or not the third BIR domain of NAIP (NBIR3) inhibits caspase-9, recombinant GST-NBIR3 protein was overexpressed, purified, and successfully used to demonstrate inhibition of this initator caspase. Through binding analyses a Smac-based peptide, which has been shown to be an IAP antagonist, and NBIR3 were shown to interact with a K_D of 52 nM and similar to the third BIR domain of XIAP (XBIR3). Interestingly, and in contrast to XBIR3, the processed Smac protein does not appear to interact with NBIR3 as association could not be detected during a pull-down study, suggesting that other interactions between the proteins are important. In a search for unique binding partners for NBIR3, a phage display library was panned for a binding consensus sequence. Following the identification of a number of human proteins

containing this sequence, TRABID a candidate protein was chosen for testing. In the TNFα signaling pathway, TRAF6 can interact with both TRABID and TAK1 while NAIP can bind TAK1 but it does not appear that TRABID and NBIR3 directly interact based on pull-down studies.

Overall, through the examination of *NAIP* induction, signaling pathways that had not previously been associated with the up-regulation of an IAP were identified and characterized. In the exploration of anti-apoptotic activity, the third BIR domain of NAIP was shown to act in a similar manner to the other IAPs containing three BIR motifs by inhibiting caspase-9 and interacting with a peptide based on the antagonist, Smac. These findings can potentially lead to therapeutic interventions in degenerative diseases with dysregulated apoptosis.

DEDICATION

To my husband, Dominic Cardy, for his patience during the two and a half years while we lived in separate countries so I could finish the research for this project.

To Zinoviev, Ershad, Yewbert, Embley, Banana and Puffin the cats; Nipper and Sausage the hedgehogs and the various fishies for their constant entertainment at home.

ACKNOWLEDGEMENTS

I am grateful to my supervisor, Alexander MacKenzie, for the opportunity to pursue a PhD in his laboratory. Nathalie Gendron provided more friendship and assistance than I could ever reciprocate. Peter Liston shared his wealth of knowledge and caffeine addiction. The principal investigators and research associates at the Apoptosis Research Centre (ARC) offered opportunities for consultation and discussion; thanks to them, all the members of ARC, and the Department of Biochemistry for friendship, technical assistance and support.

Financial assistance by Canadian Genetics Diseases Network (CGDN) and les Fonds de la recherche en santé du Québec (FRSQ).

Table of Contents

Table of Contents, continued

List of Figures

List of Figures, continued

List of Tables

ABBREVIATIONS

α	alpha
β	beta
δ	delta
ε	epsilon
η	eta
γ	gamma
κ	kappa
λ	lambda
μ	mu (micro)
θ	theta
ζ	zeta
° C	degree Celsius
ABC	ATP-binding cassette
Ask	apoptosis signal-regulating kinase
Asp	aspartic acid
ATP	adenosine triphosphate
BDNF	brain-derived neurotrophic factor
BIR	baculovirus inhibitor of apoptosis repeat
BIRC	BIR-containing
cAMP	cyclic adenosine- 3', 5'- monophosphate
Caspase	cysteinyl asparate-specific protease
CaMKII	calmodulin-dependent kinase kinase
CATERPILLAR	CARD, transcription enhancer, R (purine)-binding, pyrin, lots of LRRs
CHEO RI	Children's Hospital of Eastern Ontario Research Institute
cIAP-1	cellular inhibitor of apoptosis protein-1
cIAP-2	cellular inhibitor of apoptosis protein-2
CMV	cytomegalovirus
CNS	central nervous system
CNTF	ciliary neurotrophic factor

Cys	cysteine
DAG	diacylglycerol
DIABLO	direct IAP binding protein with low pI
DMSO	dimethylsulfoxide
DNA	deoxyribonucleic acid
ERK	extracellular regulated kinase
g	gram
GDNF	glial cell line-derived neurotrophic factor
GPCR	GTP-binding protein coupled receptor
GST	glutathione-S-transferase
h	hour
HAT	histone acetyltransferase
HDAC	histone deacetylase
IAP	inhibitor of apoptosis
IBM	IAP binding motif
IC_{50}	concentration of inhibitor that gives rise to 50% inhibition
ICE	interleukin-1β converting enzyme
IFN	interferon
IKKα	inhibitor of NF-κB kinase alpha
IL	interleukin
IP_3	inositol triphosphate
JAK	janus activated kinase
JNK1	c-jun N-terminal protein kinase
K_D	dissociation constant
K_i	dissociation constant for inhibitor binding
KO	knock out
Lgn	*Legionella*
LPS	lipopolysaccharide
LRR	leucine-rich repeats
m	milli
M	Molar

min	minute
MKK	mitogen-activated protein kinase kinase
mRNA	messenger ribonucleic acid
n	nano
NACHT	NAIP, MHC class II transcription activator (CIITA), yeast incompatibility locus protein (HET-E) and mammalian telomerase-associated protein (TP1)
NAIP	neuronal apoptosis inhibitory protein
NF-κB	nuclear factor-kappaB
NOD	nucleotide-binding oligomerization
NSE	neuron specific enolase
PAGE	polyacrylamide gel electrophoresis
PBS	phosphate-buffered saline
P_{CA}	chicken β-actin promotor
PCR	polymerase chain reaction
PDK1	3-phosphoinositide-dependent protein kinase-1
PH	Pleckstrin homology
PI3K	phosphatidylinositol 3-kinase
PIP_2	phosphatidylinositol bisphosphate
PIP_3	phosphatidylinositol triphosphate
PKA	cAMP-dependent protein kinase
PKC	protein kinase C
PKG	cGMP-dependent protein kinase
PMA	phorbol 12-myristate 13-acetate
PTX	pertussis toxin
RNA	ribonucleic acid
RPA	RNA protection assay
RSK	p90 ribosomal S6 kinase
RT-PCR	reverse transcriptase polymerase chain reaction
S6K	p70 ribosomal S6 kinase
SMA	spinal muscular atrophy

Smac	second mitochondrial activator of caspases
SMN	survival motor neuron
STAT	signal transducers and activators of transcription
TAB1	TAK1-binding protein 1
TAK1	TGF-β-activated kinase 1
TGF-β	transforming growth factor beta
TBI	traumatic brain injury
TNFα	tumour necrosis factor alpha
TNFR	TNF receptor
TRAF	TNFR-associated factor
XIAP	X-linked inhibitor of apoptosis protein

INTRODUCTION

1. Apoptosis

Apoptosis or programmed cell death is a physiological cell suicide program that plays a critical role not only during embryonic development and cellular homeostasis in the adult, but also in the clearance of invading pathogens by host tissues (reviewed in Jacobson *et al.*, 1997; Weinrauch & Zychlinsky, 1999). In mammalian systems, dysregulation of cell death pathways occurs in cancer, autoimmune and immunodeficiency diseases, reperfusion injury after ischemic episodes, and in neurodegenerative disorders. Thus, proteins involved in apoptosis regulation are of intense biological interest and many are attractive therapeutic targets.

The term apoptosis, Greek for 'dropping of leaves from trees', has been used since the 1970's to describe a type of cell death characterized by a common series of morphological changes and, thus, this name has been applied to anything that looks like apoptosis (Friedlander, 2003; Kerr *et al.*, 1972). To further clarify the meaning, it has been proposed that apoptosis be defined as caspase-mediated cell death (see caspase section below) with the following morphological features: cytoplasmic and nuclear condensation, chromatin cleavage, formation of apoptotic bodies, maintenance of an intact plasma membrane and exposure of unique surface molecules. Because of the intact plasma membrane, apoptotic cell death does not trigger an inflammatory response, in contrast to cell death by necrosis (reviewed in Fink & Cookson, 2005).

Apoptosis plays a critical role in the regulation of cellular homeostasis in the central and peripheral nervous system, both in the normal physiological state and in disease. As loss of neurons during development (Oppenheim, 1989) and in many neurodegenerative diseases occurs chiefly through the process of apoptosis (reviewed in Friedlander, 2003; Troy & Salvesen, 2002), it is crucial to understand the nature of its regulation in chronic neurodegenerative conditions such as Alzheimer's disease, ALS, Parkinson's disease, as well as in ischemia.

The childhood spinal muscular atrophies are a group of autosomal recessive neurodegenerative disorders caused by loss of the motor neurons with a consequent symmetric weakness and wasting of skeletal muscles ultimately resulting in respiratory failure. The SMAs range in severity from type I with a life expectancy of 18 months or less to type III where survival well into the adult years is the norm. The primary genetic lesion in Spinal Muscular Atrophy (SMA) is believed to be the loss or mutation of the SMN1 gene (also known as SMNt), which triggers loss of α motor neurons (reviewed in Gendron & MacKenzie, 1999). Our laboratory has proposed a link between the modulation of SMA severity and larger deletions encompassing the Neuronal Apoptosis Inhibitory Protein (*NAIP*) gene (Gendron & MacKenzie, 1999).

2. Caspases

The key enzymes orchestrating and executing apoptosis are the cysteine-dependent aspartate-directed proteases, which play a central role by cleaving key targets in the cell (reviewed in Degterev *et al.*, 2003). Initially, caspase-1 or interleukin-1β converting enzyme (ICE) was identified as the protease responsible for the maturation of

proIL-1β to its biologically active form (Cerretti *et al.*, 1992; Thornberry *et al.*, 1992). Interestingly, while studying the genetic pathway for cell death in the nematode *Caenorhabditis elegans*, it was found that the *ced*-3 gene, an essential component in this apoptotic pathway, was the homologue of mammalian ICE (Yuan *et al.*, 1993). As cellular functions have been largely conserved throughout evolution, studies of *C. elegans* genetics have proven invaluable in defining the mammalian cell death pathways (reviewed in Nicholson, 1999). The importance of these discoveries was highlighted by the award of the 2002 Nobel Prize for Physiology or Medicine to Sydney Brenner, H. Robert Horvitz and John E. Sulston, for their discoveries concerning the ''genetic regulation of organ development and programmed cell death'' in *C. elegans*.

The human genome encodes about a dozen caspases, and these can be divided into subgroups depending on inherent substrate specificity, domain composition, or presumed roles *in vivo* (reviewed in Boatright & Salvesen, 2003; Degterev *et al.*, 2003; Salvesen & Abrams, 2004). Caspases are synthesized as inactive zymogens that possess an amino-terminal prodomain as well as large and small subunits joined by a linker region. Caspases with large prodomains are thought to be involved in the initiation of the apoptotic response and are called initiator caspases. Binding motifs found in initiator caspases such as the death effector domain (DED) (caspase-8 and -10) or the caspase recruitment domain (CARD) (caspase-1, -2, -4, -5, -9, -11 and -12) appear to be involved in interactions with signaling adapter proteins while the CARD also appears to be important in promoting interactions of caspases with one another (reviewed in Boatright & Salvesen, 2003; Degterev *et al.*, 2003; Salvesen & Abrams, 2004).

The zymogens of the initiator caspases exist within the cell as inactive monomers that require dimerization to assume an active conformation, which is independent of cleavage (Boatright & Salvesen, 2003). One major pathway for the recruitment and activation of the initiator caspases is the receptor-mediated or extrinsic pathway. Within this apoptotic pathway caspase-8 activation is initiated by the binding of a ligand to the trans-membrane death receptor of the tumor necrosis factor receptor type 1 (TNFR1) superfamily, such as Fas, leading to the formation of a death-inducing signaling complex (DISC) and recruitment of caspase-8. Within this complex, the adaptor protein FADD forms the essential link to apical caspases 8 and 10 via homotypic interactions involving DED domains (Boatright & Salvesen, 2003; Degterev *et al.*, 2003). Activated caspase-8 or -10 can then activate effector caspases.

In the intrinsic apoptotic pathway, developmental and stress cues mediate mitochondrial release of cytochrome *c* combined with ATP and the apoptotic protease activating factor 1 (Apaf-1) resulting in the recruitment and activation of caspase-9 within the apoptosome complex (Boatright & Salvesen, 2003; Degterev *et al.*, 2003). This ~1 MDa oligomeric wheel-like structure contains seven Apaf-1, seven cytochrome *c*, seven ATP and seven procaspase-9 molecules. Once the apoptosome-bound procaspase-9 is activated, most likely through dimerization, this complex can mediate the activation of effector caspases, which then can cleave the cellular substrates needed for the orchestration of apoptosis (Boatright & Salvesen, 2003).

The critical point in apoptosome formation is the release of cytochrome *c* from its normal location in the intermembrane space of the mitochondria to the cytosol. This release is controlled by members of the bcl-2 family of proteins, which may mediate

either pro- or antiapoptotic functions (reviewed in Cory & Adams, 2002). Likely through a change in their conformation that results in their oligomerization and tight integration at the level of the mitochondrial membrane, the proapoptotic members such as Bax and Bak are responsible for cytochrome *c* release. Bcl-2 or bcl-xL can prevent Bax/Bak conformational changes and subsequent cytochrome *c* release and thus mediate a powerful antiapoptotic support. As an additional level of control, a subclass of bcl-2 proteins, the BH3 domain-only members, act as sentinels of cell stress and become transcriptionally or posttranslationally activated when this stress reaches a certain threshold. Upon their activation, they bind to bcl-2 or bcl-xL and prevent them from exerting their antiapoptotic effects (Cory & Adams, 2002).

Researches have demonstrated a role for caspase-2 in response to neurotrophic deprivation and DNA damage, a subset of intrinsic pathway apoptotic stimuli (Salvesen & Abrams, 2004). Following an apoptotic trigger caspase-2 appears to be activated by interaction with a high molecular weight complex that requires its CARD motif. Recently investigators have identified PIDD (p53-induced protein with a DED) as an interaction partner to RAIDD, a protein that had previously been shown to interact specifically with caspase-2 and not with any of the other CARD-containing initiator caspases. The term "PIDDosome" has thus been proposed for this caspase-2 activation complex (Tinel & Tschopp, 2004).

The initiator caspases mediate the amplification of the apoptotic system by generating substantial amounts of active executioner caspases, marking one of the most important process in a cell's life (reviewed in Degterev *et al.*, 2003). Through a cleavage event within their linker domain, the inactive zymogen caspase dimers with short

prodomains (the executioner caspases-3, -6 and -7) are activated by the apical (initiator) caspases-8, -9, or -10 (Boatright & Salvesen, 2003). At cytosolic concentrations in human cells, the caspase-3 and -7 zymogens are already dimers, but cleavage within their respective linker segments is required for activation. As an inter-subunit linker segment of the executioner procaspase blocks ordering of the active site, cleavage generates new N and C-terminal sequences to aid in active site stabilization (Boatright & Salvesen, 2003).

Caspases recognize a very short tetrapeptide sequence formed the basis for inhibitor and synthetic substrate design (reviewed in Nicholson, 1999). These proteases have an absolute requirement for Asp in P1, are promiscuous in P2, prefer Glu in P3, but have varying preferences in P4. Despite these apparently simple requirements, however, caspases are extremely stringent, indicating that three dimensional context and the appropriate surface presentation are key factors in determining whether the presence of an appropriate motif also makes it eligible for caspase proteolysis within a polypeptide. Caspase cleavage normally occurs at a single, discrete site within the target polypeptide, although examples of multiplicity, redundancy and nesting also exist (Nicholson, 1999).

Although all members of the caspase family share similarities in amino acid sequence and structure, they differ significantly in their physiologic roles. The caspases can be broadly divided into two groups: those that are centrally involved in apoptosis (caspase-2, -3, -6, -7, -8, -9, and -10) and those related to caspase-1 (caspase-1, -4, -5, -13, and -14, as well as murine caspase-11 and -12), whose primary role appears to be in cytokine processing during inflammatory responses (Salvesen & Abrams, 2004).

Caspases-1 and -5, a subgroup involved in inflammation, seem to assemble in the interleukin-1β activator complex called the inflammasome. An important function of caspase-1 is to process the pro-forms of the inflammatory cytokines, IL-1β and IL-18, to their active forms (reviewed in Fink & Cookson, 2005). Caspase-1 is not involved in apoptotic cell death and results in processing of cytokines and death of the host cell but the mechanism and outcome of this form of cell death are distinctly different from these aspects of apoptosis, which actively inhibits inflammation. Some investigators have proposed the term pyroptosis from the Greek roots "pyro," relating to fire or fever, and "ptosis" (pronounced "to-sis"), denoting falling, to describe proinflammatory programmed cell death (Fink & Cookson, 2005).

3. IAPs

Studies involving viruses were critical in the investigation of caspase inhibitors and their role in apoptosis. Researchers studying the baculoviral protein p35, which inhibits apoptosis in the insect SF-21 cell line, used a genetic complementation assay to identify additional genes that could provide cytoprotection during infection with a virus lacking a functional *p35* gene (Crook *et al.*, 1993). From the *Cydia pomonella* granulosis virus (CpGV) these investigators isolated an open reading frame capable of encoding a polypeptide of 31 kDa that was sufficient to rescue wild type infection and called this gene *iap* for inhibitor of apoptosis. They also found that expression of the CpGV *iap* gene in SF-21 cells was able to block apoptosis when the cells were exposed to the RNA synthesis inhibitor actinomycin D (Crook *et al.*, 1993).

Work completed by the same laboratory found that the *Orgyia pseudotsugata* nuclear polyhedrosis virus (OpMNPV) had a gene homologous to the *iap* from CpGV that was also able to block apoptosis in SF-21 cells during infection with the mutant *p35* virus (Birnbaum *et al.*, 1994). The nucleotide sequence of the Op-*iap* gene predicted a 30-kDa polypeptide product with approximately 58% amino acid sequence identity to the product of Cp-*iap* gene. Both proteins had a carboxy-terminal C_3HC_4 RING zinc finger-like motif, in addition to two tandem repeats of 70 amino acids found in the N-terminal regions that, based on the spacing of cysteines and histidine within these motifs, suggested the possibility of metal ion coordination and nucleic acid binding. The repeat unit was named a baculovirus iap repeat motif or BIR domain (Birnbaum *et al.*, 1994). Op-*iap* was later shown to inhibit cell death induced by ICE (caspase-1) (Hacker *et al.*, 1996; Hawkins *et al.*, 1996; Uren *et al.*, 1996).

Our laboratory was the first to identify a mammalian gene that encoded a protein with BIR-like motifs and named it the Neuronal Apoptosis Inhibitory Protein (NAIP) (Roy *et al.*, 1995), now called BIRC1 according to the new nomenclature system. Since then the human BIR-containing (BIRC) proteins have expanded to include cellular IAP1 (c-IAP1 or BIRC2), c-IAP2 or BIRC3, X-linked IAP (XIAP or BIRC4) (Duckett *et al.*, 1996; Liston *et al.*, 1996; Rothe *et al.*, 1995; Uren *et al.*, 1996), Survivin or BIRC5 (Ambrosini *et al.*, 1997), Apollon or BIRC6 (Chen *et al.*, 1999), Livin or BIRC7 (Kasof & Gomes, 2001; Lin *et al.*, 2000; Vucic *et al.*, 2000), and Ts-IAP or BIRC8 (Lagace *et al.*, 2001; Richter *et al.*, 2001). BIRC homologues have also been found in other mammals (Farahani *et al.*, 1997; Hauser *et al.*, 1998; Liston *et al.*, 1997; Scharf *et al.*, 1996; Shin *et al.*, 2003; Stehlik *et al.*, 1998a; Yaraghi *et al.*, 1998); birds (Digby *et al.*,

1996; You *et al.*, 1997), insects (Hay *et al.*, 1995; Jones *et al.*, 2000), yeast and nematodes (Uren *et al.*, 1998). With the discovery of additional homologues, the BIRC proteins have been divided into two subfamilies: the IAP group with anti-apoptotic activities and the other members that generally contain only a single BIR domain and appear to function primarily in cytokinesis and chromatin segregation (reviewed in Liston *et al.*, 2003; Miller, 1999).

Figure I-1. Domain structure of the IAP family. Individual domains are drawn to scale. The abbreviations are as follows: BIR: baculoviral IAP repeat; CARD: caspase recruitment domain; RING: RING zinc-finger and NOD: nucleotide-binding oligomerization domain. Modified from (Liston *et al.*, 2003).

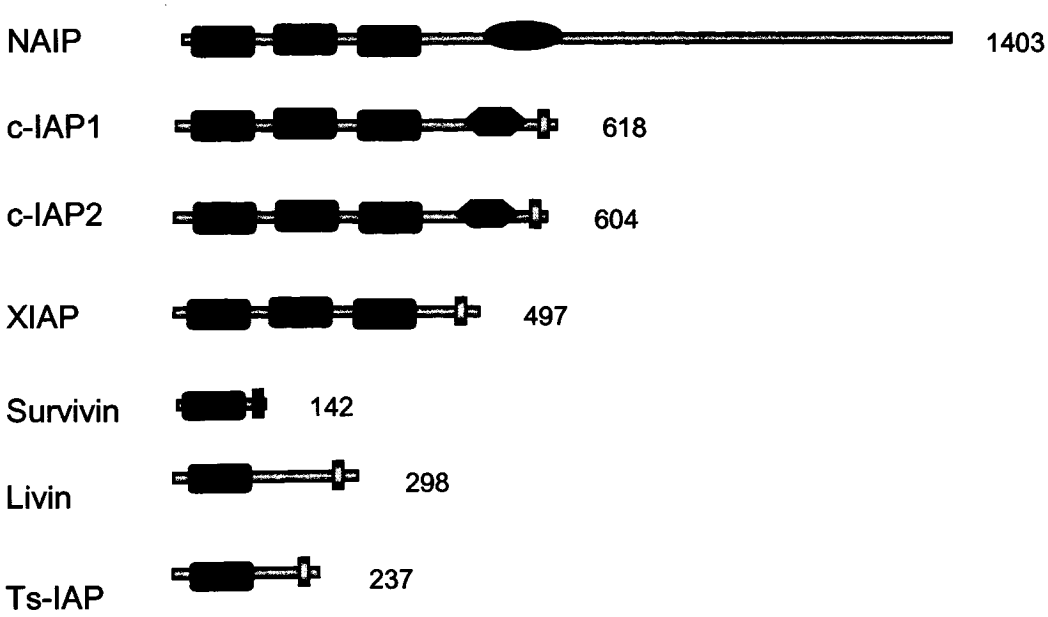
NAIP
1403
c-IAP1
618
c-IAP2
604
XIAP
497
Survivin
142
Livin
298
Ts-IAP
237
BIR Domain
RING Finger
CARD
Coiled Coil
Nucleotide Binding Domain

4. NAIP

The *NAIP* gene contains 17 exons comprising 6.2 kb of transcribed sequences and spans 50 kb of genomic DNA at 5q13.1 (Chen *et al.*, 1998). The full *NAIP* coding region is 4212 nucleotides, encoding a 1404 amino acid, 156 kD protein. Using a human fetal brain cDNA library, other investigators found an additional, shorter version of *NAIP* that encodes for a protein of 1295 amino acids and called it $NAIP_S$ (Yamamoto *et al.*, 1999). A splice variant that lacks part of the third BIR domain as well the COOH-terminal tail of regular NAIP (NAIP-DeltaEx10-11) has also be found (Notarbartolo *et al.*, 2002), in addition to the *ΨNAIP* gene, which encodes a protein lacking the first two BIR motifs (Xu *et al.*, 2002). Evidence for the corresponding polypeptide of the latter has remained elusive. NAIP has three BIR domains contained within the initial 400 amino acids of this protein but lacks the C-terminal RING zinc finger found in most other IAPs. While NAIP's structure has not been solved by NMR or X-ray crystallography, the similarity to the BIR consensus sequence of $C_{X2}C_{X6}W_{X3}D_{X5}H_{X6}C$, where X is any amino acid, means that parallels can be drawn to the other BIRC proteins, for which the structure has been delimited. Analysis of the BIR domains from c-IAP1 (Hinds *et al.*, 1999), Survivin (Chantalat *et al.*, 2000; Muchmore *et al.*, 2000; Verdecia *et al.*, 2000) and XIAP (Chai *et al.*, 2001; Huang *et al.*, 2001; Riedl *et al.*, 2001; Sun *et al.*, 1999; Sun *et al.*, 2000; Wu *et al.*, 2000) indicates that BIRs form a compact globular structure that includes a C2HC motif coordinating a zinc ion, four or five alpha helices and a variable number of anti-parallel β-pleated sheets.

5. NAIP function

To determine whether or not NAIP belonged to the IAP subfamily of BIRC proteins, our laboratory developed plasmid and adenoviral constructs that expressed *NAIP* and anti-sense *NAIP* for use in *in vitro* apoptosis suppression studies (Liston *et al.*, 1996). At the time of this publication, the DNA sequence used for the constructs was assumed to be the full-length coding region of *NAIP* but actually consisted of an alternate version that lacked exons 14 and 17 of what was eventually determined to be the full-length gene (Chen *et al.*, 1998; Roy *et al.*, 1995). This truncated form is now called *NAIPΔE14/17*. Our laboratory found that after infection with the recombinant adenoviruses, CHO cells that were induced to undergo apoptosis by serum deprivation had a survival rate of 80% in the presence of *NAIPΔE14/17*, compared to 51% with *LacZ*, while anti-sense *NAIP* lowered the survival to 45% (Liston *et al.*, 1996). In the same study, *NAIPΔE14/17* was found to increase the survival in CHO stable transfectant pools that were serum starved, and provided cytoprotection to CHO cells that were transiently transfected and then treated with menadione, a potent generator of free radicals. Similarly, *NAIPΔE14/17* delivered by the adenovirus also protected menadione-treated Rat-1 fibroblasts and HeLa cells treated with the cytokine tumour necrosis factor (TNF)-α and cycloheximide (Liston *et al.*, 1996). This study was the first to publish the anti-apoptotic activities of mammalian homologues to the baculoviral IAP proteins. Within months, the anti-apoptotic activities for XIAP, c-IAP1 and c-IAP2 were confirmed by other laboratories (Duckett *et al.*, 1996; Uren *et al.*, 1996). Furthermore, the ability of these three proteins to prevent ICE-induced apoptosis (Hawkins *et al.*, 1996; Uren *et al.*,

1996) and to directly inhibit certain caspases (Deveraux *et al.*, 1997; Roy *et al.*, 1997) was demonstrated.

Additional *in vitro* protection offered by adenoviral mediated NAIPΔE14/17, XIAP, c-IAP1 or c-IAP2 protein expression was observed in cerebellar granule neurons following potassium withdrawal for the initial 24 hours but not for longer periods of time, suggesting a delay rather than an inhibition in this system (Simons *et al.*, 1999). By measuring caspase-3/7-like activity through the cleavage of a DEVD substrate, these colleagues were the first to demonstrate that cells infected with adenoviral NAIPΔE14/17 could inhibit the appearance of a cleaved caspase substrate. Furthermore, they found that processing of the p32 proenzyme or zymogen form of caspase-3 into its small p12 and large p20 subunits was also partially blocked, suggesting that NAIP and the other IAPs tested exerted their effects upstream and/or at the level of procaspase-3 processing (Simons *et al.*, 1999). The cleavage of procaspase-3 was later determined to depend upon the activation of caspase-9, but not of caspase-8, in cerebellar ganule neurons following potassium withdrawal (Gerhardt *et al.*, 2001).

Retinoic acid (RA) differentiation of the human promyelocytic leukaemia (HL-60) cell line is a well-characterized *in vitro* model for the generation of neutrophil-like cells. When terminally differentiated, HL-60 cells die by apoptosis. Treatment of the HL-60 cells with RA resulted in a time-dependent decrease in *XIAP*, *NAIP*, *cIAP-1*, *cIAP-2* and *Survivin* mRNA expression (Doyle *et al.*, 2002). This trend was reflected by corresponding decreases in XIAP, NAIP and cIAP-2 protein levels at day 3. Western blot analyses of the protein expression during differentiation demonstrated that as XIAP, NAIP and cIAP-2 expression decreased, there was a corresponding increase in IAP

cleavage products and that this was thought to be caused by the activation of the caspases. By days 3 and 4, full-length NAIP was not detectable with an increase in a 70/80 kDa band. Finally, a 25/30 kDa band was detectable at day 5 in the absence of a caspase inhibitor. Cleavage of the IAPs was inhibited by the zVAD-fmk at 5 days, indicating that this process was dependent on caspases. Blocking caspase activity did not alter the decrease in IAP protein expression during differentiation but prevented caspase activation, IAP cleavage and the induction of apoptosis (Doyle *et al.*, 2002).

Examination of the mouse chromosomal locus that corresponds to the SMA critical region lead our laboratory and others to identify multiple copies of the *Naip*[1] gene (DiDonato *et al.*, 1997; Endrizzi *et al.*, 2000; Huang *et al.*, 1999; Scharf *et al.*, 1996; Yaraghi *et al.*, 1998). In total, seven intact *Naip* genes and three 5' truncated *Naip* pseudo-genes were found in the 13D1-D3 region in mice derived from the 129 lineage (Growney *et al.*, 2000). These genes were called *Birc1a* through to *Birc1g* (*Naip1* to *Naip7*) and the pseudogenes were named *Birc1c-ps1*, *-ps2* and *-ps3* (*Naip3-ps1* to *-ps3*). Interestingly, this region was also found to be responsible for the permissiveness to intracellular replication of *Legionella pneumophila* (Scharf *et al.*, 1996).

Using a rat PC12 cell line stably transfected with constructs expressing either a full-length mouse *Naip2* gene or a truncated *Naip2* devoid of the three BIR domains (BIR-del-Naip), another group of investigators not only confirmed that *Naip* can inhibit apoptosis induced by serum withdrawal and TNFα but that the BIR domains were required for this cytoprotective effect (Gotz *et al.*, 2000). Furthermore, when testing the inhibition of caspase-3/7 activity with a DEVD substrate following both apoptotic

[1] *Naip* refers to the murine gene whereas *NAIP* is used for human.

triggers, full-length Naip was able to block the cleavage of this substrate while the construct lacking the BIR domains was not. The authors suggest that the BIR domains of Naip might be able to block the initiator caspases-8 and -9 as these are activated by TNFα exposure or NGF withdrawal, respectively (Gotz *et al.*, 2000). Interestingly, during this study it was also discovered that Naip antagonizes NGF-induced differentiation by causing a significant delay in neurite outgrowth and that this delay was observed in PC12 cells expressing full-length Naip and the BIR-deleted Naip proteins. The effect was reversible as the addition of forskolin or the expression of the MEK kinase Cot was able to rescue neurite outgrowth in these cells (Gotz *et al.*, 2000).

Adenoviral mediated NAIPΔE14/17 or XIAP expression renders primary cortical neurons resistant to camptothecin (an agent that activates caspase-3-induced death). Through the use of glutathione-S-transferase (GST) fusions with the BIR domains of NAIP, our laboratory was successfully able to show direct inhibition of caspases-3 and -7 (Maier *et al.*, 2002). In the caspase-3 assay, the second BIR domain of NAIP (NBIR2) was the most effective inhibitor followed by the three BIR domains combined (NBIR123), which was similar to the level of inhibition demonstrated by XIAP. NBIR3 was a less effective caspase-3 inhibitor and the first BIR motif of NAIP (NBIR1) was completely ineffective at inhibiting caspase-3. Caspase-7 was inhibited by NBIR123 and XIAP only and to similar extents but slightly less than capase-3 inhibition. Neither protein inhibited caspases-1 or -8 in this *in vitro* study. A previously published study assaying for an *in vitro* recombinant NAIP and caspase interaction failed to detect any binding to the caspases (Roy *et al.*, 1997), possibly due to difficulties in protein isolation

as the BIR domains of NAIP tend to oligomerize and precipitate (J. Maier, unpublished observation).

It has now been clearly established that for the IAP subfamily of the BIRC proteins, the BIR domains and the regions surrounding them are critical for the inhibitory effect on caspase activity in apoptotic cells (reviewed in Liston *et al.*, 2003). Of the four human IAPs that possess three BIR domains, it has been shown that the second BIR domains function to inhibit caspases-3 and -7 (Maier *et al.*, 2002; Roy *et al.*, 1997; Takahashi *et al.*, 1998), whereas the third domains for XIAP, c-IAP1 and c-IAP2, but not NAIP, have been experimentally determined to bind and inhibit caspase-9 (Bratton *et al.*, 2001; Deveraux *et al.*, 1998). Of those BIRC proteins that contain only one BIR, Ts-IAP inhibits caspase-9 (Richter *et al.*, 2001), Survivin blocks caspases-3 and -7 (Shin *et al.*, 2001) and interestingly, Livin inhibits caspases-3, -7 and -9 (Kasof & Gomes, 2001; Vucic *et al.*, 2000).

The mechanism of inhibition for each caspase is slightly different. Through X-ray crystallography (Chai *et al.*, 2001; Huang *et al.*, 2001; Riedl *et al.*, 2001) and mutagenesis studies (Sun *et al.*, 1999; Sun *et al.*, 2000), the importance of the region linking the first and second BIR domains of XIAP in the inhibition of caspases-3 and -7 was demonstrated. A DISD-tetrapeptide sequence lying outside and ~11 amino acids upstream of the amino border of XIAP's second BIR domain (XBIR2) was found to be critical for binding to the catalytic groove of both proteases. While the linker region accounts entirely for the inhibition of caspases-3 (Chai *et al.*, 2001; Huang *et al.*, 2001), the XBIR2 domain is important for stabilizing the interaction of the linker in the catalytic site of caspase-7 (Suzuki *et al.*, 2001b)

The BIR3 domains of XIAP, c-IAP1, c-IAP2 (Bratton *et al.*, 2001; Deveraux *et al.*, 1998) and the single BIR domains of Livin (Vucic *et al.*, 2000) and Ts-IAP (Richter *et al.*, 2001) have been demonstrated to bind and inhibit caspase-9 (reviewed in Liston *et al.*, 2003). As described earlier, activation of the intrinsic apoptosis pathway triggers the formation of an apoptosome complex consisting of caspase-9, Apaf-1 and cytochrome *c.* and ATP (reviewed in Degterev *et al.*, 2003). Caspase-9 appears to be distinct from the effector caspases in that the binding to Apaf-1 leads to a conformational change and results in capase-9 becoming catalytically active, rather than proteolytic cleavage (Degterev *et al.*, 2003; Liston *et al.*, 2003). As an initiator caspase, activated caspase-9 can proteolytically process caspase-3 in addition to a self-cleavage event in the linker region between the large and small subunits at Asp_{315}. Through crystal structure analyses, it has been demonstrated that the XIAP BIR3 (XBIR3) domain directly engages caspase-9 by binding to the exposed amino terminus of the processed linker within a conserved surface groove. Additional contacts with caspase-9 occur with helix α5 and the linker sequence between helices α3 and α4 of XBIR3 packing closely against the hydrophobic surface of caspase-9 (Shiozaki *et al.*, 2003). The authors speculate that XBIR3 can sequester caspase-9 in a monomeric state through these interactions and trap the active site loops in a non-catalytic, inactive conformation, thus leading to its inhibition.

Smac (second mitochondrial activator of caspases) or DIABLO (direct IAP binding protein with low pI) resides in the mitochondria of healthy cells, but following an apoptotic stress is released into the cytosol where it is able to prevent and/or reverse IAP inhibition of caspases (reviewed in Verhagen & Vaux, 2002). Interestingly, Smac is synthesized as a precursor, trafficked to the mitochrondria and looses its signaling

peptide following apoptotic stress. The newly exposed N-terminus is principally responsible for its interactions with the IAPs once it is released into the cytosol. Co-crystalization of Smac and XBIR3 established that the new amino-terminal tetrapeptide sequence of Smac (AVPI) fits within a surface groove of the XBIR3 domain (Wu *et al.*, 2000), whereas the caspase-9 (A_{316}TPF) sequence was found to fit in the same groove (Shiozaki *et al.*, 2003), suggesting that Smac either competes for or displaces XIAP from caspase-9. Similar tetrapeptides have been found in the *Drosophila* proteins Reaper, Hid, Grim, Sickle and Jafrac2, as well as the human proteins Omi, GSPT1 and Chk1, and these short consensus sequences have been termed IAP-binding motifs (IBMs) (reviewed in Liston *et al.*, 2003; Salvesen & Duckett, 2002). This emerging IBM consensus appears to reflect a common mechanism in which specific proteins can interact with the BIR domains to antagonize IAP function.

Another mitochondrial IAP antagonist, called Omi or HtrA2, was identified by several groups (Hegde *et al.*, 2002; Martins *et al.*, 2002; Suzuki *et al.*, 2001a; van Loo *et al.*, 2002; Verhagen *et al.*, 2002). Interactions between XIAP and the caspases are inhibited following release of Omi from the mitochondria of apoptotic cells and processing to generate a Smac-like tetrapeptide motif. In addition, the serine protease activity of Omi contributes to cell death in a noncaspase-dependent manner, although the cellular targets of this activity have not been revealed. A third IAP antagonist, the XIAP-associated factor1 (XAF1) protein was identified by two-hybrid screening with XIAP, and encodes a novel, zinc-finger-rich protein with limited homology to TRAF6 and TNFα (Fong *et al.*, 2000). Through *in vitro* experiments direct interaction between XAF1 and XIAP was demonstrated in addition to the prevention of caspase inhibition (Liston *et*

al., 2001). When coexpressed in cell lines, XAF1 retains the normally cytosolic XIAP in the nucleus, resulting in subcellular sequestering of this IAP in addition to direct antagonism (Liston *et al.*, 2001).

Figure I-2. Role of the IAPs in regulating both the endogenous and exogenous pathways. Inhibition of both initiator (caspase-9) and effector (caspase-3 and -7) caspases uniquely situates the IAPs at the junction of both major pathways. See text for details. Modified from (Liston *et al.*, 2003).

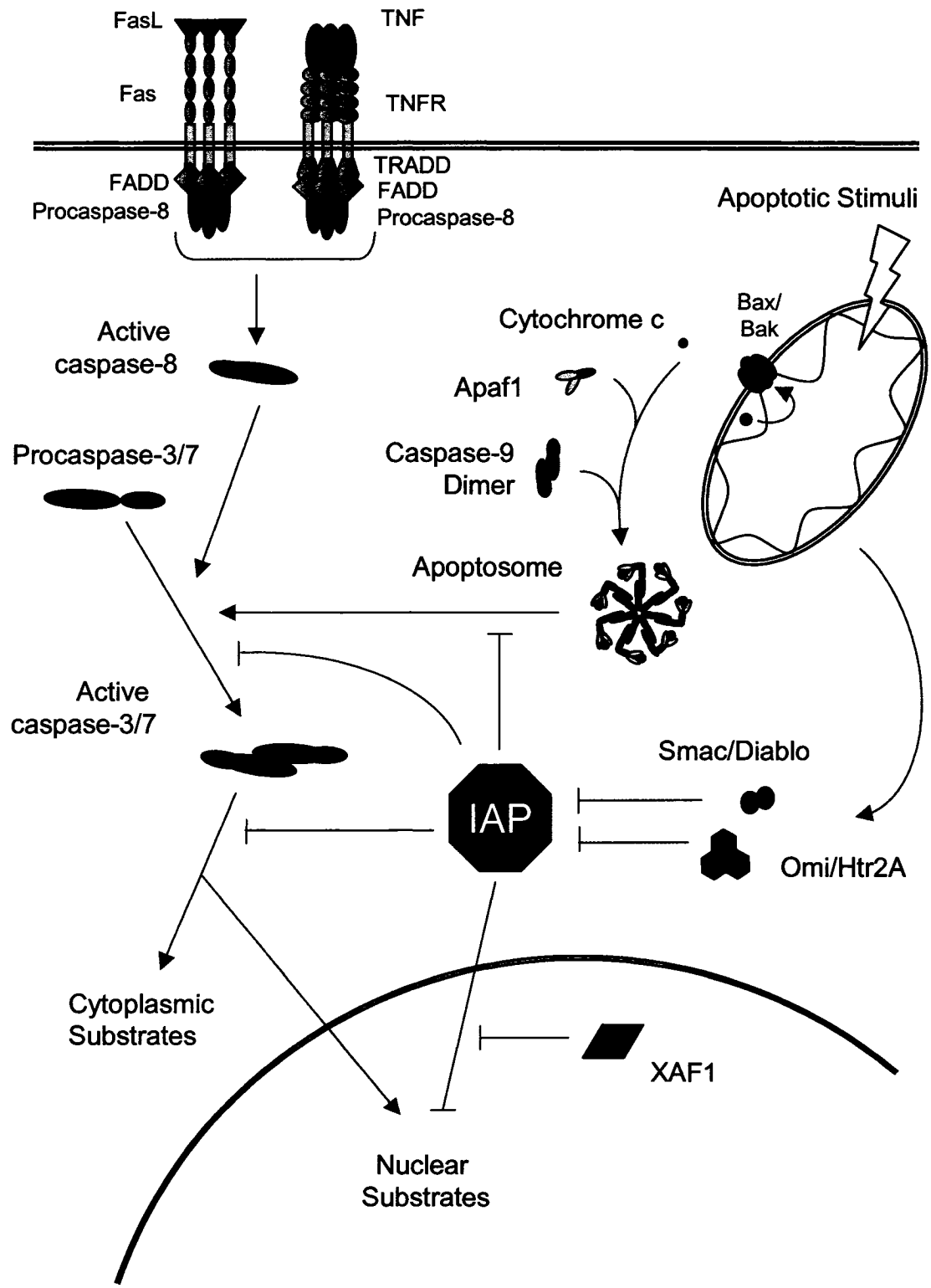
FasL
TNF
Fas
TNFR
FADD
Procaspase-8
TRADD
FADD
Procaspase-8
Apoptotic Stimuli
Active
caspase-8
Cytochrome c
Bax/
Bak
Apaf1
Procaspase-3/7
Caspase-9
Dimer
Apoptosome
Active
caspase-3/7
Smac/Diablo
IAP
Omi/Htr2A
Cytoplasmic
Substrates
XAF1
Nuclear
Substrates

6. NAIP interactions

Calcium-induced death triggered by ionomycin and thapsigargin was found to be inhibited in neuronal cell lines overexpressing the BIR domains of NAIP (Mercer *et al.*, 2000). Using a yeast two-hybrid system and a human fetal brain library, these investigators discovered that NBIR3 interacted with hippocalcin, a member of a neuron-specific family of calcium binding proteins. With stably transfected NSC-34 and neuro-2a cell lines, it was found that NBIR123 and hippocalcin could inhibit cell death induced by ionomycin and thapsigargin on their own but were much more effective when they were overexpressed together. Furthermore, this study demonstrated that NBIR123 could inhibit cleavage of the caspase-3/7 substrate DEVD following thapsigargin treatment in NSC-34 cell-line. In contrast, caspase-3/7 activity was virtually undetectable in neuro-2a cells exposed to the same trigger and while NBIR123 was only able to provide modest protection against apoptosis, NBIR3 and hippocalcin overexpressed individually were not. Interestingly, hippocalcin combined with either of the NAIP expressing cells offered significant protection against thapsigargin in this cell line. It is unclear through which apoptotic cascade thapsigargin signals in neuro-2a but it is evident that the BIR domains of NAIP and hippocalcin can act synergistically to facilitate neuronal survival in this caspase-3/7 independent cell death, as well as the caspase-3/7 dependent death in the NSC-34 cell line (Mercer *et al.*, 2000).

No defined role has yet been ascribed to hippocalcin but work by the same laboratory delineated further the binding between NBIR3 and this protein (Lindholm *et al.*, 2002). The amino acids D187 and V196 in NBIR3 were found to be involved in hippocalcin binding, and interestingly, were not present in the other IAPs possessing

three BIR domains. Hippocalcin belongs to visinin-like protein (VILIP) subfamily of the neuronal calcium sensor (NCS) gene family, which constitutes a group of calcium binding proteins that are expressed mainly in the nervous system and in neuroendocrine cells. Hippocalcin is highly expressed in the hippocampus, in pyramidal neurons, but it is also present in some other parts of the CNS (Lindholm *et al.*, 2002). In subcellular localization studies, the authors found that individual transfections of neuroblastoma cells with expression plasmids for NBIR3 and for hippocalcin resulted in distribution throughout the cytoplasm. When NAIP and hippocalcin were expressed together there was a distinct relocalization of both proteins close to the plasma membrane in the neuroblastoma cells (Lindholm *et al.*, 2002). It has yet to be determined whether or not the interaction between NAIP and hippocalcin offers a viable target for therapeutic intervention but the principle is intriguing.

Additional *in vitro* studies have demonstrated that lysates generated from 293T cells transfected with plasmids expressing NBIR123, XIAP or Livin can increase the phosphorylation of stress-activated protein kinase/c-Jun NH_2-terminal kinase-1 (SAPK/JNK1) and to a lesser extent JNK2 (Sanna *et al.*, 2002). A subfamily of the mitogen activated protein kinase (MAPK) superfamily, JNK is a key regulator of many cellular events, including apoptosis. JNK1 is ubiquitously expressed and is activated by numerous types of stress, with apoptosis resulting from some of these stimuli. Conversely, JNK-mediated cell survival has also been noted. The function of JNK in apoptosis is complex and it is probable that JNK activation modules apoptosis in a cell type and stimulus specific manner.

In apoptosis studies with TNFα or a construct encoding caspase-1 as the triggers, a catalytically inactive form of JNK1 markedly reduced the anti-apoptotic potency of XIAP, Livin and NBIR123 (Sanna *et al.*, 2002). As XIAP has been reported to interact with the bone morphogenetic protein (BMP) receptor and TAB1, which is a coactivator of TAK1 (Yamaguchi *et al.*, 1999), Sanna *et al.* assessed TAK1 involvement. TAK1 is an upstream MAP3 kinase that activates JNK1 and p38 in response to transforming growth β1 (TGF-β1). In the 293T cell line, these investigators demonstrated that the XIAP-mediated stimulation of NF-κB and JNK1 were attenuated in the presence of catalytically inactive TAK1. Furthermore, expression of catalytically inactive TAK1 significantly reduced the protective properties of XIAP, NBIR123 and Livin in TNF-α and caspase-1-induced apoptosis. Catalytically inactive TAK1 or JNK1 did not modulate XIAP, NBIR123 or Livin's protection against caspase-9 mediated apoptosis induced by BAX. In an immunoprecipitation study, XIAP, NBIR123 and JNK1 coprecipitated TAK1, although this interaction may also be through TAB1 (Sanna *et al.*, 2002).

7. Role of NAIP *in vivo*

Our identification of an IAP homologue in the SMA region in light of the postulated role for neuronal cell death in SMA (Simic *et al.*, 2000) suggests that mutations in the *NAIP* locus might lead to supraphysiologic levels of motor neuron apoptosis, contributing to SMA (Gendron & MacKenzie, 1999). In keeping with this model, studies of the neuronal localization of NAIP in the central nervous system have not only shown that there are high levels of NAIP in spinal motor neurons, but that the

overall distribution of NAIP in the brain closely matches the pattern of CNS neurodegeneration observed in acute SMA (Pari *et al.*, 2000; Xu *et al.*, 1997b).

Examination of NAIP's cytoprotective nature *in vivo* was accomplished through the use of a 4-vessel occlusion model that induced ischemia in rats (Xu *et al.*, 1997a). Our colleagues found that NAIP levels were selectively elevated by transient global ischemia in those neuronal populations that were resistant to the damaging effects of this noxious treatment. Furthermore, virally mediated overexpression of NAIP rendered rat CA1 neurons more resistant to the damaging effects of 4-vessel occlusion, reducing the level of apoptosis (Xu *et al.*, 1997a). Protection was also observed in a rat model of Parkinson disease in which the nigro-striatal pathway was selectively lesioned by injection of the catecholamine neurotoxin 6-hydroxydopamine into the striatum. Virally mediated overexpression of NAIP rendered dopamine neurons more resistant to 6-hydroxydopamine induced degeneration (Crocker *et al.*, 2001). Significantly, in both the ischemia and Parkinson's model, the NAIP-treated mice did better at the Morris water maze test and amphetamine-induced rotation, respectively than the sham protected animals. This indicated that such anti-apoptotic treatment not only rescued histologically but functionally as well (Crocker *et al.*, 2001; Xu *et al.*, 1997a; Xu *et al.*, 1997b).

The distribution of NAIP-like immunoreactivity was examined in the rat central nervous system (CNS) by using an affinity-purified polyclonal antibody (E1.0) against human NAIP (Xu *et al.*, 1997b). This investigation demonstrated a wide distribution of NAIP-like species in the rat CNS. Although low to moderate levels of NAIP-like immunoreactivity were observed in the cortex and hippocampus, intense staining was detected within a wide variety of subcortical brain regions (Xu *et al.*, 1997b). These

included the thalamus, cranial nerve nuclei, brainstem relay nuclei, cerebellum and in Clarke's column of the spinal cord. With the exception for the striatum, all of these regions display pathologic hallmarks in severe cases of SMA (Xu *et al.*, 1997b). Further studies in human neuronal tissues utilizing the same antibody were performed (Pari *et al.*, 2000), which demonstrated high immunoreactivity only in spinal cord motor neurons and in pyramidal cells of the motor cortex (Pari *et al.*, 2000). The highest expression of NAIP was found in the cells of the choroid plexus. The neuroprotective role of NAIP was revealed by the increased apoptotic vulnerability of CA1 hippocampal neurons to kainate induced seizure in mice null for *Naip1* (Holcik *et al.*, 2000).

In situ studies showed expression of the *Naip* mRNA in the brain and spinal cord of mouse embryos aged 9.5 to 14.5 days (E9.5-E14.5) (Ingram-Crooks *et al.*, 2002). *Naip* transcripts were found in the marginal zone of the lateral ventricle, the follicles of the vibrissae, in the retina and in the intestinal villi at a later stage of development (E16.5) (Ingram-Crooks *et al.*, 2002). Northern blot analysis on adult mice showed predominant expression in the liver, lung, spleen (Diez *et al.*, 2000; Matsumoto *et al.*, 1999), intestine and macrophages (Diez *et al.*, 2000). In human adult tissues, *NAIP* transcripts were detected using Northern blot analysis in placenta, liver (Roy *et al.*, 1995; Yamamoto *et al.*, 1999), spleen, lung and peripheral blood leukocytes (Yamamoto *et al.*, 1999), with minimal expression in a number of other tissues, including fetal tissues (Yamamoto *et al.*, 1999).

Motor neuron degeneration following axotomy of the sciatic nerve in 3-day-old rats can be prevented through adenoviral mediated *NAIPΔE14/17*, *c-IAP1* and *c-IAP2* expression (Perrelet *et al.*, 2000). The effect observed with these proteins was similar to

that obtained with ciliary neurotrophic factor (CNTF) or brain-derived neurotrophic factor (BDNF). After sciatic nerve axotomy NAIP immunostaining decreased, a decrease that was abolished by glial cell line-derived neurotrophic factor (GDNF) but not BDNF or CNTF treatment (Perrelet *et al.*, 2002). Co-infection of antisense *NAIP* blocked the protective effect of adeno-*NAIPΔE14/17*. Interestingly, the XIAP binding protein, XAF1 also inhibited the survival promoting effects of *NAIPΔE14/17*, showing that this antagonist is not specific to XIAP. Infection with adenoviral mediated antisense *NAIP*, antisense *XIAP* or *XAF1* induced a comparable decrease in motor neuron survival in GDNF-treated rats, but not in BDNF- or CNTF-treated rats. These results indicate that the intracellular survival mechanisms activated by GDNF and neurotrophins were different and that NAIPΔE14/17 and XIAP were shown to be essential for the GDNF-mediated rescue of axotomized motor neurons (Perrelet *et al.*, 2002).

The GDNF family ligands (GFLs), consisting of GDNF, neuturin (NRTN), persephin (PSPN) and artemin (ARTN) signal through the RET receptor tyrosine kinase and the GDNF-family receptor-α (GFRα1–α4) co-receptors to maintain several neuronal populations in the central nervous systems, including midbrain dopamine neurons and motoneurons (reviewed in Airaksinen & Saarma, 2002). In addition, GDNF, NRTN and ARTN can support the survival and regulate the differentiation of many peripheral neurons, including sympathetic, parasympathetic, sensory and enteric neurons. The cellular signaling of GFLs is complex but, in general, GFLs bind to one of the four GFRα proteins to form high-affinity homodimers, which then mediate an interaction with two molecules of RET to trigger transphosphorylation of specific tyrosine residues in their

tyrosine kinase domains and intracellular signaling (Airaksinen & Saarma, 2002; Sariola & Saarma, 2003).

RET activates several intracellular signalling cascades, which regulate cell survival, differentiation, proliferation, migration, chemotaxis, branching morphogenesis, neurite outgrowth and synaptic plasticity. In an analysis of signaling pathways required for GDNF-mediated survival, investigators have found that the survival-promoting effects of GFLs are likely mediated through p60Src via the phosphatidylinositol 3-kinase (PI3K) pathway (Encinas *et al.*, 2001). This is in contrast to nerve growth factor (NGF) - mediated survival of sympathetic neurons, which rely on additional signaling pathways in conjunction with PI3K for survival. The differences in these two survival mechanisms may offer an insight into the signaling pathways involved in IAP-dependent, GDNF-mediated neuronal survival and should be explored further.

Like GDNF, the neurotrophins can affect neuronal survival, influence synaptic function and plasticity, making them important for the development and the maintenance of the vertebrate nervous system (reviewed in Dawbarn & Allen, 2003). NGF, BDNF and neurotrophins 3, 4/5, 6 and 7 mediate neuronal survival, differentiation and growth by interacting with the Trk family of tyrosine kinases and the p75 neurotrophin receptor ($p75^{NTR}$) (reviewed in Majdan & Miller, 1999). Interestingly, it appears as if neurotrophin binding to TrkA mediates survival and $p75^{NTR}$ mediates apoptosis. If sufficient NGF is present, TrkA is robustly activated and any coincident activation of $p75^{NTR}$ is insufficient to override this survival signal. If there is a lack of NGF, TrkA is only weakly activated, whereas $p75^{NTR}$ can still be robustly activated by other neurotrophins. The net outcome of this scenario would be rapid apoptotic elimination of that neuron (Majdan & Miller,

1999). TrkA phosphorylates specific tyrosine residues within its intracellular domain which serve as protein binding/activation sites for several signaling molecules, including SHC and Ras, PLC-γ, and PI3K. Also implicated are Ras, PI3K and their downstream effector, the serine/threonine kinase Akt (Majdan & Miller, 1999).

Another family of trophic factors is represented by ciliary neurotrophic factor (CNTF), a neuropoietic cytokine that is distantly related to a number of hematopoietic cytokines (reviewed in Ip, 1998). CNTF utilizes a multicomponent "cytokine receptor" system, which includes a specificity-conferring CNTFRα component. Binding of CNTF to CNTFRα induces the heterodimerization of LIFRβ and gp130, components that are shared with its distant cytokine relatives. Activation of the nonreceptor tyrosine kinases JAK/STAT that are pre-associated with the β components and mediate the subsequent signaling events.

In a mouse model of traumatic brain injury (TBI), apoptosis occurred to the greatest extent at 24h post-TBI. The apoptosis at 24 h post-TBI occured primarily in neurons and oligodendrocytes, was preceded by increased expression of TNFα and was accompanied by microglial activation. A marked increase at 6 h in the expression of Naip followed by a decrease at 24 h post-TBI was documented in the cerebral cortex and subcortical white matter. The decrease in Naip expression was mirrored by a decrease in procaspase-3 levels, an increase in PARP cleavage and the highest level of apoptosis at 24 h post-TBI (Hutchison *et al.*, 2001). TNFα levels were approximately the same at 6 and 24 h but CD11b levels, an indicator of activated microglial cells peaked at 24 h.

While NAIP's expression profile in the CNS is consistent with an SMA modulating role for NAIP specifically and a CNS protective effect generally, the

presence of transcripts in other tissues suggests that NAIP might have a broader function. For example, *Naip* has been found to be expressed in the granulosa cells of developing ovarian follicles (Matsumoto *et al.*, 1999). These investigators found that the *Naip* gene expression was up-regulated in ovaries pretreated with gonadotropins and that the suppression of *Naip* expression using antisense oligonucleotides reduced the number of morphologically normal oocytes. The authors suggest that because *Naip* transcripts were localized in the granulosa cells of developing follicles, this gene may assist in the survival of germ cells during ovarian follicular atresia (Matsumoto *et al.*, 1999).

Another role for Naip outside the CNS has been suggested in an analysis of adipocyte differentiation as a peak of Naip protein expression was observed at day 4 of an 8-day long differentiation process of the mouse adipocyte 3T3-L1 cell line (Magun *et al.*, 1998). Interestingly, this peak was correlated with an enhanced resistance against apoptosis induced by growth factor deprivation. Differentiation was induced by the combination of insulin, dexamethasone and isobutylmethylxanthine but the individual agents were unable to induce Naip expression on their own. Rapamycin, a p70 S6 kinase inhibitor that blocks adipocyte differentiation by inhibiting the induction of a critical adipogenic transcription factor, C/EBPα, was also able to abrogate the increase in Naip expression (Magun *et al.*, 1998).

NAIP was found to be strongly expressed in human placenta, both during the first trimester and at term. Immunoreactivity was found in the cytoplasm of villous cytotrophoblast cells, syncytiotrophoblast, villous mesenchymal cells, and villous endothelial cells (Ka & Hunt, 2003). These studies were performed using a rabbit polyclonal antibody (AF829) from R&D Systems for the immunoblotting and, for

immunohistochemistry, a rabbit polyclonal antibody (PC245) from Oncogene Research Products. The authors do not explain why a 35 kD band for NAIP was detected instead of the full-length protein. We have found through Western blotting using a polyclonal anti-Naip antibody (J2) that NAIP was present in the placenta and by immunohistochemisty that its expression was stronger in the decidual cells of the decidua basalis, the maternal portion of the placenta (Maier *et al.*, 2004). Preliminary work using lysates isolated from cells stably transfected with NAIP has shown that our in-house antibody, J2 was able to recognize a band around 160 kD, whereas the R&D Systems antibody did not (C. Coffill and A. MacKenzie, unpublished observation). It is also possible that the 35 kD band could have been produced as a cleavage product from full-length, as in the mouse (Hutchison *et al.*, 2001). Further studies will be needed to determine if these discrepancies are caused by the specificity of the different antibodies used.

8. Role of NAIP in *Legionella* susceptiblity

The C57BL/6 mice and the Legionnaire's disease susceptible A/J strain have a similar chromosomal arrangement to each other but differ from the 129 strain in that they possess only *Birc1a, b, c, e, f* and *c-ps3* (Diez *et al.*, 2003). Further refinement of the *Lgn1* locus led our colleagues and others to discover that *Birc1e* (*Naip5*) was the gene associated with resistance to the *Legionella* gram negative bacteria (Diez *et al.*, 2003; Wright *et al.*, 2003).

In permissive hosts, *Legionella* enters macrophages through a unique phagocytosis mechanism and replicates within maturation-defective phagosomes that do not acidify or fuse to the lysosomes (reviewed in Roy & Tilney, 2002). Instead, the

phagosome-containing *Legionella* recruits endoplasmic reticulum (ER) vesicles to form an ER-like vacuole studded with ribosomes, in which the bacteria replicate. The bacteria continue to grow and eventually lyse the host cell, releasing more bacteria to initiate a new infection cycle (Roy & Tilney, 2002). *Legionella* that have infected macrophages from mouse strains not permissive to replication are still able to rapidly inhibit the phagosome-lysosome fusion after phagocytosis but the infection cannot spread further (Wright *et al.*, 2003). It has been hypothesized that the role of Naip5 might be able to prevent the bacterium from gaining access to the replicative phagosome as it has been previously documented that *Lgn1* alleles affect intracellular *Legionella* targeting (Watarai *et al.*, 2001) and it has been shown that Naip protein expression is increased in macrophages after phagocytosis (Diez *et al.*, 2000). The authors who discovered Naip5 involvement do not, however, preclude Naip from having a function in the suppression of apoptosis at later points of the infection (Diez *et al.*, 2003; Wright *et al.*, 2003).

9. Outline of thesis

Redundancy in the Inhibitory of Apoptosis gene family suggests specific roles and consequently specific functions, mechanisms of control and interactions for each member of the family. While the suppression of apoptosis has been established for truncated portions of NAIP (reviewed in Liston *et al.*, 2003), cytoprotection mediated by the full-length human protein has not been fully explored. In the first part of this project I established stable cells with an inducible construct for the selective overexpression of NAIP to assess the suppression of apoptosis provided by the full-length protein and explore its cytoprotective mechanisms. The initial hypothesis proposed in this study is

that overexpression of the full-length NAIP protein can suppress apoptosis. Furthermore, as trophic factors and adenoviral-mediated *NAIPΔE14/17* overexpression have been shown to be cytoprotective, it is proposed that if sufficiently divergent signaling pathways are mediated by these agents an additive or synergistic suppression of apoptosis will be achieved. It was established that BDNF, CNTF and NGF trophic factors use similar signaling pathways to NAIP in the suppression of apoptosis as the combined treatment does not result in an additive or synergistic effect

The signaling pathways controlling *NAIP* expression in neuronal cells have yet to be identified. Following high-throughput screening analyses, that identified compounds resulting in the up-regulation of murine *Naip1* transcription levels in a neuroblastoma cell line, sodium butyrate was chosen as an inducer for the elucidation of cell signaling pathways. It is proposed that through the inhibition of specific kinases known to be affected by sodium butyrate, and by monitoring the transcript level of *Naip1*, signaling pathways involved in the sodium butyrate induced up-regulation of *Naip1* will be elucidated. It was determined that an H-7-sensitive kinase (other than PKA) plays a fundamental role in the expression of *Naip1* as this inhibitor can down-regulate basal *Naip1* levels, in addition to the attenuation of NaB-induced up-regulation.

As it is known that NBIR3 mediates cytoprotection, yet is less effective at inhibiting caspase-3/7 activity than NBIR2, it is proposed that NBIR3 can inhibit caspase-9, similar to the third BIR domain of XIAP (Davoodi *et. al.*, 2004) and that NBIR3 can interact with Smac, an IAP antagonist. To further study the mechanisms through which NBIR3 may mediate the suppression of apoptosis, potential binding partners of NBIR3 were investigated. Through phage display library screening, pull-

down studies and surface plasmon resonance analyses, potential binding partners of NBIR3 were identified. Based on the phage display data it is proposed that TRABID can interact with NBIR3. While no interaction was noted with TRABID, the BIR domains of NAIP were found to have similar roles to those of XIAP as it was demonstrated that both NBIR2 and NBIR3 can bind a Smac-based peptide and that NBIR3 can inhibit caspase-9.

By increasing our awareness of signaling pathways through which NAIP transcription is up-regulated and through which this protein mediates suppression of apoptosis, our understanding of its biochemical characteristics will be enhanced and perhaps lead to therapeutic interventions for diseases in which apoptosis is dysregulated.

MATERIALS AND METHODS

Materials

The human dopaminergic neuroblastoma cell line, SH-SY5Y was obtained from June Biedler at the Sloane-Kettling Institute. The human cervical epithelioid carcinoma HeLa and the rat adrenal pheochromocytoma PC12 Tet-Off™ cell lines, the pTRE and pTK-Hyg vectors, doxycycline and Hygromycin B were all purchased from Clontech. The murine neuro-2a cell line was acquired from ATCC (CCL-131). Dulbecco's Modified Eagle's Medium (DMEM) culture media, α-MEM, fetal bovine serum (FBS) and antibiotics were purchased from Wisent, Inc., while the horse serum acquired from Invitrogen. Tissue culture flasks and plates were obtained from Corning.

Trophic factors, doxorubicin and Hoescht 33258 were all from Sigma. WST-1 was obtained from Roche. Triton-X-100 from Pierce/Chromatographic Specialities Inc. Vectashield mounting medium from Vector Labs Inc. Lipofectamine Plus™, Lipofectamine 2000, Opti-MEM, restriction enzymes, pCR®2.1-TOPO vector and 4-12% NuPAGE® pre-cast gels were purchased from Invitrogen. The broad range protein marker was from New England Biolabs while the anti-rabbit Ig linked to horseradish peroxidase and ECLplus reagents were obtained from Amersham Pharmacia Biotech (Roche). The primary polyclonal anti-NAIP J2 (or J3) was generated and characterized in our laboratory. The secondary anti-rabbit Cy3-conjugated antibody was purchased from Jackson ImmunoResearch Laboratories. Anti-phospho JAK1/2 antibodies were from BioSource International while the anti-phospho Erk, anti-phospho CREB and anti-CREB

antibodies were purchased from Cell Signaling. Rat monoclonal anti-HA was obtained from Roche Molecular Biochemicals and the anti-β-actin antibody was from Sigma. Immobilon™-P polyvinylidene fluoride (PVDF) membrane was purchased from Millipore.

Sodium butyrate, cAMP analogs and kinase inhibitors were purchased from Calbiochem. Other chemicals were obtained from Sigma. Substrates and enzymes for the caspase-9 activity assay were purchased from BIOMOL Research Laboratories Inc. The adenoviral constructs expressing *NAIPΔE14/17* and *LacZ* had been previously generated by our group (Liston *et al.*, 1996) but further amplified and purified by Quantum (Qbiogene).

Isopropyl β-D-thiogalactoside (IPTG) and reduced glutathione were purchased from Sigma. The pGEX4T3 vector and glutathione sepharose 4B were obtained from Amersham Biosciences (Roche). The Ph.D.-7 phage display peptide 7-mer library kit was purchased from New England Biolabs, Inc. Following identification by phage display, ResGen™ Invitrogen Corporation was commissioned to synthesis the candidate seven-amino-acid sequences with a biotin moiety conjugated to the carboxyl terminus. A mouse monoclonal antibody against myc was obtained from Invitrogen. Our laboratory had previously modified Invitrogen's pcDNA3 vector to incorporate a 6x-myc epitope (Liston *et al.*, 1996). Bradford reagent was obtained from BioRad. The ABI Prism 7700 Sequence Detection System, the TaqMan EZ RT-PCR kit and the TaqMan GAPDH Control Reagent were obtained from Perkin Elmer Applied Biosystems.

Methods

Cell survival assay The SH-SY5Y cells were maintained in DMEM with 10% non-heat-inactivated FBS containing 100 units/ml penicillin G sodium and 100 µg/ml streptomycin sulfate at 37°C and 5% CO_2. 72 hours before exposure to adenovirus, the cells were seeded into 96 well dishes at a density of 3.5 x 10^5 cells per well. Following a 90-minute incubation with either adeno-*NAIPΔE14/17* or adeno-*LacZ* at an MOI of 200, the cells were washed once with fresh media and then incubated with medium containing one of the trophic factors. 48 hours after exposure to the adenovirus, the cells were treated with 100 ng/ml doxorubicin for 4 hours. Following this incubation period the media was replaced and cell survival assay was performed 18 hours later.

To determine the percentage of cells that survived the doxorubicin treatment, WST-1 reagent was added according to the manufacturer's protocol. After two to four hours of incubation at 37°C and 5% CO_2, the difference in absorbency readings at 450 versus 650 nm was obtained using a Spectra Max 340 microtitre plate reader from Molecular Devices. Cell survival was determined as the percentage of cells treated versus those not treated with doxorubicin.

Confocal microscopy Processing of coverslips for immunofluorescence labeling of proteins was performed as previously described (Chaly *et al.*, 1984). To obtain micrographs, 4.5 x 10^5 cells were seeded in 12 well dishes containing round glass cover slips and were fixed with 3% paraformaldehyde before permeabilisation in 0.2% Triton-X-100. All dilutions were made in PBS. Samples were incubated with primary

antibody/PBS (dilution 1:25-50, 1 hour) and secondary antibody/PBS (dilution 1:600, 45 minutes). Coverslips were washed with PBS between each antibody and before and after counterstaining with Hoescht 33258 (1 μg/ml, 1 minute). Cells were mounted in Vectashield mounting medium. Confocal fluorescence microscopy was performed with a Zeiss Axiovert 135 LSCM (Carl Zeiss) using a 40x oil Planapo objective lens (Zeiss, NA 1.3). Confocal series were collected at 0.6 μm increments. Images were stored on a computer and processed with Adobe Photoshop Software.

SDS-PAGE and Western analyses To prepare whole cell lysates, cells were harvested and resuspended in a lysis solution containing 7.2 mM phosphate buffer, pH 7.4, 150 mM NaCl, 1% IGEPAL, 1% taurocholic acid, 0.1% SDS, 1 mM EDTA, 1 mM phenylmethysulfonyl fluoride (PMSF), 10 μg/ml leupeptin, 1 μg/ml aprotinin and 10 μg/ml pepstatin. Proteins were separated on a 4-15% gel and subjected to Western blotting analyses as recommended by the manufacturer's protocol. The primary polyclonal anti-NAIP antibody J2 was generated and characterized in our laboratory. ECLplus was used according the manufacturer's protocol to detect the presence of the anti-rabbit antibody linked to horseradish peroxidase.

Subcloning of NAIP in pTRE vector An adapter nucleotide sequence and its complement were synthesized to incorporate *Sal*I, *Xho*I, *Nhe*I and *Xba*I restriction sites into the MCS of the pTRE vector at the *Xba*I site. Another reaction was used to introduce an *Sst*II site and a Kosak consensus sequence. A pGBT9-NAIP template previously generated by our laboratory was used to amplify a 320 bp PCR fragment of *NAIP*. This

product was then ligated into the pCR®2.1-TOPO vector. The restriction enzymes *Sst*II and *Eco*RI were used to isolate the fragment. This initial 5' fragment of *NAIP* was then ligated into the adapted pTRE vector. The restriction enzymes *Not*I and *Sal*I were used to excise the remaining portion of *NAIP* from the pGBT9-*NAIP* template and subclone the fragment in pTRE-5'-*NAIP*. The new construct, containing the entire 4209 bp coding region of *NAIP*, was named pTRE-*NAIP*.

Generation of stable transfectants overexpressing NAIP The Hela Tet-Off™ cell lines were maintained in DMEM with 10% heat-inactivated FBS containing 100 units/ml penicillin G sodium and 100 µg/ml streptomycin sulfate at 37°C and 5% CO_2. The PC12 Tet-Off™ cell lines were maintained in DMEM with 10% horse serum, 5% non heat-inactivated FBS containing 100 units/ml penicillin G sodium and 100 µg/ml streptomycin sulfate at 37°C and 10% CO_2.

The day before transfection, the cells were seeded into 60mm dishes at a density of 7 x10^5 cells per plate. 1.8 µg total of pTRE-NAIP and pK-Hyg DNA were added at a molar ratio of 20:1, combined with Lipofectamine Plus™ reagents in Opti-MEM media. Following a 3-hour incubation at 37°C and the appropriate CO_2 concentration, the transfection mixture was removed and replaced by complete medium. Two days following transfection, hygromycin was added to the media at a concentration of 200 µg/ml for the HeLa and 100 µg/ml for the PC12 cells, and this complete medium was changed every 2 days. Approximately 3 to 4 weeks after the transfection, clones were transferred to individual wells by aspiration of single colonies. RNA and protein were

isolated from the clones for analyses by quantitative RT-PCR and Western blot, respectively, to determine the presence of the transgene.

Caspase-9 assay Caspase-9 assays were performed in 100 mM MES pH 6.5, 10% polyethylene glycol, 0.1% CHAPS and 10 mM DTT using 100 units of Caspase-9 and 2mM Ac-LEHF-pNA as a substrate. The hydrolysis of the substrate was monitored once every 60 seconds at 405 nm at 30°C for 90 min in a 96 well dish using a Spectra Max 340 microtitre plate reader from Molecular Devices.

Preparation of samples for Kinexus analysis The cell pellet was homogenized in an ice-cold lysis buffer containing 20 mM MOPS, pH 7.0, 2 mM EGTA, 5 mM EDTA, 30 mM NaF, 40 mM b-glycerophosphate, 10 mM sodium pyrophosphate, 2 mM sodium orthovanadate, 1 mM PMSF, 3 mM benzamidine, 5 μM pepstatin A, 10 μM leupeptin and 0.5% Nonidet P-40. Following centrifugation at 100,000 x g for 30 min, supernatant were mixed with sodium dodecylsulphate-polyacrylamide gel electrophoresis (SDS-PAGE) sample buffer (Laemmli, 1970) at a final protein concentration of 1 mg/ml. and boiled. Samples were stored at room temperature until assessed at Kinexus, Inc.

NBIR3 constructs and protein generation The BIR3 domain of *NAIP* was PCR-amplified with a 5' *Bam*HI site and a 3' *Xho*I site. The forward and reverse primers are listed in table M-1. This fragment was then subcloned, in-frame, into the MCS of the pGEX4T3 vector, yielding a GST-NBIR3$_S$ (amino acids 252 to 353) chimeric protein. Other GST fusion proteins used were described previously (Maier *et al.*, 2002).

Following transformation of *E. coli* BL21, selection and sequencing, a single colony was chosen for protein expression. An overnight inoculation of 100 ml of LB medium containing 100 μg/ml ampicillin at 37°C with vigorous shaking was transferred to 1L of LB-Amp and continued at 37°C until the $OD_{600nm} \approx 1$. At this point the flask was moved to a 30°C shaking incubator and IPTG was added to a final concentration of 300 μM. One ml aliquots were taken every hour for five hours for testing on SDS-PAGE, as described previously.

The isolation of the GST-fusion protein was performed as described by the manufacturer's protocol with minor modifications. Following the five-hour induction, the culture was centrifuged at 7,700 x *g* for 10 minutes at 4°C, the supernatant was discarded and the pellet was resuspended in 25 mM Tris-HCl (pH 8), 150 mM NaCl, 5 mM β-mercaptoethanol. The pellet was stored overnight at -80°C. The next day, the pellet was allowed to thaw on ice for one hour. Protease inhibitors were added and then cells were disrupted by sonication. Triton X-100 and taurocholic acid were added to a final concentration of 1% each and allowed to mix gently for 30 minutes. The mixture was then centrifuged at 12 000 x *g* for 10 minutes at 4°C. The supernatant was transferred to a fresh container, glutathione sepharose 4B beads were added and allowed to mix gently overnight at 4°C.

The next day, the suspension was centrifuged at 500 x *g* for 5 minutes to sediment the gel. The gel was washed with at least 10 bed volumes of 25 mM Tris-HCl (pH 8), 150 mM NaCl, 1mM β-mercatoethanol. Following the washes, the suspension was centrifuged as above to isolate the gel. The purified proteins were eluted in 10 mM reduced glutathione, 50 mM Tris-HCl (pH 8) at room temperature for 10 minutes. The

elution process was repeated a total of five times with each supernatant set aside. A Bradford assay was used to measure the protein concentration of the samples, as this can be performed in the presence of glutathione. The samples were then analyzed by SDS-PAGE and stained with Coomassie Blue.

Phage display peptide library The panning technique was performed as described by the manufacturer's protocol with minor modifications. Using a 96-well microtitre plate, 150 µl of a 0.1 M $NaHCO_3$ solution containing either 15 µg of GST or 3 µg of GST-NBIR3 were aliquoted into individual wells and incubated overnight at 4°C in a humidified container. The next day, the wells were the blocked with 5 mg/ml BSA, 0.1 M $NaHCO_3$, washed with 50 mM Tris-HCl, 150 mM NaCl, 0.1% Tween-20 and then 2 x 10^{11} virions were added to the well containing the GST. After 30 minutes of incubation time, the solution containing non-binding phage was transferred to the well containing GST-NBIR3. Following another 30-minute incubation, the non-binding phage from this well were discarded, the well was washed and the bound phage were eluted with a buffer of 0.2 M Glycine-HCl (pH 2.2), 1 mg/ml BSA and then neutralized 1 M Tris-HCl (pH 9.1).

Isolated phages were amplified and the panning process was repeated for a total of four times, raising the Tween-20 concentration in the wash steps to 0.5 % in the second round and to 1 % in the third and fourth rounds. Amplification of individual colonies was carried out according to the manufacturer's procedure and the resulting phage DNA was sent for sequencing.

Surface plasmon resonance The interactions of GST-BIR fusion proteins with the immobilized biotinylated peptides were observed using a BIAcore 3000 biosensor system (Biacore, Piscataway, NJ) as described previously (MacKenzie *et al.*, 1997). The immobilization and running buffer was 10 mM HEPES, 150 mM NaCl, and 0.005% P20 (Tween 20), pH 7.4. The surfaces of four flow cells were activated for 1 min with a 1:1 mixture of 0.1 M N-hydroxysuccinimide and 0.1 M 3-(N,N-dimethylamino) propyl-N-ethylcarbodiimide at a flow rate of 20 µl/min. Approximately 2500 resonance units of Streptavidin were immobilized on research grade CM5 sensor chips by amine coupling. The remaining activated groups were blocked by ethanolamine. 22 resonance units of the biotinylated peptides were then captured on the streptavidin surface at a flow rate of 5 µl/min. Preparations of GST-BIR fusion proteins were diluted in running buffer and injected over the differently coated flow cells at 20 µl/min to view association with the biotinylated peptides. Binding was observed as an increase in resonance units (RU) over time. Dissociation was shown by a decrease in RU when the injection was terminated, and flow was switched to running buffer. To determine specificity, preparations of GST were injected over flow cells coated with the biotinylated peptides. Surfaces were regenerated with 100 mM HCl. Sensorgram data were analyzed using the BIAevaluation 3.0 software package (Biacore AB).

Basic Local Alignment Search Tool (BLAST) analyses The sequences of the seven amino acid peptides that NBIR3 was found to bind were used for homology searches in the protein databases at the National Center for Biotechnology Information web site (http://www.ncbi.nlm.nih.gov/) according to (Altschul *et al.*, 1997).

Pull down analysis Cell lysates for pull-down analysis were prepared as previously described (Hunter *et al.*, 2003). Briefly, 100-mm dishes of untransfected, and Ub-_AVPI-Smac-transfected 293A cells were scraped and mixed with lysis buffer (50 mM Tris-HCl, pH 8.0, 150 mM NaCl, 0.1% Triton X-100, 10 mM EDTA) and protease inhibitors. Lysates were collected in Eppendorf tubes, incubated on ice for 20 min, and centrifuged at 17,000 x *g* for 5 min. For pull-down analysis, 100 µg of total cell lysate and 2.5 µg of GST fusion protein were mixed in an Eppendorf tube, and 500 µl of lysis buffer were added to allow for adequate mixing on a rotating shaker. After a 2-h incubation at 4 °C, the protein-bead complexes were washed three times in ice-cold lysis buffer. Beads were syringe-dried and resuspended in a small volume of 1x sample buffer prior to SDS-PAGE.

Neuro-2a cell culture The mouse neuroblastoma, neuro-2a cell line was cultured in minimum essential medium (MEM) supplemented with 10% fetal bovine serum (FCS), penicillin (50 units/ml) and streptomycin (50 units/ml) at 37°C in 5% CO_2. Cells were subcultured once a week and for experimentation seeded at a density of 12.5 X $10^3/cm^2$, with drug addition at 24 h or 48 h. The drugs were dissolved in the appropriate solvent according to the manufacturer and the same volume was added to the controls. For each experiment, cell viability was determined by trypan blue exclusion, to ensure that there was no cytotoxicity induced by the solvents at the working concentrations. Cellular morphology was assessed with an inverted phase-contrast microscopy.

RNA extraction Neuro-2a cells were plated at 3.6 X 10^5 cells in 60 mm-diameter dishes. Cellular extracts were passed through Qiagen RNeasy Mini Kit spin columns including a DNase treatment step of the samples while on the column as per manufacturer's instructions (Qiagen). Briefly, cells were lysed with buffer RLT, homogenized by passing lysate through a 21-gauge needle. One volume of 70% ethanol was added to the homogenized lysate, which was then applied to an RNeasy column. After centrifugation, the column was washed once with Buffer RW1. The DNase I incubation mix was pipetted directly onto the spin column membrane, and place on the benchtop for 15 min. The column was washed with Buffer RW1 once and buffer RPE twice before the RNA was eluted with RNase-free water.

Quantitative RT-PCR For real time quantitative RT-PCR, 100 ng of total RNA for each sample was assayed for expression of *Naip* RNA simultaneously with human *GAPDH* mRNA. RT-PCR reactions were performed in the ABI Prism 7700 Sequence Detection System with the TaqMan EZ RT-PCR kit and TaqMan GAPDH Control Reagent. Reactions were performed according to manufacturer's recommendations. Briefly, 25 µl RT-PCR reactions contained: 1X TaqMan EZ Buffer, 3mM Mn(OAc), 300µM deoxy-ATP, -CTP, -GTP, 600 µM deoxyUTP, 100nM rodent GAPDH primers and probe, 600nM Naip1 primers, 200 nM NAIP probe, 0.25u AmpErase UNG and 2.5U rTth DNA Polymerase. RT-PCR conditions were: 2 min at 50°C, 30 min at 60°C, 5 min at 95°C, followed by 40 cycles of 15 sec at 94°C and 1 min at 60°C. Samples were normalized for *GAPDH* mRNA content and then expressed as the % change relative to non-treated

control samples arbitrarily set at 100 %. Primers and probes used for *Naip1* are listed in Table M-1.

Statistical analysis Results were analyzed statistically using Student's t test. Values are considered significant when $p < 0.05$; very significant when $p < 0.01$; and extremely significant when $p < 0.001$.

Table M-1. Primers used for PCR.

ID		Sequence (5' to 3')
Adapters to incorporate additional restriction sites in the pTRE construct		
CC1	forward	TCTAGTCGACTCGAGCTAGCATCTAGA
CC2	reverse	TCTAGATGCTAGCTCGAGTCGACTAGA
Incorporation of additional restriction sites in NAIP for subcloning into the adapted pTRE vector		
CC3	forward	CTGGAGCCGCGGCCACCATGGCCACCC
CC4	reverse	GGCACCAAAGAGGATTAGGCT
Incorporation of additional restriction sites in NAIP for subcloning into the pGEX4T3 vector		
CC5	forward	GGATCCTCAGAGGAAATTACC
CC6	reverse	CTCGAGATAGGACCAACTGCTATTGAA
Quantitative RT-PCR primers and probe		
NG1	forward	GCCATTTTATGTCCAAGGGATATC
NG2	reverse	CTTCCCAATTTCCTAAACATCCA
NG3	probe	CTGTACCGTGTCCTGTTTACCAAAGACAAAGC

RESULTS, CHAPTER ONE

NAIP is the founding member of the mammalian BIRC proteins and because it has been demonstrated to suppress apoptosis, NAIP belongs to the IAP subfamily of these proteins. Our laboratory and others have shown that overexpression of NAIP is cytoprotective in model cellular systems (Gotz *et al.*, 2000; Lindholm *et al.*, 2002; Liston *et al.*, 1996; Maier *et al.*, 2002; Mercer *et al.*, 2000; Sanna *et al.*, 2002; Simons *et al.*, 1999) and *in vivo* (Crocker *et al.*, 2001; Perrelet *et al.*, 2002; Perrelet *et al.*, 2000; Xu *et al.*, 1997a).

Trophic factors play an essential role in the growth, survival and differentiation of neurons in both the peripheral and central nervous systems. Brain-derived neurotrophic factor (BDNF) and nerve growth factor (NGF) belong to the family of neurotrophic factors known as the neurotrophins while ciliary neurotrophic factor (CNTF) is a neuropoietic cytokine that is distantly related to a number of hematopoietic cytokines and is representative of a second family of neurotrophic factors (reviewed in Dawbarn & Allen, 2003; Ip, 1998). To investigate if combining NAIP with trophic factors would result in an additive or synergistic cytoprotective effect in the SH-SY5Y cell line, the effects of BDNF, CNTF and NGF were examined with or without overexpression of NAIP. This dopaminergic neuroblastoma cell line was chosen because it possesses the receptors for the three trophic factors used in this study (Ehrhard *et al.*, 1993; Johnson *et al.*, 1994). Previous studies by our group showed that NAIP was effective at suppressing apoptosis in the SH-SY5Y cell line following exposure to doxorubicin, thus, this drug was selected as the apoptotic trigger. Due to the difficulty in transfecting SH-SY5Y cells

using traditional methods, an adenoviral vector was used to overexpress NAIP in these cells.

The adenoviral construct expressing NAIP had been previously generated by our group and further amplified and purified by Quantum (Qbiogene). The NAIP nucleotide sequence used for this construction was based on the initial cloning efforts in our laboratory (Roy *et al.*, 1995) but actually represented a variant version that lacked exons 14 and 17 of the final designated full-length *NAIP* gene (Chen *et al.*, 1998). This truncated mRNA version results in a protein that was ~140 kD instead of the expected ~160 kD. This truncated NAIP expressing adenovirus will be referred to as adeno-*NAIPΔE14/17*.

Before treating the cells with trophic factors and adeno-*NAIPΔE14/17* it was necessary to establish the dose of doxorubicin needed to kill 50% of the SH-SY5Y in the model system to be used (Figure 1-1). SH-SY5Y cells seeded in 96-well dishes were incubated for 3 days and treated for four hours with doxorubicin concentrations ranging from 25 to 300 ng/ml and cell survival was determined 18 hours later. The response to the drug was dose dependent with approximately half of the cells surviving between 100 to 125 ng/ml. Cell survival experiments with this cell line were therefore performed at a dose of 100 ng/ml of doxorubicin.

To study the effect of combination therapies on cell survival, SH-SY5Y cells were pretreated with adeno-*NAIPΔE14/17* or adeno-*LacZ* for 90 minutes, trophic factors were added to the media and 48 hours after exposure to the adenovirus, the cells were treated with doxorubicin for 4 hours. The media was replaced following the incubation

Figure 1-1. Survival of SH-SY5Y cells in the presence of increasing concentrations of the apoptotic trigger doxorubicin. SH-SY5Y cells were seeded in 96-well dishes, treated with a range of doxorubicin concentrations and cell survival was determined by the colorimetric assay WST-1 as described in Materials and Methods. The values represent the average of three wells ± STD. The experiment shown is representative of three independent trials.

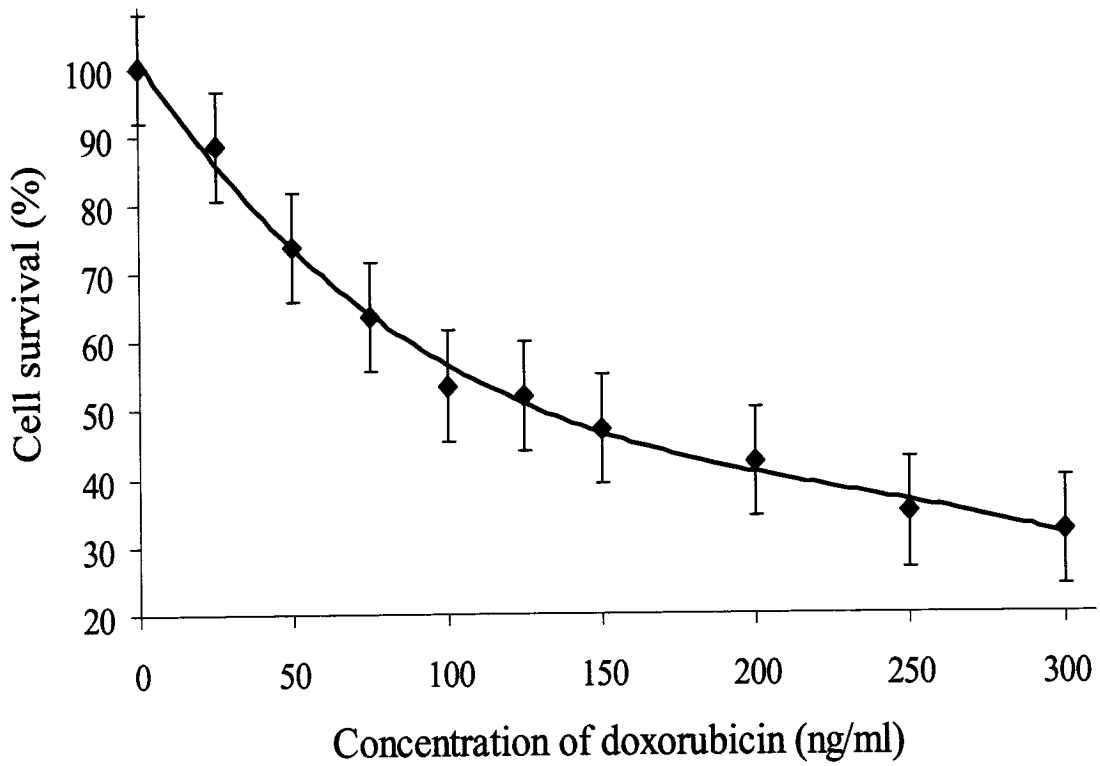
Cell survival (%)
100
90
80
70
60
50
40
30
20
0
50
100
150
200
250
300
Concentration of doxorubicin (ng/ml)

period with the drug and cell survival assay was performed 18 hours later (Figure 1-2). As expected, and in accordance with the dose response curve, those cells pretreated with only *LacZ* and then exposed to doxorubicin had a 48% survival rate. Pretreatment with *LacZ* in combination with BDNF, CNTF or NGF raised the survival rates to 63%, 60% or 65%, respectively. Interestingly, the 80% cytoprotection offered by pretreatment with adeno-*NAIPΔE14/17* alone could not be augmented by the addition of trophic factors. Thus, in this model system using an adenovirus vector for overexpression, NAIP conferred greater protection then that observed with the trophic factors and its anti-apoptotic effects could not be enhanced by the combination therapy.

To explore the possibility that the markedly supraphysiologic levels of NAIP delivered by adenovirus, may have masked any cooperation with the trophic factors in the prevention of cell death, and to further elucidate the mechanism of NAIP's anti-apoptotic activity, a cell line with stably expressed full-length NAIP was established.

While all studies to date have shown that various truncated products of human NAIP, such as NAIPΔE14/17 and the BIR domains, were effective at preventing cell death, it had not been clearly demonstrated that the full-length protein was cytoprotective. Therefore, before establishing the stable cell lines expressing full-length NAIP, it was necessary to confirm by transient transfection that full-length NAIP was effective at suppressing apoptosis. The human cervical epithelioid carcinoma HeLa, a cell-line that was easily transfected, was used for the transient transfections and etoposide was chosen as the apoptotic trigger as the BIR domains had been found to be effective at preventing cell death following treatment with this drug (Maier *et al.*, 2002). To compare the effects

Figure 1-2. The effect of adeno-NAIPΔE14/17 and trophic factor pretreatments on the survival of SH-SY5Y exposed to doxorubicin. SH-SY5Y cells were seeded in 96-well dishes, pretreated with either adeno-NAIPΔE14/17 or adeno-LacZ at a MOI of 200, incubated with PBS or 50 ng/ml of BDNF, CNTF or NGF and then exposed to 100 ng/ml of doxorubicin. Cell survival was determined by the colorimetric assay WST-1 as described in Materials and Methods. Cells that were pretreated as described above but not exposed to doxorubicin were used to establish 100% survival. The values represent the average of three wells ± STD. Results were analyzed statistically using Student's t test. Values are considered significant when $p < 0.05$ (*); very significant when $p < 0.01$ (**); and extremely significant when $p < 0.001$(***).

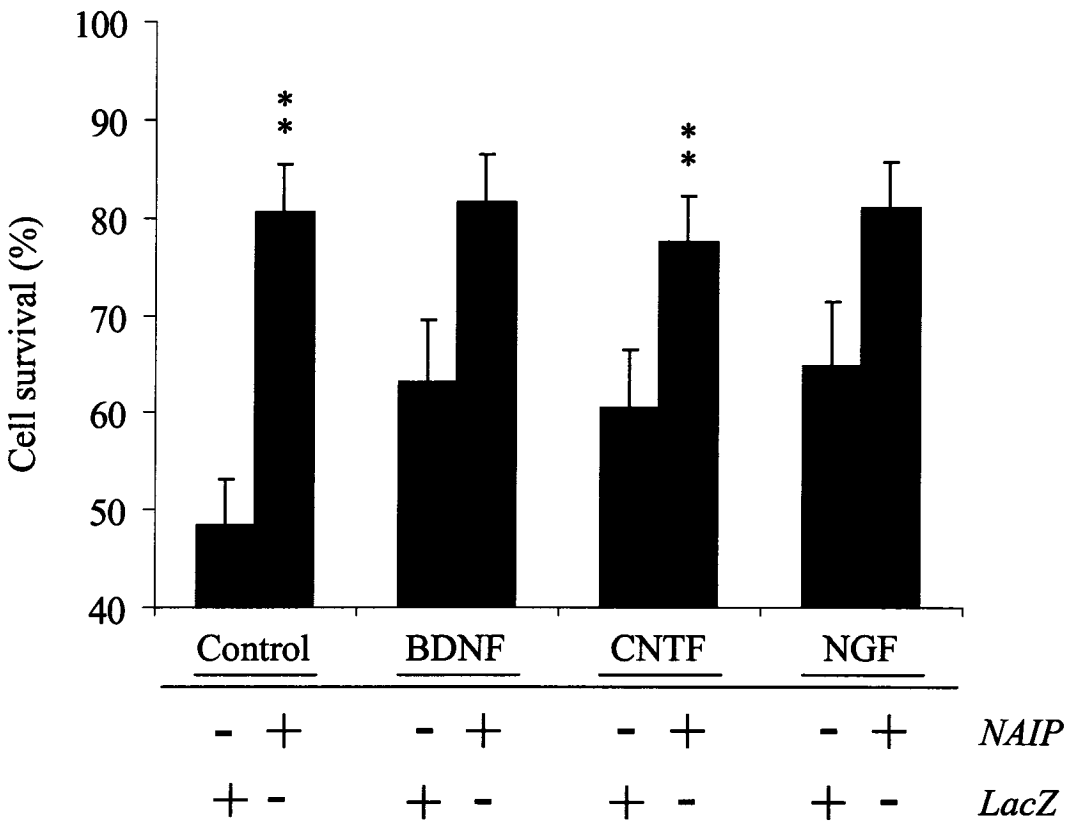
100
90
80
70
60
50
40
Cell survival (%)
**
**
Control
BDNF
CNTF
NGF
- + - + - + - +
+ - + - + - + -
NAIP
LacZ

of truncated and full-length NAIP on the survival of HeLa cells exposed to etoposide, cells were transiently transfected with pCDNA3 constructs expressing either NAIPΔE14/17 or the full-length gene and then treated with 30 μM etoposide (Figure 1-3). While half of the HeLa cells that were mock-transfected and then exposed to etoposide died, the survival of cells transiently transfected with NAIPΔE14/17 was 64% and for those expressing the full-length protein the survival rate increased to 74%. Based on these results, the full-length coding region of the gene was used for the stable cell line development.

To study the overexpression of full-length NAIP in a cell model system that allowed for selectable expression, the development of stable cell lines was pursued using the pTRE vector that has a tetracycline-responsive promoter controlled through the concentration of tetracycline in the media (Figure 1-4). Because the vector did not have suitable restriction enzyme sites in its multiple cloning site to match the cDNA available in the laboratory, a PCR was performed to introduce a *Sac*II site and a Kozak consensus sequence (Kozak, 1984) at the 5' end of NAIP. For the 3' end, oligomers were synthesized to introduce *Sal*I, *Nhe*I, *Xho*I, *Xba*I and *Bam*HI sites into an existing *Xba*I site within the pTRE vector (Panel C). A 300 bp fragment at the 5' end of NAIP was next ligated to the pTRE vector followed by a restriction digest with *Sac*II and *Eco*RI. The remaining 4000 bp of NAIP cDNA was excised with *Not*I and *Sal*I from an existing construct and ligated to the pTRE vector containing the 5' region. The overall ligation scheme is depicted in Panel A, while the 4359 and 3135 bp fragments generated from a restriction enzyme digest of the completed construct is shown in Panel B. Sequencing

Figure 1-3. The effect of transient transfections of truncated and full-length NAIP on the survival of HeLa cells exposed to etoposide. Cells were transiently transfected with pCDNA3-NAIPΔE14/17 or pCDNA3-full-length NAIP and then treated with 30 μM etoposide. Cell survival was determined by the colorimetric assay, WST-1 as described in Materials and Methods. Cells that were transfected with each construct but not exposed to doxorubicin were set to 100% survival. The values represent the average of three independent experiments ± STD. Results were analyzed statistically using Student's t test. Values are considered significant when $p < 0.05$ (*); very significant when $p < 0.01$ (**); and extremely significant when $p < 0.001$(***).

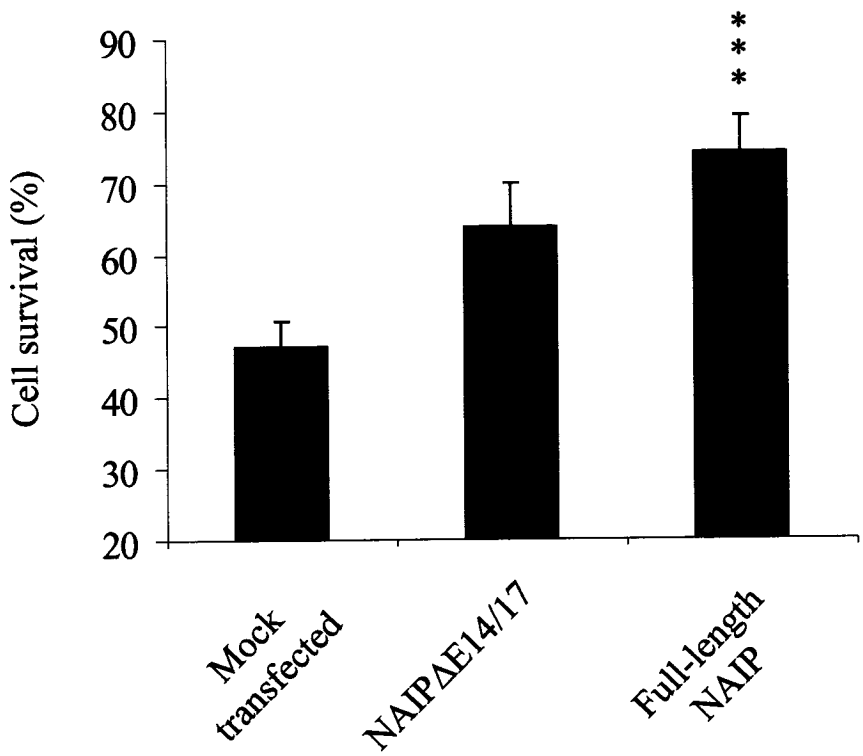
Cell survival (%)
90
80
70
60
50
40
30
20
***
Mock transfected
NAIPΔE14/17
Full-length NAIP

Figure 1-4. Development of the selectively inducible vector pTRE-NAIP. Panel A, schematic of the pTRE vector containing the full 4209 bp of the *NAIP* coding region. Panel B, restriction enzyme digest with *Nco*I and *Sal*I of pTRE-NAIP resulting in bands at 4359 and 3135 bp (lane 2). Panel C, sequences within the completed pTRE-NAIP construct illustrating the introduction of the *Sac*II site and a Kozak consensus sequence (5' section, bp 433-458) and the inclusion of adapter oligomers for the introduction of novel restriction sites into the pTRE vector (3' section, bp 4807-4836).

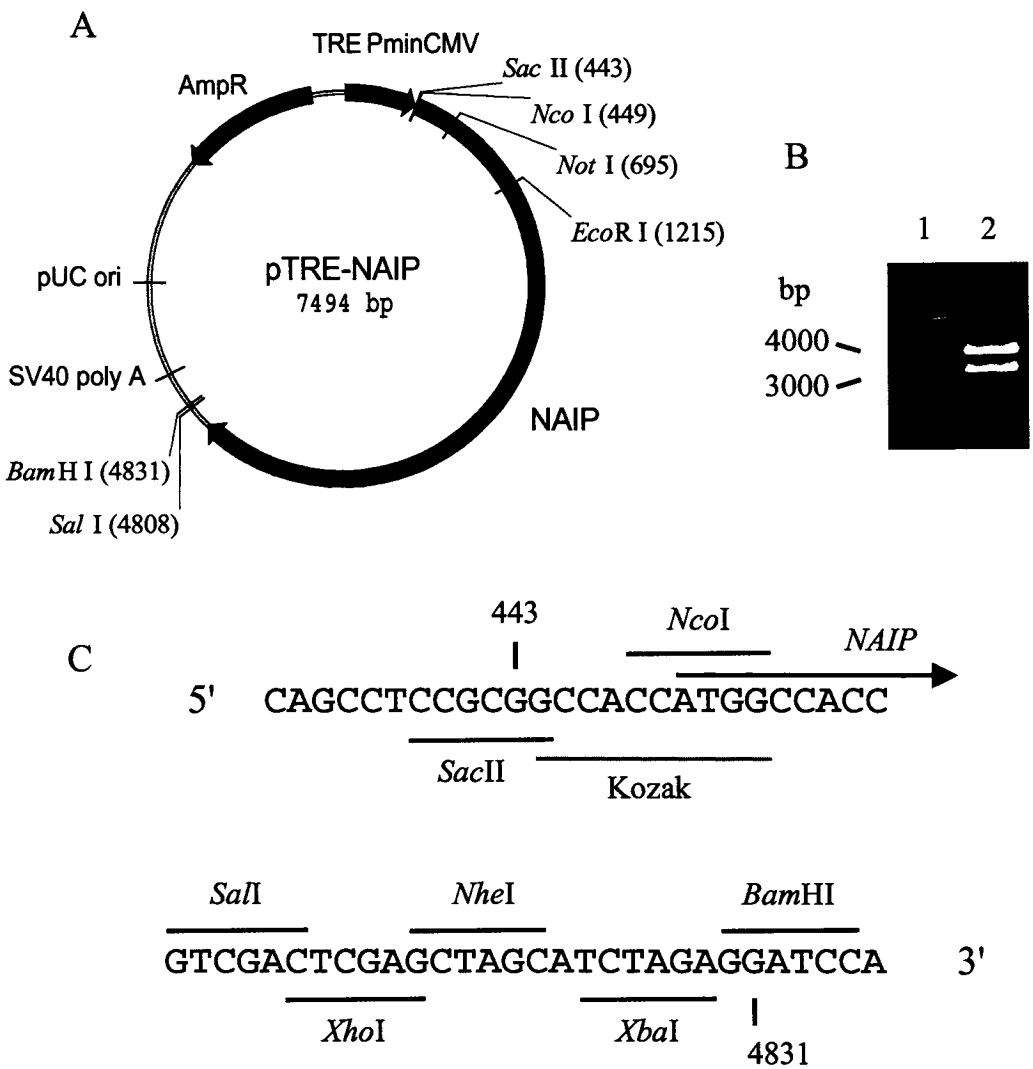
A
TRE PminCMV
AmpR
Sac II (443)
Nco I (449)
Not I (695)
EcoR I (1215)
pUC ori
pTRE-NAIP
7494 bp
SV40 poly A
NAIP
BamH I (4831)
Sal I (4808)
B
1 2
bp
4000
3000
C
443
NcoI
NAIP
5' CAGCCTCCGCGGCCACCATGGCCACC
SacII
Kozak
SalI
NheI
BamHI
GTCGACTCGAGCTAGCATCTAGAGGATCCA 3'
XhoI
XbaI
4831

was performed to rule out translationally significant mutations (data not shown).

Continuing with the development of stable cell lines with selectable expression of NAIP, HeLa and the rat adrenal pheochromocytoma PC12 cells stably transfected with pTet-Off, and thus expressing the tetracycline-responsive element, were purchased from Clontech. HeLa cells were selected because of other work performed by our group with this cell line (Liston *et al.*, 1996; Maier *et al.*, 2002) and the PC12 cells were chosen for differentiation and trophic factor studies (Gotz *et al.*, 2000). Following the co-transfection of the pTRE-NAIP and pHyg constructs and then selection with hygromycin, surviving clones were tested by quantitative RT-PCR (PC12) and Western blot (PC12 and HeLa) for the overexpression of NAIP (Figure 1-5). Relative *NAIP* RNA levels in individual stable transfectants were determined by quantitative RT-PCR (Panel A) while the level of protein was detected with an anti-NAIP antibody (J2) by probing immunoblots of individual stable clones transfected with either mock DNA (1) or full-length NAIP (2) in Panel B.

Overexpression of NAIP was also visualized in stable PC12 clones by indirect immunofluorescence with the anti-NAIP polyclonal antibody, J2 (Figure 1-6). Cells were fixed, permeablized, probed with anti-NAIP J2 and a CY3-conjugated secondary antibody, counter-stained with Hoechst and viewed by confocal microscopy. Anti-NAIP immunofluorescence was only faintly detectable in the mock transfected (A) but was highly visible in the cytoplasm, particularly in the perinuclear area in the stable NAIP cells seen in a Z-axis cross-section in panels B through D. The corresponding Hoechst-stained nuclei can be seen in panels E through H.

Figure 1-5. Identification of individual clones with stable over-expression of full-length NAIP by at the mRNA and protein levels. Panel A, relative Naip RNA levels in individual stable transfectants. Transfection, isolation of individual clones, RNA collection and NAIP analysis by quantitative RT-PCR were performed as described in Materials and Methods. Panel B, anti-NAIP Western blot of individual stable clones transfected with either mock DNA (1) or full-length NAIP (2). Lysate preparations and Western blotting were performed as described in Materials and Methods.

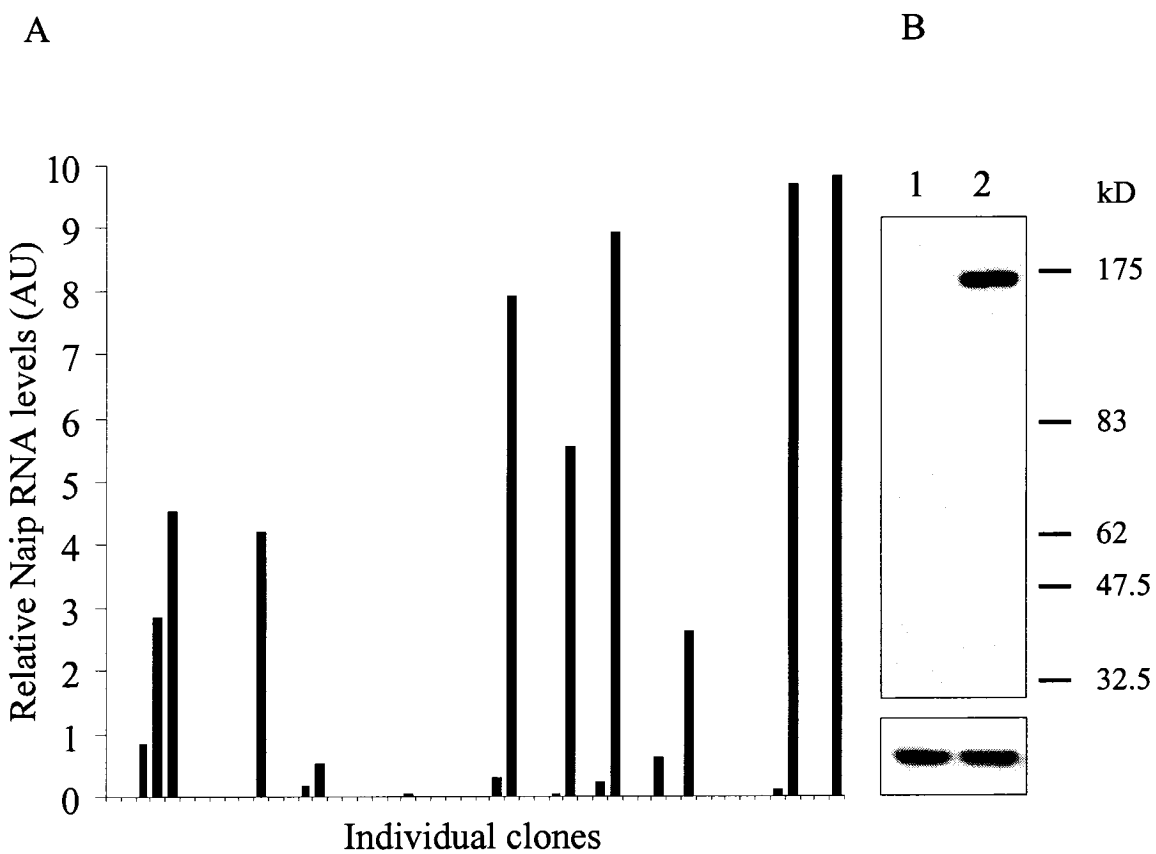
A
B
Relative Naip RNA levels (AU)
10
9
8
7
6
5
4
3
2
1
0
Individual clones
1
2
kD
175
83
62
47.5
32.5

Figure 1-6. Indirect immunofluorescence of stable NAIP PC12 clones using a polyclonal anti-NAIP antibody. Cells were fixed, permeablized, probed with anti-NAIP J2 and a CY3-conjugated secondary antibody and then counter-stained with Hoechst. Anti-NAIP immunofluorescence was only faintly detectable in the mock transfected (A) but was highly visible outside the nuclear area in the stable NAIP cells seen cross-sectioned in panels B through D. The corresponding Hoechst-stained nuclei can be seen in panels E through H. Stable transfection, isolation of individual clones, immunocytochemistry and confocal microscopy were performed as described in Materials and Methods.

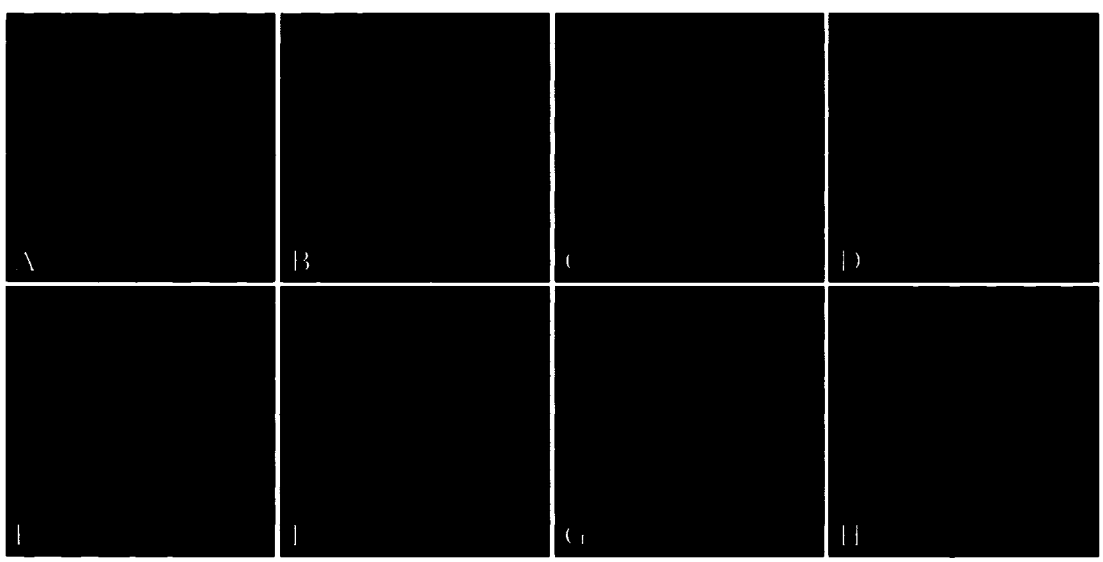
A
B
C
D
E
F
G
H

Once overexpression of NAIP was confirmed in the cell lines, they were tested for increased survival following treatment with apoptotic triggers (Figure 1-7). Surprisingly and in contrast to what was seen when HeLa cells were transiently transfected with a construct expressing full-length NAIP (Figure 1-3), the NAIP stable HeLa cell lines did not offer increased protection against etoposide (data not shown). Our group had previously demonstrated adenoviral mediated *NAIPΔE14/17* cytoprotection in HeLa when treated with TNFα and cycloheximide (Liston *et al.*, 1996) yet in the present experiment the mock-transfected and the NAIP stable HeLa cell lines each displayed a equivalent survival rate (Panel A). Similarly, SH-SY5Y cells infected with adeno-*NAIPΔE14/17* and treated with doxorubicin had an increased survivial rate (Figure 1-2) but in the present experiment there was no significant difference in survival noted between the mock-transfected Hela cell and the stable NAIP cells (Panel B). In addition, when the PC12 cell line stably expressing full-length NAIP was tested for increased cytoprotection, no increased survival was found (data not shown).

Further experiments are required to determine why transient transfection of a construct expressing full-length NAIP is cytoprotective but stable, long-term overexpression of NAIP is not. While our group has some interesting data to suggest that the C-terminus of NAIP may block the BIR domains under certain conditions (J. Davoodi, unpublished observation), the difference between the transient and stable cell lines seems to relate to the length of time NAIP was overexpressed in the cell. Other groups attempting to develop stable XIAP cell lines have discovered a loss in cytoprotection and attributed it to a compensatory mechanism to counter the continuous

Figure 1-7. Survival of stable cell lines after treatment with apoptotic triggers. Panel A, stable cell lines treated with 1 ng/ml TNFα and 30 μg/ml cycloheximide. Panel B, stable cell lines treated with 3 μg/ml doxorubicin. Negative control cells were exposed to vehicle only and were set to 100% survival. Cell survival was determined by the colorimetric assay, WST-1 as described in Materials and Methods. The values represent the average of three wells ± STD. The experiments shown are representative of three independent trials.

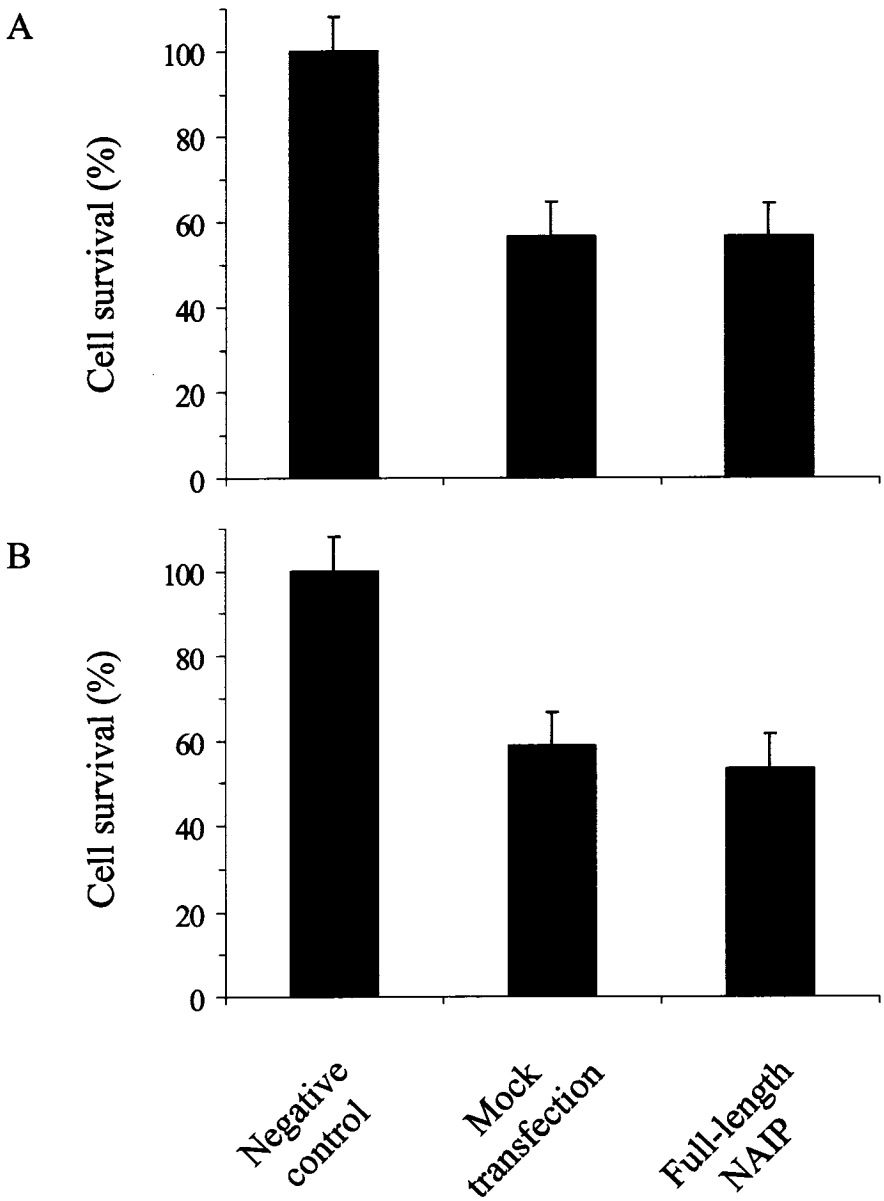
A
Cell survival (%)
100
80
60
40
20
0
B
Cell survival (%)
100
80
60
40
20
0
Negative control
Mock transfection
Full-length NAIP

expression of an IAP (Colin Duckett, personal communication). As the stable cells developed in this present study were produced with continuous overexpression of NAIP, those cell lines that survived the lengthy selection process may have offset the cytoprotective nature of this protein. As a result, a different approach was needed to further elucidate the function of NAIP.

DISCUSSION, CHAPTER ONE

The binding of neurotrophic factors BDNF and NGF to the Trk receptors initiates signaling cascades through the phosphorylation of tyrosine residues and the docking of adapter proteins to the receptor. The intracellular signaling cascades activated include the phosphatidylinositol-3-kinase/Akt kinase pathway, phospholipase C γ and the Ras kinase pathway (Dawbarn & Allen, 2003). Because the cytoprotection offered by NAIPΔE14/17 could not be improved upon through the pretreatment with these two trophic factors, it implies that similar signaling pathways are involved. CNTF, however, uses the CNTFRα receptor coupled to LIF and gp130 for signaling through the JAK/STAT pathways. Interestingly, CNTF was shown to up-regulate NAIP in the axotomized rat optic nerve (B. VanAdel and A. MacKenzie, unpublished observation). The slight increase in cytoprotection in the presence of CNTF and NAIPΔE14/17 when compared to CNTF alone could be due to additional up-regulation of endogenous NAIP. Overall, there was no additive or synergistic protection with the trophic factors and NAIPΔE14/17, suggesting either that the NAIP levels were too high at an MOI of 200 for a subtle effect to be observed or similar signaling pathways were engaged.

Using a vector with a tetracycline inducible promoter allows for the expression of potentially toxic genes to be turned off during the selection process of stably transfected clones. While it was not anticipated that NAIP would exert any undesirable effects during the selection process, its expression was left on in the present study. Quantitative RT-PCR and Western analyses revealed increased NAIP in the cell lines yet increased survival was not demonstrated. In contrast, transient transfection of full-length NAIP was

shown to suppress apoptosis. Although the possibility that full-length NAIP self-inhibits and only becomes active under some triggers cannot be formally excluded, this explain why a transient transfection in the same cell line exposed to the same trigger is protective. Ectopic localization of NAIP in the stable transfection does not appear to be a factor given that the cytoplasmic localization of NAIP, as determined by confocal microscopy analyses, was expected and has been seen previously with transient transfections (D. Barnes and A. MacKenzie, unpublished observation). The length of time for the overexpression of NAIP seems key to understanding why cytoprotective effects could no longer be demonstrated.

RESULTS, CHAPTER TWO

As the suppression of apoptosis can be mediated by the transient overexpression of exogenous NAIP in model cellular systems, the elucidation of signaling pathways through which endogenous NAIP expression is controlled at the transcriptional or translational level, therefore, would be a logical next step in the pursuit of understanding the regulation of this protein. To understand the intracellular signals that control *Naip* expression following treatment with various kinase modulators, an analysis of *Naip* RNA and protein levels in the murine neuroblastoma cell line, neuro-2a was undertaken. This cell line was chosen as a representative of a neuronal-like system in which NAIP-BIR123 had been shown to protect against calcium-induced cell death (Mercer *et al.*, 2000) and in which *Naip* expression had been demonstrated previously (Z. Yaraghi, personal communication).

High-throughput screening of compound libraries (~10,000) by our group had identified that cAMP or sodium butyrate (NaB) could up-regulate *Naip* transcript levels (C. Craig and A. MacKenzie, unpublished observation) in addition to genistein and serum withdrawal (Z. Lahoua and A. MacKenzie, unpublished observation). These compounds have been previously characterized in the scientific literature for their effects on intracellular pathways. Although cyclic adenosine 3', 5'-monophosphate (cAMP) is most recognized for binding to the cAMP-dependent protein kinase (PKA), which in turn phosphorylates protein substrates that regulate a large number of cellular processes, a small number of PKA-independent but cAMP-dependent pathways have also been discovered (reviewed in Chin *et al.*, 2002). NaB is a naturally occurring four-carbon fatty

acid that, in addition to activating a number of signaling pathways, acts as a histone deacetylase (HDAC) inhibitor resulting in hyperacetylation of core histones, transcription factors, and proteins involved in transcription (reviewed in Davie, 2003). Genistein is a potent plant-derived isoflavone that displays estrogenic activity at nanomolar concentrations and can be antiproliferative or induce apoptosis at higher concentrations (above 10-50 μM). (Linford *et al.*, 2001). At these higher doses genistein has multiple intracellular effects, including inhibition of the activity of certain tyrosine kinases such as Src and the epidermal growth factor receptor (Akiyama *et al.*, 1987) and the inhibition of topoisomerase II (Markovits *et al.*, 1989). The structural analog daidzein has estrogen receptor agonist properties similar to genistein but is inactive with respect to tyrosine kinase inhibition (Lavens *et al.*, 1992).

To determine the extent of *Naip* transcript up-regulation in neuro-2a cells following various treatments, the *Naip* RNA levels were measured by quantitative RT-PCR (Figure 2-1). As the baseline control, neuro-2a cells were treated with water and the level of *Naip* transcript present was set to a value of one. Treatment with the cAMP analogs [N6, O2'-dibutyryl cAMP (db-cAMP) and 8-bromo-cAMP (8-Br-cAMP)] resulted in an averaged increase of 2.7 times above the control level whereas NaB resulted in a 2.2 fold increase in transcript levels. A 3-fold increase in *Naip*, the most induction seen in this experiment, was brought about by serum starvation. When the active kinase inhibitor genistein was added to the media, a 2-fold increase in *Naip* levels was observed while the inactive form, daidzein had a minimal effect.

Figure 2-1. Induction of *Naip* RNA levels in neuro-2a cells following various treatments. Neuro-2a cells were treated with water; 2 mM db-cAMP, 8Br-cAMP or sodium butyrate; 50 μM genistein or daidzein; or serum starved for 48 hours. Cell treatment, RNA collection and *Naip* analysis by quantitative RT-PCR were performed as described in Materials and Methods. Each value represents the mean ± SEM (N=3) and the data presented is representative of three independent experiments. Statistical significance with respect to the control: * $p < 0.05$; ** $p < 0.01$ and *** $p < 0.001$.

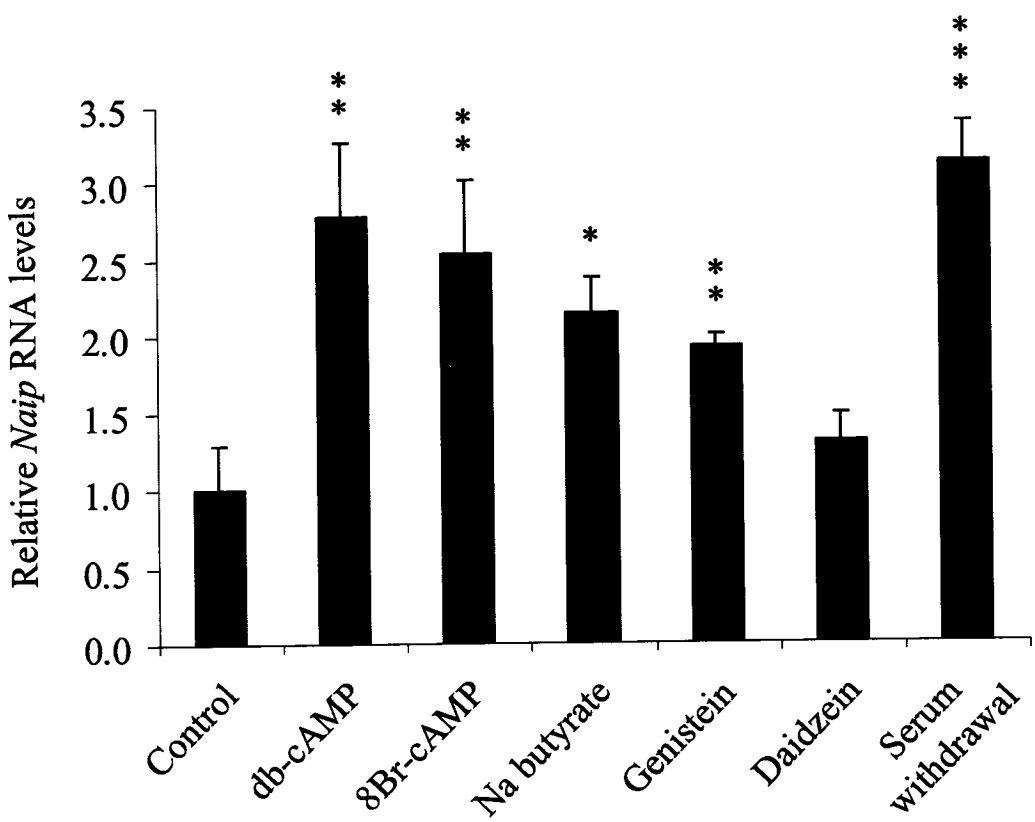
Relative *Naip* RNA levels
3.5
3.0
2.5
2.0
1.5
1.0
0.5
0.0
***
**
*
**
***
Control
db-cAMP
8Br-cAMP
Na butyrate
Genistein
Daidzein
Serum withdrawal

For the purpose of this study, I chose to focus on one of the up-regulators (NaB) was to elucidate the signaling pathways involved. Other investigators have shown that NaB treatment of SMA-like mice resulted in increased expression of SMN protein and in significant improvement of SMA clinical symptoms (Chang *et al.*, 2001) so it was logical to study this compound first given our hypothesis that NAIP can act as a modulator in the severity of SMA (Gendron & MacKenzie, 1999). To obtain an indication of the signaling pathways that were involved in the up-regulation of *Naip* by NaB in neuro-2a cell lysates, a collaboration was established with Kinexus Bioinformatics Corporation. Through Western blot analyses, this company is able to detect 78 known protein kinases in a single assay and then display that data visually (Figure 2-2) or through densitometry values (Table 2-1). The differences in various kinase protein expression levels in neuro-2a cells following NaB treatment (Figure 2-2, Panels B and D) can be readily seen when compared to the cell lysates only treated with water (Panels A and C). Each numbered arrow indicates a change in the expression levels of one of more kinase, the names of which and the degree of change can be seen in Table 2-1. Other bands that were not numbered but displayed a change in intensity were not identified in the 78 kinase panel and, therefore, represented cross-reactions with the antibodies used.

With few exceptions, phosphorylation of the tyrosine residues in the activation loop of tyrosine kinases leads to an increase in enzymatic activity while phosphatases restore the kinases to their basal state of activity (reviewed in Hubbard & Till, 2000). Because the phosphorylation status of a kinase can be a stronger indicator of activation within a particular signaling pathway than change in absolute expression level, the densitometry values given were meant more as a reflection of those kinases that might be

Figure 2-2. Western blot analyses of various kinase protein expression levels in neuro-2a cells following sodium butyrate treatment. Panels A and C correspond to cells exposed to water while those in panels B and D were treated with sodium butyrate. Within each panel, the same lysate sample was electrophoresed in every lane but each lane was probed individually with a different antibody. The Western blots in panels A and B were probed with one series of antibodies while those of panels C and D were incubated with a second series. The arrows indicate changes in expression levels of the following kinases: 1, the extracellular regulated kinases (ERK) (see Figure 2-5 for more details); 2, Cyclin-dependent kinase 7 (35); 3, Ribosomal S6 kinase 1 (73); 4, Casein kinase 2 (35, 37 and 39); 5, Inhibitor of NF κB kinase alpha (83); 6, Calmodulin-dependent kinase kinase (52); 7, Protein kinase G1 (cGMP-dependent protein kinase) (70); 8, Protein kinase A (cAMP-dependent protein kinase) (38); 9, ZIP kinase (death associated protein kinase 3) (48); and 10, Janus kinase 2 (116). Cell treatment and lysate preparations were performed as described in the Materials and Methods while the Western blots were completed at Kinexus Bioinformatics Corporation.

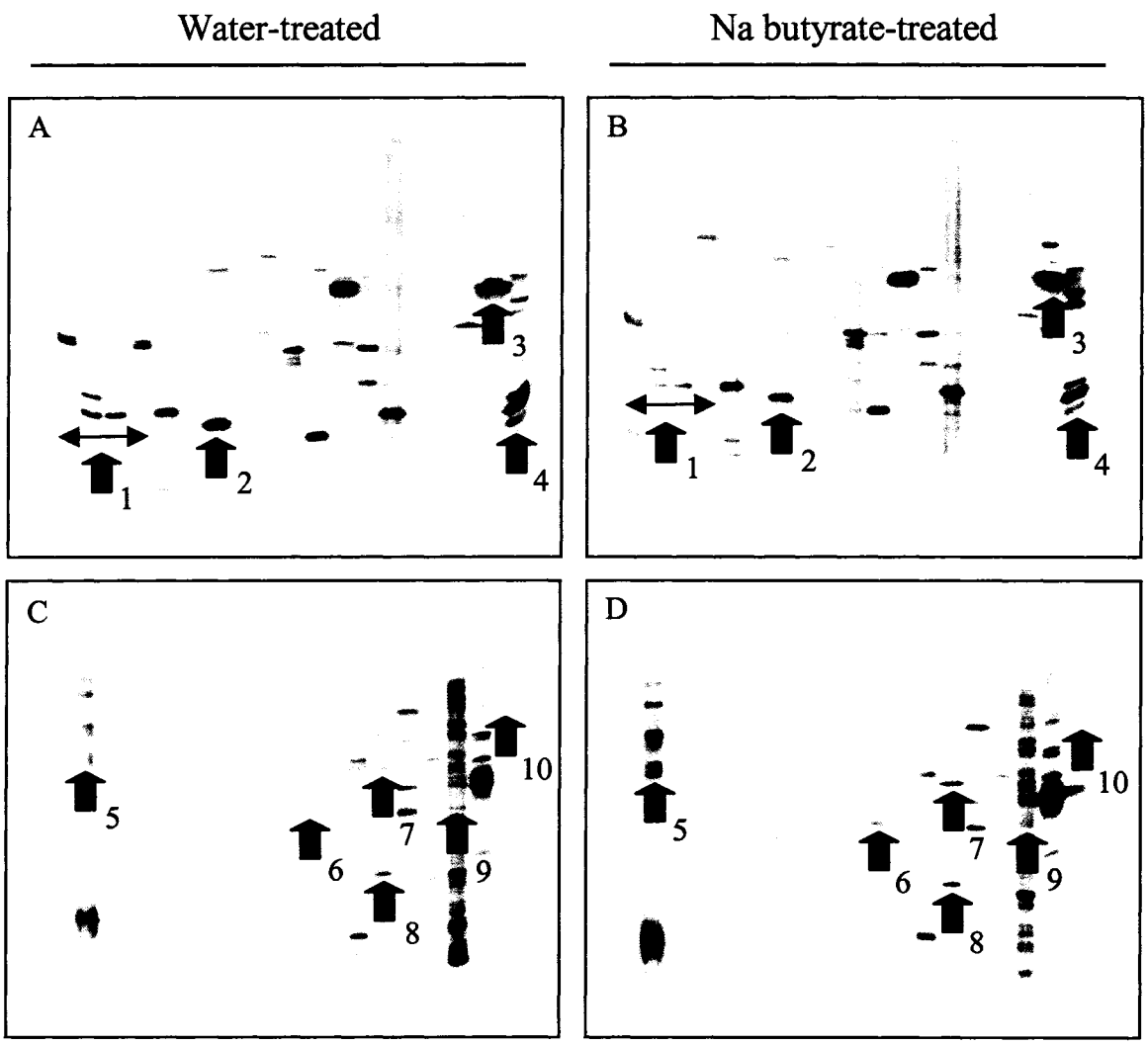
Water-treated
Na butyrate-treated
A
B
C
D
1
2
3
4
5
6
7
8
9
10

Table 2-1. Kinase expression levels following treatment with sodium butyrate.

#	Kinase name	Abbrev.	Density value[a] Water	NaB	Change	
1	extracellular regulated kinase 1 (40)	ERK1	4856	2323	↓	0.48
	extracellular regulated kinase 2 (37)	ERK2	7045	2253	↓	0.32
	extracellular regulated kinase 3 (56)	ERK3	5282	1915	↓	0.36
	Protein kinase C mu (120)	PKCμ	1381	nd	↓	
2	Cyclin-dependent kinase 7 (35)	CDK7	26589	10275	↓	0.39
3	Ribosomal S6 kinase 1 (73)	RSK1	5097	22140	↑	4.34
4	Casein kinase 2 (35)	CK2	6137	4037	↓	0.66
	Casein kinase 2 (37)	CK2	19042	17562	↓	0.92
	Casein kinase 2 (39)	CK2	17766	5699	↓	0.32
5	Inhibitor of NF κB kinase alpha (83)	IKKα	4674	15400	↑	3.30
6	Calmodulin-dependent kinase kinase (52)	CaMKII	4878	8946	↑	1.83
7	Protein kinase G1 (cGMP-dependent protein kinase) (70)	PKG1	5127	11447	↑	2.23
8	Protein kinase A (cAMP-dependent protein kinase) (38)	PKA	9497	10507	↑	1.11
9	ZIP kinase (death associated protein kinase 3) (48)	ZIP	6209	nd	↓	
10	Janus kinase 2 (116)	JAK2	1525	nd	↓	

[a] The quantity of a band was measured by the area under its intensity profile curve (intensity x mm)

involved in NaB signaling. Furthermore, because this analysis was only performed once at Kinexus and as some of the values were representative of expression and not activation levels, the phosphorylation status of each kinase in the table or the effect of a specific inhibitor needed to be tested to determine its true involvement in NaB-induced *Naip* up-regulation.

A decrease in the following kinases was observed after NaB treatment: ERK1, ERK2, ERK3, PKCμ (all above double headed arrows 1); CDK7 (arrow 2); CK2 (arrow 4); ZIP (arrow 9) and JAK2 (arrow 10). The following kinases displayed increased protein expression after treatment with NaB: RSK1 (arrow 3); IKKα (arrow 5); CaMKII (arrow 6); PKG1 (arrow 7); and PKA (arrow 8). The greatest changes were 4-fold and 3-fold increases in the amount of RSK1 and IKKα, respectively and decreases that lead to undetectable amounts of PKCμ, ZIP and JAK2 following NaB treatment.

It has been demonstrated that Janus kinase (JAK)2 is tyrosine phosphorylated immediately after stimulation with lipopolysaccharide (LPS), a major component of the outer membrane of gram-negative bacteria (Okugawa *et al.*, 2003). Investigators have found that *cIAP2* mRNA is up-regulated by LPS in a human monocyte cell line after differentiation by phorbol 12-myristate 13-acetate (PMA) (Cui *et al.*, 2000), a treatment that has been shown to up-regulate *cIAP2* in colon cells through the activation of PKCδ and NF-κB (Wang *et al.*, 2003). Researchers from the former study did not investigate *NAIP* in the monocyte cell line and those from the latter study did not find a significant change in human *NAIP* levels as determined by RNase protection assay (RPA) but the amount of *NAIP* in the colon cell line used was initially very low. Similarly, using the RPA technique, other researchers found minimal change in *NAIP* levels in non-

differentiated monocytes following LPS incubation (Perera & Waldmann, 1998) but did not investigate post-differentiated levels. However, a significant increase in *Naip* RNA and protein was noted in murine macrophages following intracellular infection with *Legionella pneumophila*, a gram-negative bacteria (Diez *et al.*, 2000). The differences in these results seem to reflect cell specificity, differentiation status and techniques used for detection. However, due to the importance of JAK2 in LPS-induced signaling in macrophages (Okugawa *et al.*, 2003) and the role of Naip5 in *Legionella* susceptibility (Diez *et al.*, 2003), JAK2 was chosen for the initial investigation of *Naip* up-regulation following NaB treatment in the neuro-2a cell line.

The relative *Naip* RNA levels were measured in neuro-2a cells following NaB treatment in the presence of AG490, a JAK2 inhibitor (Figure 2-3). As AG490 was dissolved in DMSO, the level of *Naip* transcript found in cell lystates treated with only this solvent was set to one and used as the control (Panel A). Following pretreatment with AG490 but not NaB resulted in a 1.8 times increase in expression level. Exposure to NaB in the absence of AG490 gave an expected 2.5-fold increase. In a dose response manner and with additive results, those cells that were exposed to a constant level of NaB but increasing concentrations of AG490 displayed increased levels of *Naip* transcript to a maximum of 5-fold above control. See Table 2-2 for a list of the kinase inhibitors and what effect they had on NaB induction of *Naip* expression.

As the expression level of JAK2 was not detectable following NaB treatment (Table 2-1) nor, as determined in the present study, was the phosphorylation status of JAK1 or JAK2 significantly different when compared to water or DMSO (Figure 2.3,

Figure 2-3. Relative *Naip* RNA levels in neuro-2a cells following sodium butyrate treatment in the presence of a JAK2 inhibitor. Panel A, Following pretreatment with various concentrations of AG490 and exposure to 2 mM sodium butyrate, the level of *Naip* message was determined. RNA collection and *Naip* analysis by quantitative RT-PCR were performed as described in Materials and Methods. Each value represents the average ± STD (N=3) and the data presented is representative of three independent experiments. Panel B, comparison of JAK 1 or 2 phosphorylation levels following cellular treatment with water (1); DMSO (2); 2 mM sodium butyrate (3); or serum withdrawal for 48 h (4). Cell treatment, lysate preparations and Western blotting were performed as described in the Materials and Methods. Statistical significance with respect to the control: * $p < 0.05$; ** $p < 0.01$ and *** $p < 0.001$.

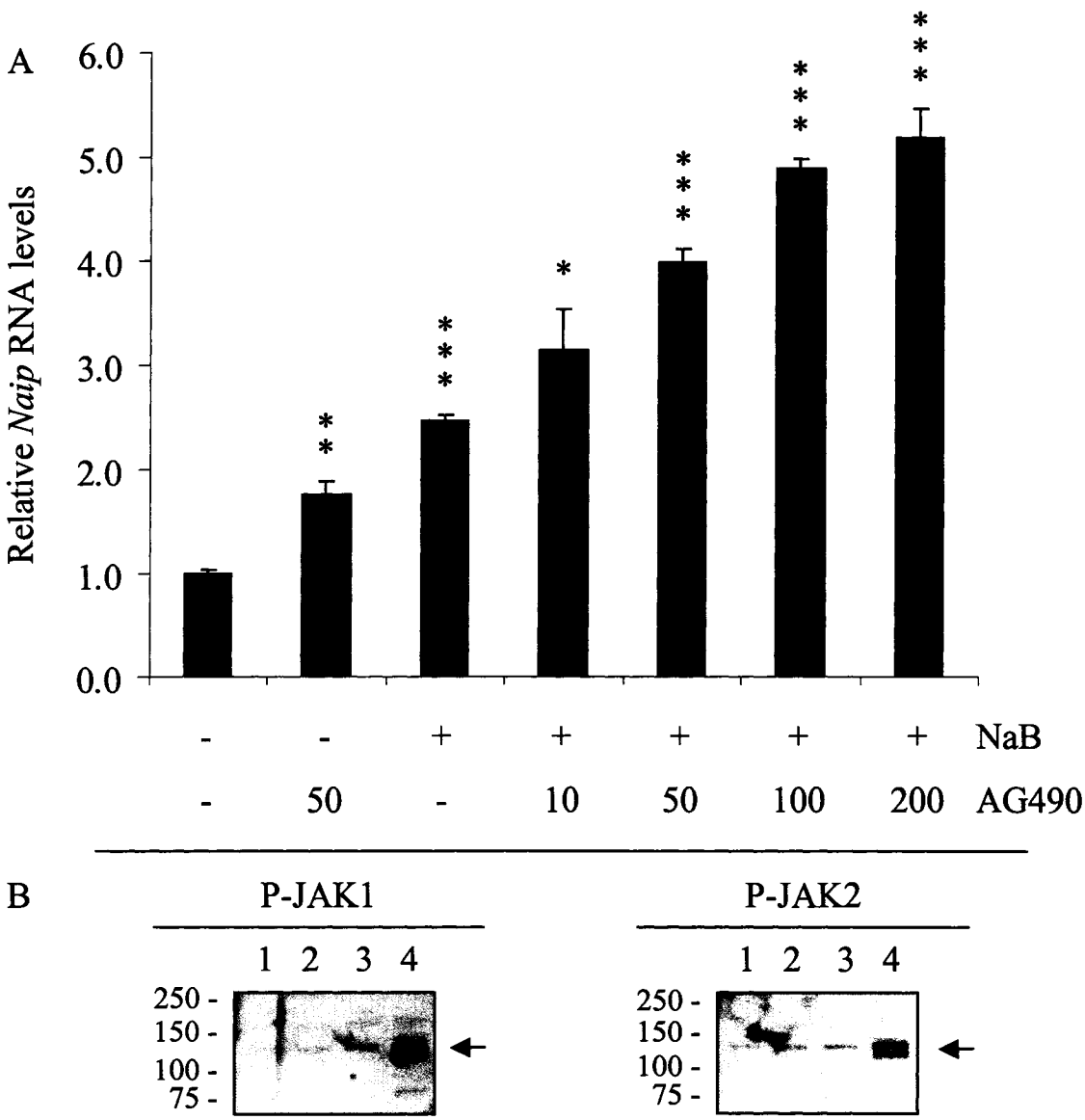
A
Relative Naip RNA levels
6.0
5.0
4.0
3.0
2.0
1.0
0.0
- - + + + + + NaB
- 50 - 10 50 100 200 AG490
B
P-JAK1
P-JAK2
1 2 3 4
250 -
150 -
100 -
75 -

Table 2-2. Kinase inhibitors and their effects on *Naip* up-regulation induced by sodium butyrate treatment.

Inhibitor	Kinases affected	NaB-induced *Naip*
AG490	JAK2	1.6
PD98059	MEK/ERK	0.8
SB203580	p38	0.8
Rp-8-cAMP	PKA	0.9
H-89	PKA	1.0
H-7	PKA, PKC, PKG	0.1

* *Naip* RNA level in cells preincubated with the kinase inhibitor followed by treatment with NaB divided by the level of *Naip* transcript in cells treated with NaB treatment alone

Panel B), it can be surmised that activation of JAK2 is not critical for NaB-induced up-regulation of *Naip* in the undifferentiated neuro-2a cell line. In contrast, the inhibition of JAK2 mediated an induction of *Naip*, as demonstrated by the AG490 results (Figure 2-3, Panel A). Because the NaB and AG490 treatments were additive, two or more separate *Naip*-inducing signaling pathways were probably involved. While it is possible that JAK2 activation following LPS-mediated signaling in macrophages may play a role in the up-regulation of *Naip5*, the inhibition of this kinase leads to the up-regulation of *Naip1* in undifferentiated neuronal-like cells. Further studies comparing and contrasting *Naip1* versus *Naip5* transcript levels could help clarify these different signaling mechanisms. However, as the NaB-dependent induction of *Naip* in neuro2A cells did not appear to be mediated through the activation of JAK2 pathway, the involvement of other kinases needed to be investigated to elucidate this compound's method of action.

Researchers demonstrated the involvement of kinases other than the JAK family in NaB signaling in the K562 chronic myeloid leukemia cell line through the use of a MEK-ERK inhibitors and monitoring the change in G-protein α-subunit, $G\alpha_{i2}$ mRNA levels (Yang *et al.*, 2001). These investigators found that when the ERK pathway was blocked, the NaB-induced increase in $G\alpha_{i2}$ levels was inhibited as was the ability of NaB to induce differentiation. The mitogen-activated protein kinases (MAPKs) have four subfamilies: the extracellular signal-regulated kinases (ERK1/MAPK1 and ERK2/MAPK2), which generally function in the control of cell division; the c-Jun NH2-terminal kinases (JNK1, JNK2 and JNK3) or stress-activated protein kinases (SAPKs)

Figure 2-4. Relative *Naip* RNA levels in neuro-2a cells following sodium butyrate treatment in the presence of either ERK or p38 MAPK family inhibitors. Following pretreatment with 20 μM PD98059 or 6 μM SB203580 and exposure to 2 mM sodium butyrate, the levels of *Naip* message were determined. Cell treatment, RNA collection and *Naip* analysis by quantitative RT-PCR were performed as described in Materials and Methods. Each value represents an average ± STD (N=3). Statistical significance with respect to the control, * $p < 0.05$ and *** $p < 0.001$ or with respect to the NaB treated cells, ‡ $p < 0.05$.

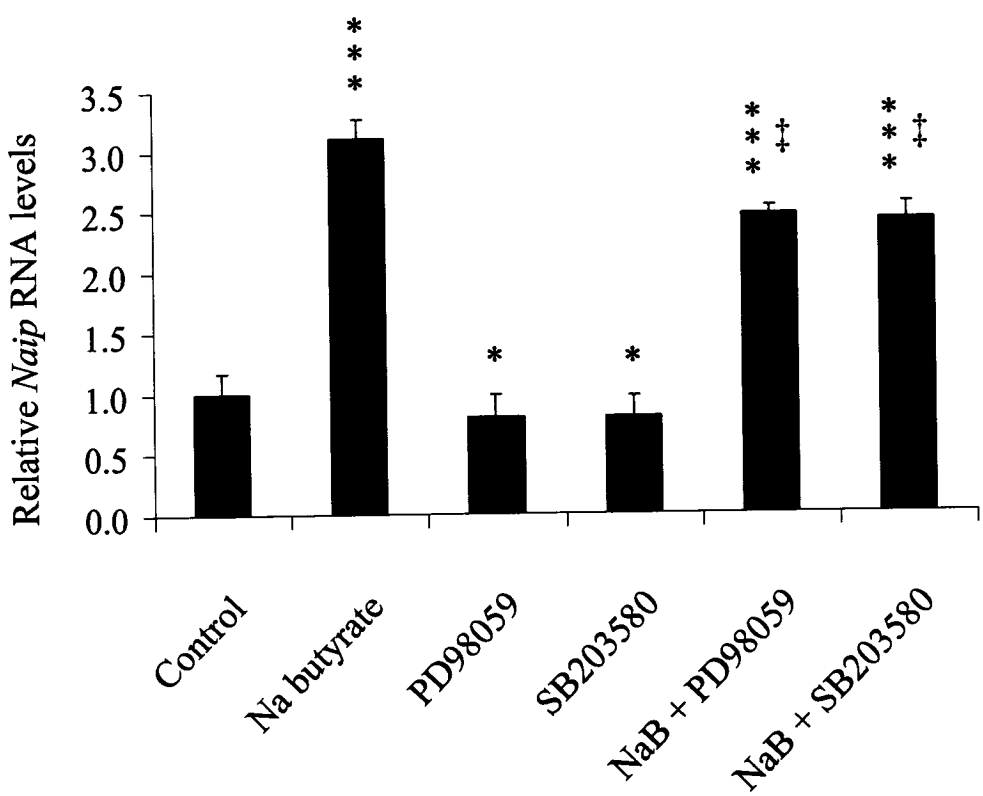
Relative *Naip* RNA levels
3.5
3.0
2.5
2.0
1.5
1.0
0.5
0.0
Control
Na butyrate
PD98059
SB203580
NaB + PD98059
NaB + SB203580

that are critical regulators of transcription; the p38 MAPKs (p38α, p38β, p38γ and p38δ) that are activated by inflammatory cytokines and environmental stresses; and the recently identified fourth kinase pathway, ERK5 (reviewed in Johnson & Lapadat, 2002). The MAPKs are phosphorylated by the MAPK kinases (MEKs, MKKs or MAP2Ks).

Given the importance of the ERK and p38 in the NaB-mediated induction of $G\alpha_{i2}$ mRNA levels in the K562 cell line, inhibitors of these kinases were examined next for effects on *Naip* up-regulation (Figure 2-4). The level of *Naip* transcript found in neuro-2a cells treated with only DMSO was set to one and used as the control. Treatment with NaB resulted in an expected 3-fold increase in transcript levels while pretreatment with PD98059, an inhibitor of ERK activation, or SB203580, an inhibitor of p38 activation, only slightly altered *Naip* from baseline levels. Likewise, combining pretreatment of the ERK and p38 inhibitors with exposure to NaB did not block the *Naip* induction mediated by the latter treatment alone. The up-regulation of *Naip* by NaB, therefore, was not dependent on either the ERK or p38 subfamily of MAPKs.

In parallel with the *Naip* mRNA level assessment, cell lysates were collected to examine the phosphorylation levels of ERK1 and 2. As can be seen in Figure 2-5 (which is an enlargement of the area above arrow #1 from Figure 2.2) the levels of the ERK family of MAPKs decreased following treatment with NaB when compared to the controls of either water or DMSO while the levels of p38 levels remained constant (Panel A). Although not a member of the MAPK family, PKCμ expression was included in these lanes and shown to decrease following NaB treatment but the significance of this finding is not known. Comparison of ERK 1 or 2 phosphorylation levels following

Figure 2-5. Western blot analyses of protein expression and phosphorylation levels of the ERK family of MAP kinases. Panel A, comparison of the protein expression levels of ERK1-3, p38 and PKCμ following cellular treatment with either water, DMSO or 2 mM sodium butyrate for 48 h. Panel B, comparison of ERK 1 or 2 phosphorylation levels following various cellular treatments. The gel was loaded as follows: Marker (1); cellular treatment with water (2); DMSO (3); 2 mM sodium butyrate (4); NaB + 20 μM PD98059 (5); NaB + 6 μM SB203580 (6); PD98059 (7) and SB203580 (8). Cell treatment and lysate preparations were performed as described in Materials and Methods. In panel A the Western blots were completed at Kinexus while those in panel B were carried out according to Materials and Methods.

A

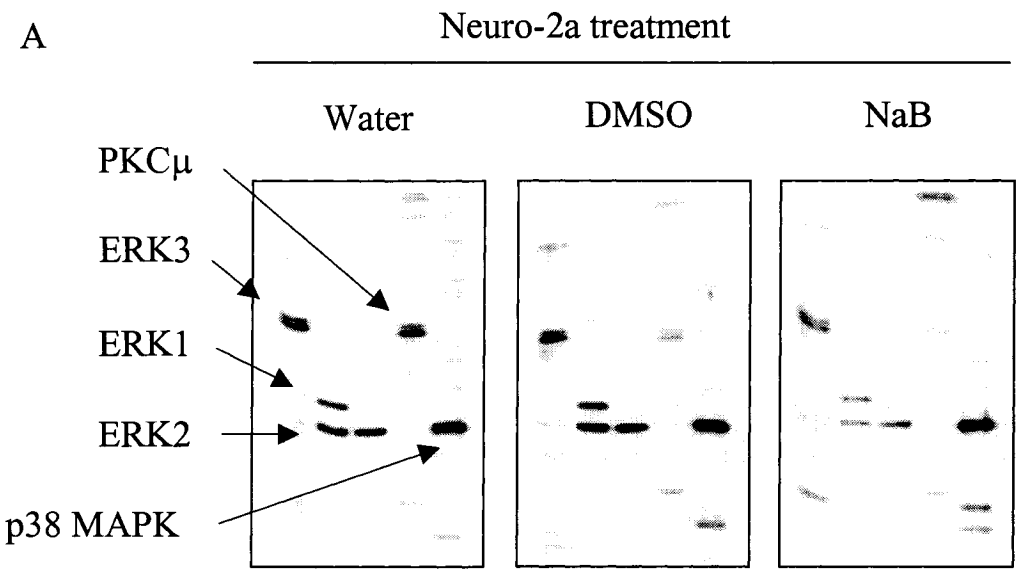
Neuro-2a treatment
Water
DMSO
NaB
PKCμ
ERK3
ERK1
ERK2
p38 MAPK

B

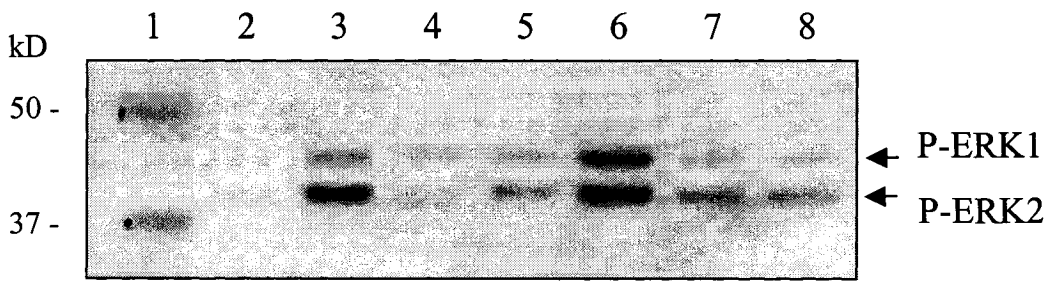
kD
1
2
3
4
5
6
7
8
50 -
37 -
P-ERK1
P-ERK2

various treatments can be seen in Panel B. No significant activation was observed following cellular treatment with water (lane 2); NaB, which was dissolved in PBS (lane 4); pretreatment with PD98059 alone (lane 7) or when followed by NaB exposure (lane 5). DMSO strongly activated this family of kinases, especially ERK2 (lane 3) but did not significantly stimulate *Naip* transcription. Pretreatment with the p38 inhibitor in combination with NaB, however, did result in activation of ERK-1 and 2 (lane 6). An activation that did not occur with either treatment alone (lanes 4 and 8) so the combined effect was probably due to cross-talk between the pathways but *Naip* levels remained unaffected. Overall the change in ERK phosphorylation status did not correlate with the *Naip* transcript level (Figure 2-4). Given that the ERK pathways are important for NaB-mediated induction of $G\alpha_{i2}$ mRNA levels in the K562 chronic myeloid leukemia cell line (Yang *et al.*, 2001), the discrepancy with the present experiment in neuro-2a may be due to cell line specificity or different signaling mechanisms responsible for the up-regulation of separate genes.

As a further indication of differences due to cell line specificity, other investigators have demonstrated that when the human colonic adenocarcinoma Caco-2 and the rat small intestinal IEC-6 cell lines were both transfected with a construct encoding the promoter region for the Na^+/H^+ *exchange 3* (*NHE3*) gene and then exposed to NaB, only in the Caco-2 cells displayed a significant expression of the reporter (Kiela *et al.*, 2001). These researchers found that two specific inhibitors of PKA, Rp-cAMPS and H-89, as well as cotransfection with a dominant-negative form of the regulatory subunit of PKA, inhibited the induction of the *NHE3* promoter by NaB (Kiela *et al.*, 2001). To determine if PKA was involved in the up-regulation of *Naip*, Rp-cAMP and H-

89 were used in the presence of NaB in the neuro-2a cell line (Figure 2-6). The level of *Naip* transcript found in those cells treated with only DMSO was set to one and used as the control. Treatment with NaB resulted in an expected 3-fold increase in transcript levels while pretreatment with Rp-8-cAMP or H-89 did not significantly alter *Naip* from baseline levels. Combining pretreatment with the PKA inhibitors and NaB exposure did not attenuate the levels of *Naip* message produced by the latter treatment alone. Despite the increase in *Naip* by cAMP on its own (Figure 2-1), the cAMP-dependent PKA was not critical in the NaB-induced up-regulation of *Naip*. These results indicated that the increase in *Naip* brought about by NaB treatment was either through a cAMP-dependent but PKA-independent pathway or that a different pathway to that of cAMP was involved.

In parallel to the mRNA experiment to evaluate PKA involvement in *Naip* induction, cell lysates samples were collected to analyze the activation of the cAMP response element (CRE)-binding protein (CREB). PKA, ERK, Ca^{2+}/calmodulin-dependent protein kinases (CaMKs), Ribosomal S6 kinases (S6K/RSKs) and stress signaling can result in the phosphorylation of the transcription factor CREB, which then activates downstream target genes through CRE (reviewed in Shaywitz & Greenberg, 1999). In order to examine whether or not activation of this important transcription factor occurred following NaB treatment in neuro-2a cells, Western blot analyses were performed on cell lysates (Figure 2-7). Interestingly, even though NaB treatment was shown to mediate a 2.5-fold increase in *Naip* transcription over those cells exposed to DMSO, both of these cell lysates displayed CREB phosphorylation. This result indicated either a lack of correlation between CREB activation and NaB-induced up-regulation of *Naip* or a more complicated regulatory mechanism.

Figure 2-6. Relative *Naip* RNA levels in neuro-2a cells following sodium butyrate treatment in the presence of PKA inhibitors. Following pretreatment with 200 μM Rp-8-cAMP or 0.5 μM H-89 and exposure to 2 mM sodium butyrate, the levels of *Naip* message were determined. Cell treatment, RNA collection and *Naip* analysis by quantitative RT-PCR were performed as described in Materials and Methods. Each value represents an average ± STD (N=3). Statistical significance with respect to the control, *** $p < 0.001$.

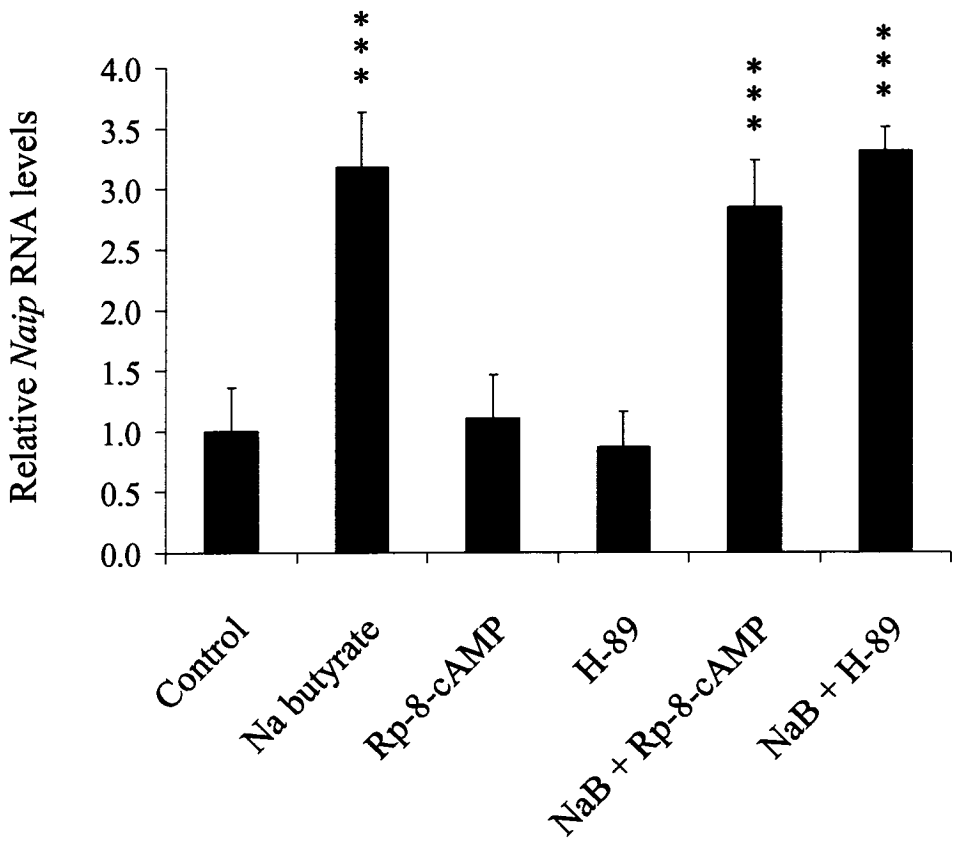
Relative *Naip* RNA levels
4.0
3.5
3.0
2.5
2.0
1.5
1.0
0.5
0.0
****
****
****
Control
Na butyrate
Rp-8-cAMP
H-89
NaB + Rp-8-cAMP
NaB + H-89

Figure 2-7. Western blot analyses of the phosphorylation levels of CREB. Comparison of CREB phosphorylation levels following cellular treatment with water, DMSO or 2 mM sodium butyrate. For the loading control the membrane was stripped and re-probed with anti-CREB (bottom panel). Cell treatment, lysate preparations and Western blotting were performed as described in Materials and Methods.

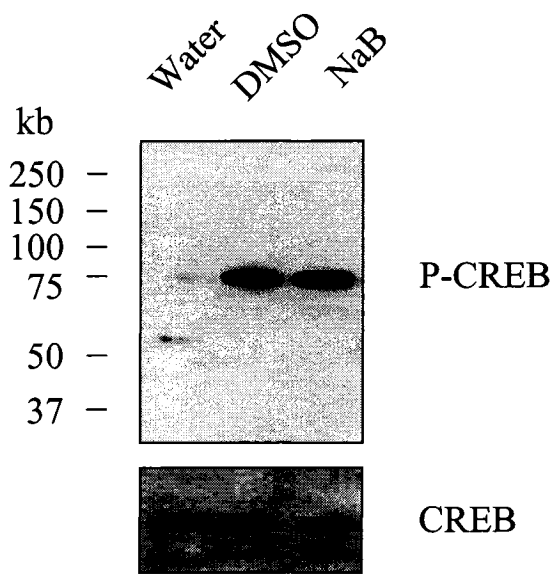
Water
DMSO
NaB
kb
250
150
100
75
50
37
P-CREB
CREB

Because CREB can be activated by diverse stimuli, the regulation of distinct programs of gene expression and specificity is mediated by a number of phosphorylation sites and associated proteins (Shaywitz & Greenberg, 1999). It is worth noting that the *Naip* promoter contains CREB recognition sites (N. Gendron and A. MacKenzie, unpublished observation) and thus, the role of CREB activation in the up-regulation of *Naip* by NaB may be best determined by technologies such as dominant negative mutants. Alternatively, it may be valuable to examine additional kinases that are known to phosphorylate CREB and that were elevated in the Kinexus screen, such as RSK and CMKII.

As specific kinase inhibitors did not result in an attenuation of NaB-induced *Naip* up-regulation, a broader kinase inhibitor was tested. The investigators who demonstrated the induction of *NHE3* by NaB, not only modulated this activity by specific PKA inhibitors but also demonstrated an effect through the use of H-7, a broader kinase inhibitor (Kiela *et al.*, 2001). Because the isoquinoline derivative H-7 can inhibit protein kinases A, C and G within the low micromolar range (reviewed in Ono-Saito *et al.*, 1999), it would be interesting to determine if NaB mediates signaling in neuro-2a cells through either PKC or PKG, as inhibition of PKA was previously determined not to affect *Naip* up-regulation (Figure 2-6). Interestingly, other researchers demonstrated that pre-treatment of macrophages with H-7 reduced the Stat1 phosphorylation at Ser727 resulting from bacterial infection or treatment with either LPS or interferon-γ (IFN-γ) (Kovarik *et al.*, 1998) and recent data has data has implicated a PKC isoform in this phenomenon (Deb *et al.*, 2003). As *Naip* can be induced by the incubation of murine

macrophages with *Legionella*, it is intriguing to consider that this up-regulation might be mediated through an H-7 sensitive pathway.

The broad based serine-threonine kinase inhibitor H-7 was, therefore, assessed for an effect on NaB-induced *Naip* up-regulation in neuro-2a cells (Figure 2-8). A value of one was assigned to those cells treated with only water while those treated with NaB gave an expected 2.3-fold increase in the level of *Naip* transcript. Interestingly, pretreatment with H-7 lowered *Naip*'s basal expression to half of the control level and furthermore, completely blocked the induction brought about by NaB. As a role for PKA in this phenomenon was not supported by Rp-8-cAMP and H-89 experiments (Figure 2-6), the other kinases through which the H-7 inhibitor acts, PKC and/or PKG, become likely candidates. Further experimentation to elucidate the roles of these kinases is being conducted in our laboratory.

In summary, NaB was shown to induce a two- to three-fold increase of the *Naip* transcript level in the mouse neuroblastoma neuro-2a cell line. Pre-incubation with the JAK2 inhibitor AG490 demonstrated an increase in *Naip* induction that was additive with the NaB treatment. Activation of CREB was noted with NaB but further examination of the *Naip* promoter is required as well down-regulation of this transcription factor to determine its importance. Additional analysis of the *Naip* promoter would also allow for the assessment of the importance of the GC box located at -335 from the putative transcriptional initiation site (Xu *et al.*, 2002) since the action of NaB can be mediated through Sp1/Sp3 GC boxes, such as for $p21^{Waf1/Cip1}$ (reviewed in Davie, 2003). And finally, the attenuation of NaB-induced *Naip* up-regulation by H-7 provides an opportunity to investigate the role of non-PKA kinases that are inhibited by this

isoquinoline derivative in this phenomenon. The further elucidation of signaling pathways for *Naip* looks promising and will hopefully develop additional biologic insight and, possibly, prospects for therapeutic invention.

Figure 2-8. Relative *Naip* RNA levels in neuro-2a cells following sodium butyrate treatment in the presence of a broad based serine-threonine kinase inhibitor. Following pretreatment with 60 μM H-7 and exposure to 2 mM sodium butyrate, the levels of *Naip* message were determined. Cell treatment, RNA collection and *Naip* analysis by quantitative RT-PCR were performed as described in Materials and Methods. Each value represents an average ± STD (N=3). Statistical significance with respect to the control, *** $p < 0.001$ or with respect to the NaB treated cells, ‡‡‡ $p < 0.001$.

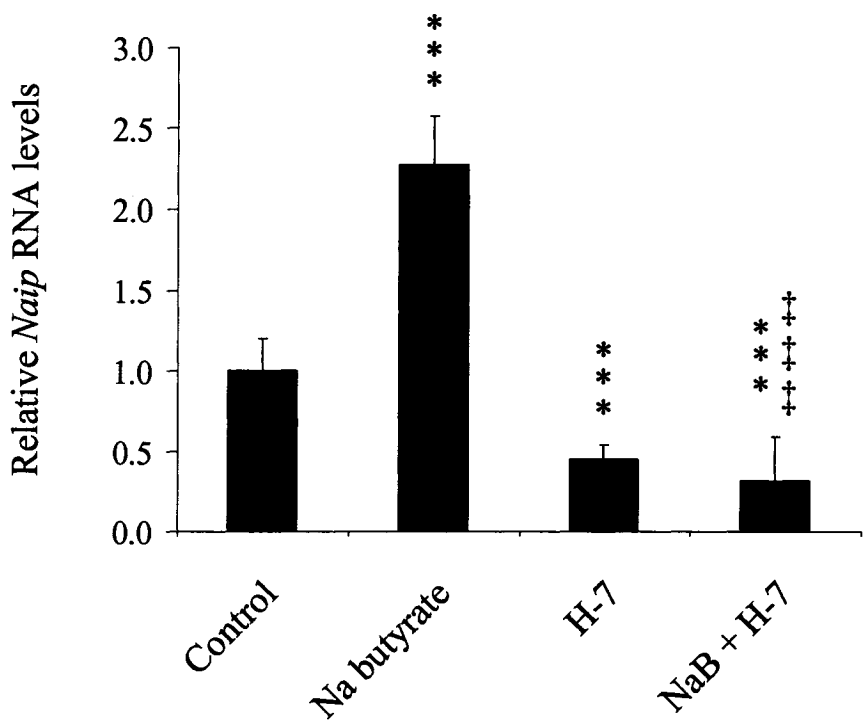
Relative *Naip* RNA levels
3.0
2.5
2.0
1.5
1.0
0.5
0.0
***
***
***
†††
Control
Na butyrate
H-7
NaB + H-7

DISCUSSION, CHAPTER TWO

As a method of delaying cell death under severe stress, the induction of pro-survival genes could be viewed as providing enough protection to allow the situation to be resolved and for any damage to be repaired. However, apoptosis can occur if an unfavourable condition (such as serum withdrawal) continues beyond a threshold level. Overexpression of *NAIPΔ14-17* has been shown to suppress cell death mediated by serum withdrawal (Liston *et al.*, 1996) and the present study has demonstrated that endogenous *Naip* was induced in those cells that survived this type of deprivation. Because of the harshness of this treatment, however, individual inducers were chosen to dissect the molecular mechanisms that mediate the up-regulation of *Naip*.

In order to elucidate the signaling pathways involved in the up-regulation of *Naip* transcription, experimental treatments were based on the scientific literature and the results were examined for any similarities or differences. *Naip* was induced by genistein, a soy isoflavone known to inhibit tyrosine kinases, but not by the inactive isoform daidzein, which indicated that kinases and phosphatases were most likely required for the modulation of *Naip* transcript levels. Genistein has been found to bind and activate the G-coupled adenosine A1 receptors, triggering a number of signaling pathways (reviewed in Jacobson *et al.*, 2002). These receptors have been reported to act through phosphoinositide 3-kinase (PI3K), Akt/protein kinase B (Akt/PKB), tyrosine kinases, protein kinase C (PKC), and MAPK signaling cascades (Jacobson *et al.*, 2002). Further examination of these individual pathways, however, would be necessary to determine which ones were specifically involved in the genistein-induced up-regulation of *Naip*.

Although NaB was chosen for these studies, it was interesting to note that while the cAMP analogs and NaB both resulted in an up-regulation of *Naip*, the former are best known as inducers of PKA, while in contrast, the latter was shown to be independent of PKA. Clearly, a PKA-independent *Naip*-inducing pathway exists but whether the up-regulation mediated by NaB is a cAMP-dependent pathway was not apparent and would have to be examined further. Likewise, it needs to be determined if the cAMP-induction of *Naip* was dependent on PKA. Combining cAMP with NaB to see if their effects are additive or using the PKA inhibitors with cAMP treatment would shed more light on this issue.

Despite not yet having been identified in mammals, cAMP receptors (cARs) have been well characterized in the amoeba *Dictyostelium discoideum,* which expresses four different cARs during its development into a multicellular organism (reviewed in Bankir *et al.*, 2002). cARs belong to the superfamily of seven transmembrane domain G protein-coupled receptors that mediate increases in cGMP and inositol 1,4,5-trisphosphate (IP_3) production, as well as the recruitment of the pleckstrin homology domain-containing Akt/PKB and cytosolic regulator of adenylyl cyclase (CRAC). In addition, the activation of these receptors mediates a dramatic rise in the proportion of polymerized actin followed by the phosphorylation of myosin I and II and leads to a transient influx of calcium (Bankir *et al.*, 2002). Further examination of transduction through these various pathways might lead to an increased understanding of how cAMP analogs induce *Naip* transcription.

The receptors for NaB and other short chained fatty acids (SCFAs) have now been identified in humans as other G protein-coupled receptors (GPR), GPR41 and

GPR43 (Brown *et al.*, 2003; Le Poul *et al.*, 2003; Nilsson *et al.*, 2003; Senga *et al.*, 2003). Murine M1 myeloid leukemia cells that differentiate into macrophages upon stimulation with leukemia inhibitory factor (LIF) or interleukin-6 (IL-6) mediate the up-regulation of a leukocyte-specific STAT-induced GPR (LSSIG), which is an orthologue to the human GPR43 (Senga *et al.*, 2003). In this cell line, LIF and IL-6 bind gp130 activating the JAK/STAT pathway, through STAT3 and/or STAT5 to induce *LSSIG/GPR43* expression. Although many possibilities exist, the additive *Naip* up-regulation observed with NaB and AG490 may be mediated by an increase of NaB receptors on neuro-2a cells as a means to compensate for the JAK2 inhibition. Because this class of receptors has tissue-specific expression patterns (Brown *et al.*, 2003; Nilsson *et al.*, 2003), the prevalence of the GPR41/43 receptors in the neuro-2a cell line needs to be determined experimentally.

Although the specific receptor activations have yet to be investigated, the examination of kinase expression changes following exposure of the cells to NaB treatment revealed an increase in the inhibitor of NF-κB kinase alpha (IKKα) (Table 2-1). This observation takes on significance given that XIAP has been shown to be a strong stimulator of NF-κB (Hofer-Warbinek *et al.*, 2000) and, in a positive feedback loop, can be up-regulated by NF-κB (Stehlik *et al.*, 1998b). The inhibitory subunits (IκBα, IκBβ and IκBε) prevent NF-κB translocation to the nucleus, and thus, the activation of NF-κB requires the phosphorylation and dissociation of IκB, which is mediated by IKK-α and IKK-β. It has been demonstrated that XIAP and/or TAK1 can stimulate IKKβ kinase activity and that TAK1 interacts with NIK, a kinase upstream of both IKKs. (Hofer-Warbinek *et al.*, 2000). Although other reports have indicated that the XIAP-induced

upregulation of NF-κB is independent of TAK1 (Birkey Reffey *et al.*, 2001). An interaction between with NAIP and TAK1 has also been demonstrated (Sanna *et al.*, 2002) and consequently the *Naip* up-regulation may lie upstream of and contribute to NF-κB induction. Conversely, it also possible that *Naip* is downstream of NF-κB as this transcription factor was found to be important for the PMA-induced up-regulation of human *NAIP* in Jurkat cells (Busuttil *et al.*, 2002).

NF-κB can be induced by a number of pathways, including through the activation of several G-protein coupled receptors (reviewed in Ye, 2001) and by NaB treatment (Mayo *et al.*, 2003). The induction of diverse biological functions mediated by the heterotrimeric G-proteins can be accomplished through varying complexes of the 18 α, 12 β, and 5 γ subunits (Ye, 2001). Investigators have found that SCFAs may activate the G_i, G_q, and G_{12} subunits (Brown *et al.*, 2003), which can contribute to the activation and/or transactivation of NF-κB. Although the exact signaling mechanisms involved in the NaB-induced up-regulation of *Naip* need to be explored further, other investigators have implicated a PI3K/Akt-dependent manner in NF-κB activation (Mayo *et al.*, 2003).

In conclusion, analyses employing a series of kinase inhibitors demonstrated that NaB-induced *Naip* up-regulation in neuro-2a cells was not dependent upon ERK1/2, p38 or PKA. A small but significant reduction in the *Naip* transcript level was detected in the presence of MAPK inhibitors for ERK1/2 and p38 but these compounds did not block the *Naip* induction caused by NaB. Treatment with the broad-based kinase inhibitor H-7, however, did result in a complete attenuation of NaB-induced *Naip* up-regulation. As PKA involvement was ruled out with this treatment, these results implicate either PKC or PKG in the induction of *Naip*, which needs to be clarified by further experimentation. As

both PKC and PKG can be activated in a PI3K-dependent manner, it can be assumed that PI3K is involved in NaB-induced *Naip* up-regulation, similar to NaB-induced NF-κB transcriptional activity. Whether this is the case and whether Naip is up- or downstream of NF-κB activation needs to be determined experimentally.

To bring this work to publication, it would be valuable to differentiate the NaB-mediated HDAC inhibitor activity from the phosphorylation activity, similar to an approach used by other investigators in the examination of $p21^{WAF1/CIP1}$ transcription (Kobayashi *et al.*, 2004). These researchers first used a chromatin immunoprecipation assay to observe the acetylation of H3 and H4 in a time course following NaB treatment and then noted which transcription factors were recruited to the promoter during that time. Although NaB is well known to inhibit HDAC and cause hyperacetylation of histones, the authors observed no change in p300, CBP, or HDAC1 association with the promoter region of the $p21^{WAF1/CIP1}$ gene (Kobayashi *et al.*, 2004). Because binding of these factors was not affected by NaB, the investigators aimed to examine the role of phosphorylation to influence association between the $p21^{WAF1/CIP1}$ promoter and total acetylated histone H3 and H4. A similar approach would be useful with the *Naip* gene to determine the time course for histone acetylation and the transcription factors involved.

An examination of the promoter region for the murine *Naip* genes would allow the identification of potential transcription factors that may be affected by NaB. A cursory inspection of the 5'-flanking region of the murine *Naip1* gene (Accession # AF242432) indicates seven putative Sp1 sites and one NF-κB site on the sense strand with a log-likelihood score above 12 using Transcription Element Search Software (TESS) (Schug & Overton, 1998). The Sp1 binding site has been defined as the butyrate

response element (Davie, 2003). The NF-κB site is in close proximity to one of the Sp1 sites and is a good candidate to allow for synergy between the two transcription factors (Majello *et al.*, 1994).

In the *p21*$^{WAF1/CIP1}$ study (Kobayashi *et al.*, 2004), the kinase inhibitor H-7 suppressed mRNA in both the absence and presence of NaB without influencing the butyrate-induced hyperacetylation of H3 and H4 associated with the *p21*$^{WAF1/CIP1}$ promoter. In addition, the induction of *p21*$^{WAF1/CIP1}$ transcription by the phosphatase inhibitor okadaic acid, in the absence of changes in association of acetylated histones with the promoter, provided further evidence of the importance of phosphorylation to *p21*$^{WAF1/CIP1}$ transcription. As hyperacetylation of histones by NaB was not sufficient to increase *p21*$^{WAF1/CIP1}$ mRNA levels and there were no changes in the phosphorylation, dual modification, or methylation of histone H3, the investigators plan to examine which kinase is responsible for the induction of the *p21*$^{WAF1/CIP1}$ gene by NaB (Kobayashi *et al.*, 2004).

For the *Naip1* gene, it would be valuable to examine the level of NaB-induced acetylated histones in the presence and absence of H-7 and okadaic acid to evaluate the roles acetylation and phosphorylation play. Assuming that phosphorylation is important, and as H-7 is known to inhibit PKA, PKG and PKC (Ono-Saito *et al.*, 1999) it would be valuable to assess these kinases. In the present study, PKA did not attenuate the NaB-induced *Naip* up-regulation (Figure 2-6) so an increase in the concentration of the H-89 inhibitor could be used to test for the role of PKG. If PKG was found not to play a

significant role, then the various PKC isozyme inhibitors, peptides and anti-sense oligonucleotides could be evaluated (Way *et al.*, 2000).

In the $p21^{WAF1/CIP1}$ study, the investigators did not evaluate the phosphorylation levels of Sp1 itself (Kobayashi *et al.*, 2004). The ever-growing list of kinases that phosphorylate Sp1 now includes DNA-PK, PKA, PKC-ζ, casein kinase II, ERK, cyclin-dependent kinase, and others identified by only molecular weight and kinase activity (Chu & Ferro, 2005). Furthermore, several groups have found that okadaic acid increases the level of Sp1 · phosphorylation suggesting that the steady state levels of Sp1 phosphorylation are suppressed by the protein phosphatases (Chu & Ferro, 2005). For the Naip study, it would be interesting to test the phosphorylation levels of Sp1 to see if this transcription factor can also be affected by the kinase inibitor H-7. If it is, then PKC-ζ, would be a good candidate to assess. For the future Naip studies it would also be valuable to use $p21^{WAF1/CIP1}$ probes in the quantitative RT-PCR as a positive control. Primers and probe sequences for TaqMan have previously been established for murine $p21^{WAF1/CIP1}$ (Burns *et al.*, 2001).

RESULTS, CHAPTER THREE

The ability to up-regulate NAIP and its corresponding cytoprotection mark preliminary stages in exploring options of therapeutic intervention to prevent unwanted programmed cell death. To further understand the role NAIP plays in the suppression of apoptosis, other proteins with which it interacts in the cellular environment need to be identified. The IAP subfamily of BIRC proteins all inhibit apoptosis and block caspases-3, -7 and/or -9, yet can also possess distinct differences (reviewed in Liston *et al.*, 2003). cIAP-1 and -2 bind tumor necrosis factor receptor associated factor 1 (TRAF1) or TRAF2, forming part of a protein complex that is located on the cytoplasmic tail of TNFα receptor 2 (Rothe *et al.*, 1995). Survivin plays a unique role through its association with chromatin structures and expression during the G_2/M transition in the cell cycle (Li *et al.*, 1998) while Livin also seems to be localized primarily in the nucleus but not with a particular structure (Kasof & Gomes, 2001). It is likely, therefore, that NAIP interacts with a subset of proteins that are distinct from other IAP interactions, especially given the unique aspects of NAIP structure.

Hippocalcin, a member of a neuron-specific family of calcium binding proteins, interacts with the BIR3 domain of NAIP as shown by yeast two-hybrid and a human fetal brain library (Mercer *et al.*, 2000). While the investigators found a synergistic protection against calcium-induced apoptosis conferred by these two proteins, no defined role has yet been ascribed to hippocalcin. Ulevitch's group found that NAIP-BIR123 and XIAP bind to TAK1, a MAP3 kinase that activates JNK1 and p38 in response to transforming growth factor β1 (TGF-β1) (Sanna *et al.*, 2002). These two studies are the only published

investigations into NAIP's protein-protein interactions, other than direct binding with the caspases. We thus undertook an effort to identify additional protein-binding partners in an effort to find other potential therapeutic targets and to increase our understanding of NAIP's function. In this regard, it is important to note that, out of the 1404 amino acids that compose NAIP, the most cytoprotective section identified thus far is the 100 amino acids encompassing the third BIR domain (Maier *et al.*, 2002). Interestingly, in the same study, our group also found that NBIR3 was not as proficient as NBIR2 at the inhibition of caspases-3 or -7. These observations raised the questions of whether NBIR3 also inhibited caspase-9 or, if an intermediary protein enhanced NBIR3's cytoprotection, did hippocalcin, TAK1 or unidentified partners play a role.

To identify protein-binding partners for the most cytoprotective region of NAIP, a plasmid construct expressing GST-NBIR3 was generated, the protein produced in *E. coli* and purified (Figure 3-1). With increasing time after induction by IPTG, a protein band at the expected size of 43 kD can be seen developing in intensity within the bacterial cell lysates that were separated on 4-15% polyacrylamide gels and then visualized with Coomassie blue (lanes 3-7). After the bacterial lysates were incubated with glutathione-sepharose beads, washed and eluted, a single band can be seen for the purified GST-NBIR3 (lane 8). Following dialysis to remove the excess glutathione, the purified protein was ready to be used for protein-protein interaction experiments.

The BIR3 domains of XIAP, c-IAP1, c-IAP2 (Bratton *et al.*, 2001; Deveraux *et al.*, 1998) and the single BIR domains of Livin (Vucic *et al.*, 2000) and Ts-IAP (Richter *et al.*, 2001) have been demonstrated to bind and inhibit caspase-9 (reviewed in Liston *et al.*, 2003). Activation of the intrinsic apoptosis pathway triggers the formation of an

Figure 3-1. Production and purification of GST-NBIR3 fusion protein. Coomassie stained 4-15% gels. *E. coli* previously transformed with a construct expressing GST-NBIR3 were grown overnight and used to inoculate a larger culture. Once an OD of 1 was reached, a sample of the culture was taken and IPTG was added to the remainder for a final concentration of 3 mM. Protein production continued for five hours with samples taken every hour. The culture was centrifuged and the pellet was frozen at -70 °C until purification could take place. Lane (1), MW marker; (2) pre-induction bacterial lysate; (3) one hour post-induction; (4) two hours; (5) three hours; (6) four hours; (7) five hours; (8) purified GST-NBIR3; (9) MW marker. Purification of GST-NBIR3 and PAGE were performed as described in Materials and Methods.

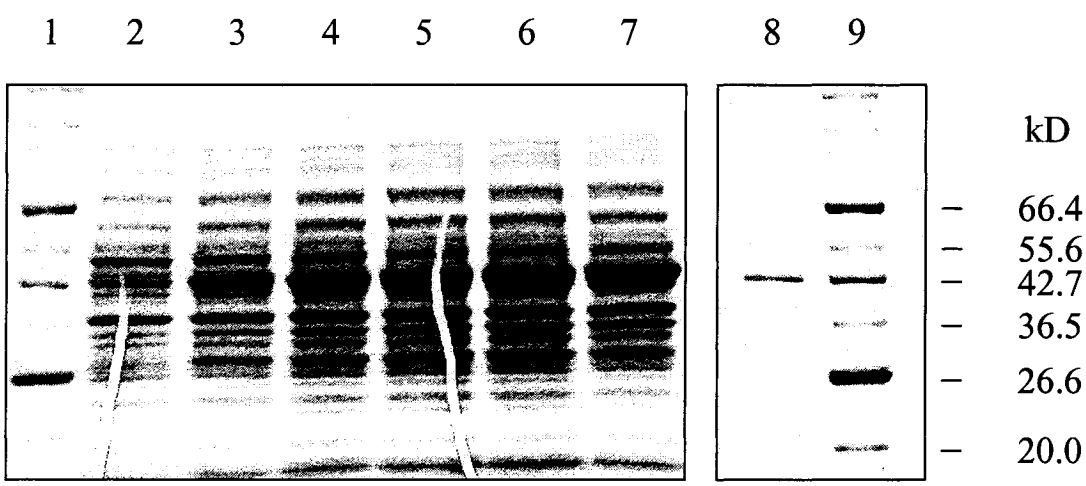
1
2
3
4
5
6
7
8
9
kD
66.4
55.6
42.7
36.5
26.6
20.0

"apoptosome" complex consisting of capase-9, Apoptosis Protease Activating Factor-1 (Apaf-1), ATP and cytochrome *c*. (reviewed in Degterev *et al.*, 2003). Caspase-9 appears to be distinct from the effector caspases in that the binding to Apaf-1 leads to a conformational change and results in capase-9 becoming catalytically active, rather than being proteolytic cleaved (Degterev *et al.*, 2003; Liston *et al.*, 2003). As an initiator caspase, activated caspase-9 can proteolytically process caspase-3 in addition to a self-cleavage within the linker region between the large and small subunits at Asp_{315}. Through crystal structure analyses, it has been demonstrated that the XIAP BIR3 (XBIR3) domain directly engages caspase-9 by binding to the exposed amino terminus of the processed caspase-9 linker within a conserved surface groove. Additional contacts with caspase-9 occur with helix α5 and the linker sequence between helices α3 and α4 of XBIR3 packing closely against the hydrophobic surface of caspase-9 (Shiozaki *et al.*, 2003). The authors speculate that XBIR3 can sequester caspase-9 in a monomeric state through these interactions and trap the active site loops in a non-catalytic, inactive conformation, thus leading to its inhibition. Because the other IAPs that possess three BIR domains were able inhibit caspase-9, it was logical to assume that NBIR3 could as well.

To determine if NBIR3 was able to inhibit capase-9 as had been determined for c-IAP1, c-IAP2 and XIAP, an *in vitro* colorimetric assay with recombinant caspase-9 and purified GST-NBIR3 was performed (Figure 3-2). Although it was not clear why the initial enzymatic activity of capase-9 was greater in the presence of GST-NBIR3 for the first 30 minutes of the experiment, it can be seen that in the absence of GST-NBIR3 (black) there was more cleavage of the LEHD-pNA substrate after 90 minutes than in the

Figure 3-2. Inhibition of caspase-9 by the third BIR domain of NAIP. An *in vitro* colorimetric assay showing that in the absence of GST-NBIR3 (black) there is more enzymatic cleavage of the LEHD-pNA substrate after 90 minutes than in the presence of GST-NBIR3 (red). GST-NBIR3 purification and the caspase-9 assay were performed as described in Materials and Methods. The values represent the average of two experiments with a maximum variation between the two of 0.01 absorbance units at any given time point.

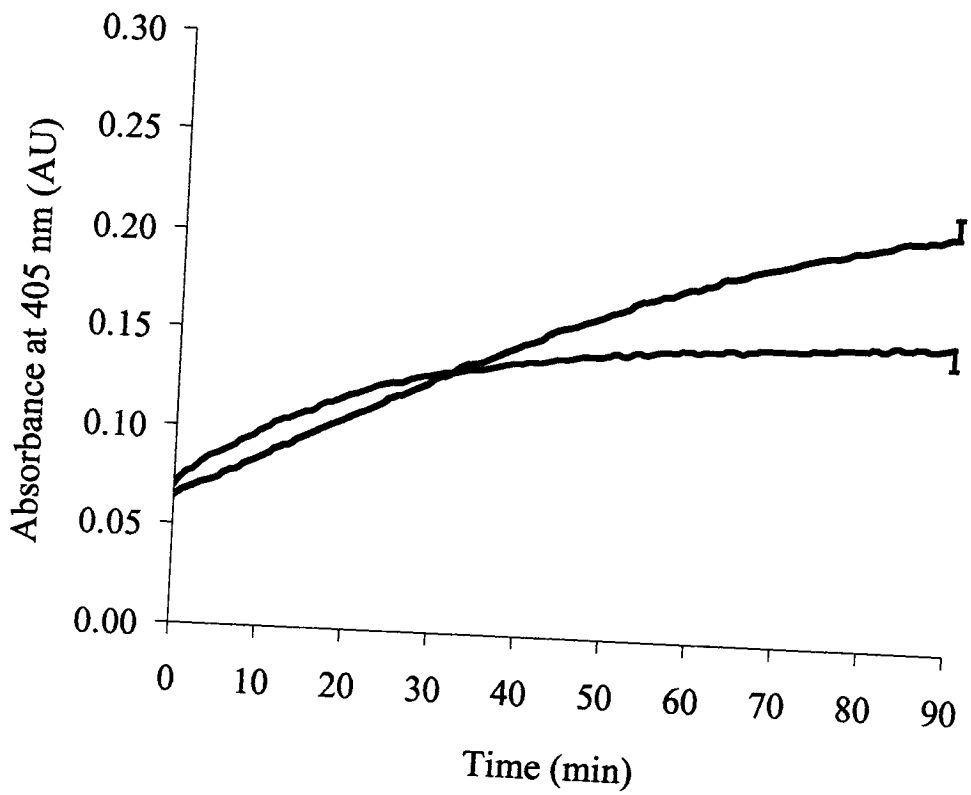
0.30
0.25
0.20
0.15
0.10
0.05
0.00
Absorbance at 405 nm (AU)
0
10
20
30
40
50
60
70
80
90
Time (min)

presence of GST-NBIR3 (red). Given that caspase-9 was inhibited by GST-NBIR3 and not by GST alone (data not shown), we concluded that a direct inhibition of caspase-9 was mediated by the third BIR of NAIP. Having documented inhibition of caspase-9 by NAIP I next assessed NAIP interaction with Smac.

Smac resides in the mitochondria of healthy cells, but following an apoptotic, stress is released into the cytosol where it is able to prevent and/or reverse IAP inhibition of caspases (reviewed in Verhagen & Vaux, 2002). Interestingly, Smac is synthesized as a precursor, trafficked to the mitochrondria and loses its signaling peptide upon import (Du *et al.*, 2000; Verhagen *et al.*, 2000). The newly exposed N-terminus is principally responsible for its interactions with the IAPs once it is released into the cytosol. Co-crystalization of Smac and XBIR3 established that the new amino-terminal tetrapeptide sequence of Smac (AVPI) fits within a surface groove of the XBIR3 domain (Wu *et al.*, 2000), whereas the caspase-9 (A_{316}TPF) sequence was found to fit in the same groove (Shiozaki *et al.*, 2003), suggesting that Smac competes for and/or displaces XIAP from caspase-9. Similar tetrapeptides have been found in the *Drosophila* proteins Reaper, Hid, Grim, Sickle and Jafrac2, as well as the human proteins Omi, GSPT1 and Chk1, and these short consensus sequences have been termed IAP-binding motifs (IBMs) (reviewed in Liston *et al.*, 2003; Salvesen & Duckett, 2002). This emerging IBM consensus appears to reflect a common mechanism in which specific proteins can interact with the BIR domains to antagonize IAP function. The NBIR3 mediated inhibition of caspase-9 *in vitro* suggests that the ATPF sequence of caspase-9 and/or the AVPI sequence of Smac can interact with NBIR3 in a manner similar to that of XBIR3.

To evaluate the binding between NBIR3 and a Smac-based peptide, Surface Plasmon Resonance (SPR) was chosen as these biosensors provide several advantages in the analysis of protein interactions when compared to other sensors (reviewed in Yuk & Ha, 2005). The principal benefits for the use SPR spectroscopy include the real-time measurement of biomolecular interactions without labeling and with a simple optical system device. In the present study, a ten amino acid peptide based on the N-terminus of processed Smac (AVPIAQKSEP) was synthesized with a biotin tag for use in a plasmon resonance binding experiment. Once the peptide was bound to the plasmon resonance chips through a streptavidin interaction (solid phase), increasing concentrations of GST (data not shown), GST-XIAP (Figure 3-3, Panel A) and GST-NBIR3 (Panel B) in solution were used as the analyte (mobile phase).

In the initial part of each the curve, from 100s to 275s, there was an increase in optical response with an increase in time that reflected binding between GST-BIR3 and biotin-labeled peptides while the mobile phase flowed over the solid phase. As the concentration of GST-BIR3 increased, from the bottom of each panel towards the top, there was an increased change in optical response, which indicated increase binding with more analyte present. Once the flow of GST-BIR3 was stopped at 275s, the optical response decreased with time and thus the remaining part of the curve reflected dissociation. The equilibrium dissociation constants (K_D) were found to be 24 nM for GST-XBIR3 and 52 nM for GST-NBIR3 (Figure 3-3), 140 nM for GST-NBIR2 (data not shown). GST alone did not display binding.

As determined by fluorescence polarization-based competition assays using a Smac-based peptide, the K_D for XBIR3 was found to range between 430 nM (Liu *et al.*, 2000)

and 810 nM (Srinivasula *et al.*, 2001). These are approximately 20 to 40 times the value of 24 nM found in this experiment. These disparate results could be explained by deviations from simple pseudo-first order binding curves and potential matrix contributions to transport limitation of the analyte (reviewed in Schuck, 1997). While the sources of discrepancy need to be further explored to determine the accuracy of the K_D value calculated, the SPR technique can still be used successfully to demonstrate interactions between macromolecules and ranking of different binding partners. The published and experimental K_D's for XBIR3-Smac-based peptide interactions are similar, suggesting that SPR is a reliable method that demonstrates NBIR3 also interacts with this IBM.

Given that NBIR3 binds the Smac-based peptide, full-length Smac was tested next in a pull-down study due to crystal structure analyses showing that Smac recognizes XBIR3 on two interfaces (Wu *et al.*, 2000). First, the N-terminal four residues in mature Smac (AVPI) bind a surface groove on XBIR3 formed by the strand β3, the helix α3 and the intervening loop. Two of the four residues, Val2 and Pro3, form a short anti-parallel β-strand with the three-stranded β-sheet of XBIR3. Second, the H2 and H3 helices in Smac contact the XBIR3 residues surrounding the helix α1. The authors speculate, however, that compared to the binding of the Smac N-terminal tetrapeptide to the surface groove on BIR3, this second interface may play a minor role, given that N-terminal deletion mutants of Smac failed to bind XBIR3 (Wu *et al.*, 2000).

To test binding of NBIR3 with processed Smac, purified GST-BIR3 fusion proteins were used in pull-down study with a ubiquitin-Smac-HA-tagged fusion construct (Figure 3-4). Our colleagues generated this unique construct to bypass the mitochondrial

Figure 3-3. GST-XBIR3 and -NBIR3 binding of a Smac-based peptide as determined by surface plasmon resonance. Panel A, concentrations of XBIR3 used were as follows: 5.7, 11.4, 17.2, 22.9, 34.3, 57.2 and 114 nM from the bottom curve to the top. Panel B, concentrations of NBIR3 used were as follows: 12.4, 24.8, 49.6, 74.5, 89.3, 124 and 186 nM from the bottom curve to the top. The Smac-based peptide synthesized for the binding study had the following sequence: AVPIAQKSEP-biotin. Peptides generated from the cleavage of caspase-6 were also generated to contain a biotin label at their C-terminus. Streptavidin was bound to the chip, followed by the addition of the biotin-labelled peptides. GST-fusion proteins were then flowed over the chips at differing concentrations to see if a change in the electrical response would indicate binding to the peptides. The binding experiments took place in the laboratory of Dr. R. MacKenzie at the NRC.

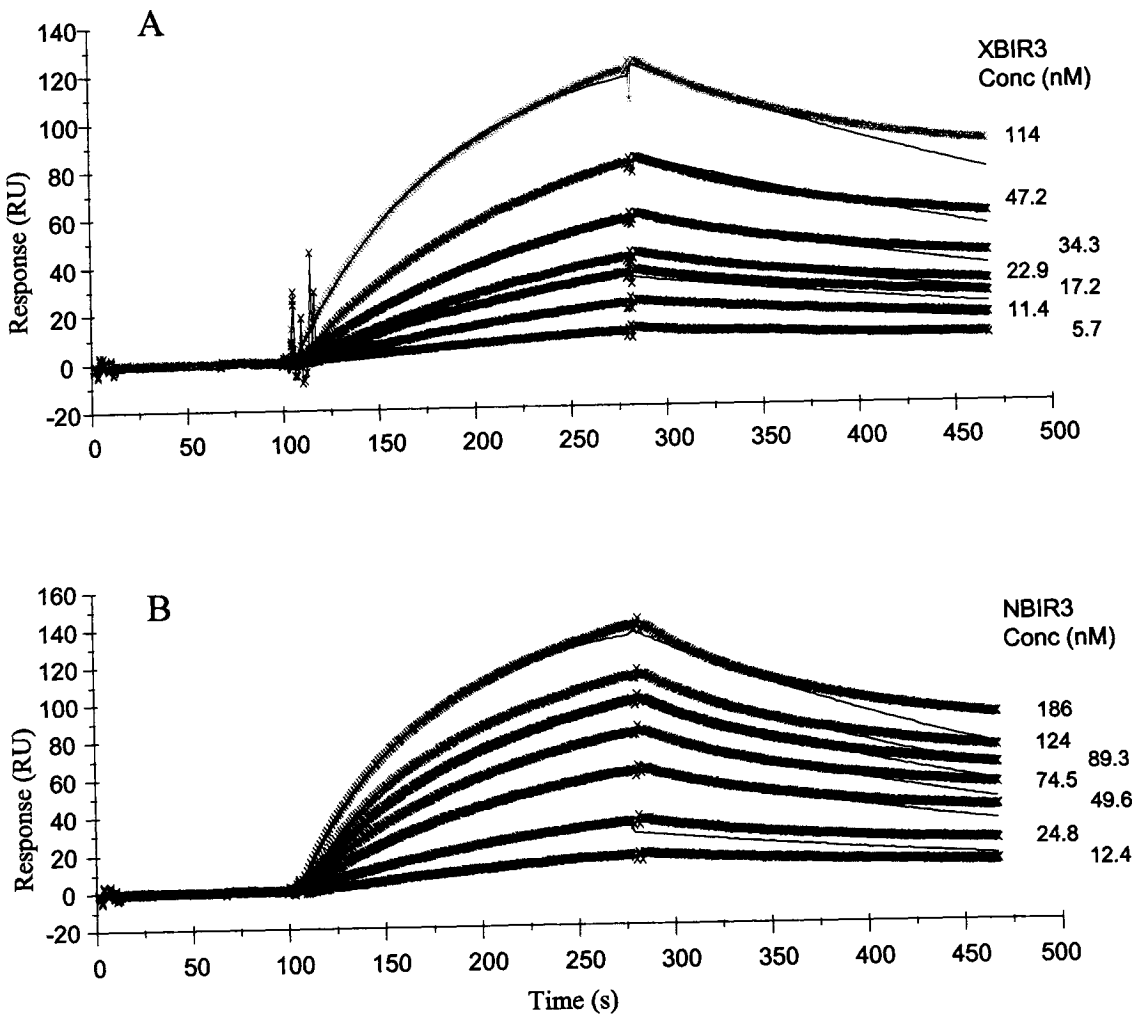
A
XBIR3
Conc (nM)
114
47.2
34.3
22.9
17.2
11.4
5.7
Response (RU)
140
120
100
80
60
40
20
0
-20
0
50
100
150
200
250
300
350
400
450
500
B
NBIR3
Conc (nM)
186
124
89.3
74.5
49.6
24.8
12.4
Response (RU)
160
140
120
100
80
60
40
20
0
-20
0
50
100
150
200
250
300
350
400
450
500
Time (s)

requirement for Smac processing by developing a fusion protein that would be cleaved by endogenous ubiquitin-specific proteases yielding processed, cytosolic Smac with the correct AVPI amino terminus (Hunter *et al.*, 2003). The purified GST-NBIR3 can be seen on the Coomassie stained 4-15% gel as a distinct band around 43 kD with a fainter band representing cleaved GST around 26 kD (lane 2). In this experiment, GST-NBIR3$_L$ (amino acids 231 to 392), in lane 2, and GST-NBIR3$_S$ (amino acids 252 to 353) were used to have more than one independent sample for testing. The pull-down with GST-NBIR3 and cell lysate containing the processed HA-Smac did not show a detectable interaction. The HA-Smac can be seen in the transfected cells in lane 11. When a substantially lower quantity of cell lysate was incubated with GST-XBIR3, an interaction with Smac could be clearly detected (lane 12). This positive control indicated that the technique was working properly but that GST-NBIR3 was not interacting with the processed Smac protein. Further studies are required to elucidate the reasons underlying the discrepancy between the pull-down, which did not show binding, and the SPR experiment that demonstrated a concentration-dependent interaction between NBIR3 and a Smac-based peptide.

NBIR3's failure to bind mature Smac suggests the possibility of additional functional differences. It is possible, therefore, that NBIR3 interacts with unique Smac-equivalents. In designing a search for such an equivalent ligand, it was important to consider that many IAP-protein interactions require proteolytic processing (i.e. Smac, omi/HtrA2, caspase-3/7/9) and, thus would be overlooked using yeast two-hybrid. Phage-display on the other hand may be more informative and has been successfully used to identify peptide sequences that bind Livin and XIAP (Franklin *et al.*, 2003).

Figure 3-4. GST-BIR3 pull-downs with HA-Smac. Coomassie stained 4-15% gel (1) MW marker; (2) purified GST-NBIR3. Western blot showing Smac-transfected cell lysates used in a pull-down experiment with GST-tagged constructs. 1 mg of lysate was incubated with 10 μg of fusion protein bound to glutathione sepharose beads. The proteins that remained associated to the beads following a series of washes were separated on a 4-15% gel and transferred to PVDF. The Western blot was then probed with anti-HA. The following lanes indicate pull-downs with GST fusion protein and either Smac-transfected or untransfected cell lysates (3) NBIR3L-Smac; (4) NBIR3S-Smac; (5) GST-Smac; (6) NBIR3L-untransfected; (7) NBIR3S-untransfected; (8) GST-untransfected; (9) MW marker. Cell lysates showing over-expression of (10) HA-Smac or (11) untransfected. (12) Positive control pull-down of 200 μg Smac-transfected lysate with 10 μg of GST-XBIR3 fusion protein. Production of GST-fusion proteins, transfection of cells, pull-down experiments, PAGE and Western blotting were all performed as described in Materials and Methods.

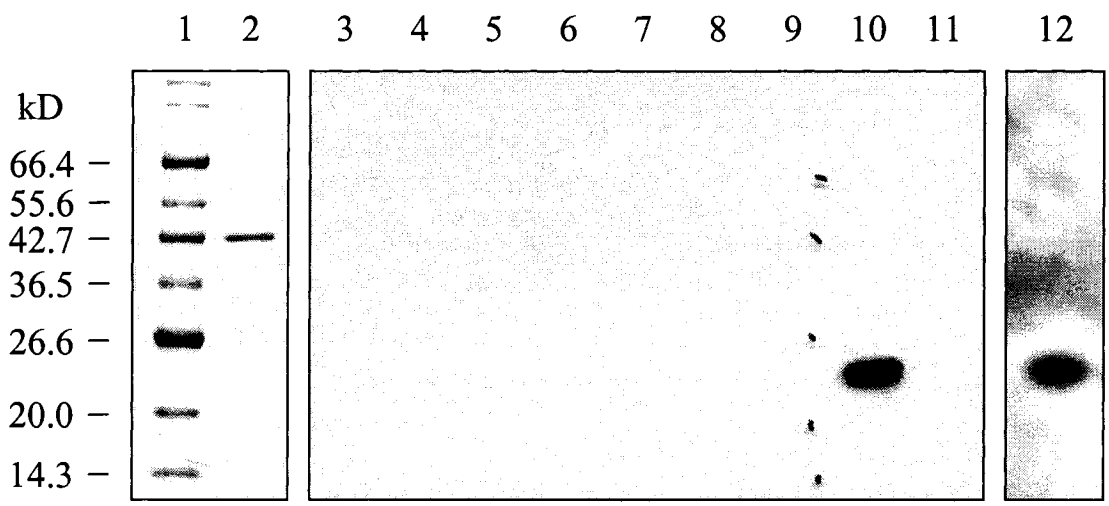
1 2 3 4 5 6 7 8 9 10 11 12
kD
66.4
55.6
42.7
36.5
26.6
20.0
14.3

The second BIR domain of XIAP (XBIR2) was found to bind the sequence CEFESC through phage display (Tamm *et al.*, 2003). The EFES motif occurs in caspase-3 and is located within a loop that is important in the binding of BIR2 to caspases-3 and -7. Furthermore, this motif was found to mimic the XIAP-binding site within specific caspases insofar as binding of the peptide to XIAP was inhibited by preincubation with caspase-3 and -7 but not -9. Binding was also specific to XBIR2 and not of the other IAP members, such as c-IAP1, c-IAP2, NAIP or Survivin (Tamm *et al.*, 2003). The use of phage display allowed these researchers to identify an interaction that could be seen with full-length proteins and thus was considered an option for NBIR3 interaction studies.

Purified GST-NBIR3 was incubated with a phage display library and following four successive pannings, a series of amino acid sequences that bound NBIR3 were identified (Figure 3-5). Of the 14 phage plaques that were sequenced from the fourth pan, half represented the amino acid heptapeptide of FHENWPS. Other similar sequences of FHEAWPQ and FHESWPR were each present once, leading to a proposed hexapeptide binding consensus sequence of FHEXWP, where X represents any non-charged amino acid. The other two peptides, HYPIYNI and SHALSNS, found at an abundance of 4/14 and 1/14 respectively, do not seem to resemble the consensus sequence described above. A BLAST search (Altschul *et al.*, 1997) was used to identify human proteins that possess the FHEXWP consensus sequence or a portion of it and thus can be considered potential NAIP binding partners (Table 3 and Appendix 1).

TRABID was chosen as the initial candidate to test for NBIR3 binding due to its ability to interact with the TNF-receptor-associated factor 6 (TRAF6) (Evans *et al.*, 2001). TRAFs have emerged as the major signal transducers for the TNF receptor superfamily

and the interleukin-1 receptor/Toll-like receptor (IL-1R/TLR) superfamily and lack of TRAF6 leads to defective signaling by IL-1 and IL-18 as well as hypo-responsiveness to bacterial lipopolysaccharides (LPS), the cell wall component of Gram-negative bacteria (Lomaga *et al.*, 1999). Signal amplification by TRAF6 involves the activation of multiple kinase cascades including IκB Kinase (IKK), MAP kinases and Src-family tyrosine kinases. The activation of both IKK and MAP kinases by TRAF6 appears to involve the MAP3K, TAK1 (Wu & Arron, 2003). As mentioned earlier, other investigators found through coimmunoprecipitation studies that NAIP's BIR123 and XIAP bound to TAK1 (Sanna *et al.*, 2002) and our colleagues discovered that not only was Naip protein expression in macrophages increased following *Legionella pneumophila* infection (Diez *et al.*, 2000) but that the mouse Naip5 gene was responsible for resistance to this Gram-negative bacteria (Diez *et al.*, 2003). Connecting the interaction of NAIP and TAK1 to the binding of TRABID and TRAF6 would increase our understanding of the signaling pathways in LPS responsiveness and perhaps provide a key to NAIP's role in the susceptibility to Legionnaire's disease.

To investigate a potential interaction between TRABID and NAIP, lysates from cells transiently transfected with a construct expressing HA-tagged TRABID were used for a pull-down experiment with GST-BIR fusion proteins and analyzed by Western blot (Figure 3-6). Unfortunately, no apparent interaction between the BIR domains of NAIP and the TRABID protein could be detected using this method. Successful transfection of the cells with the construct expressing HA-tagged TRABID can be seen in lane 6 as a band of the expected size, near the 83 kD marker, was present in a sample of the cell lysate. As our laboratory did not have constructs expressing either TAK1 or hippocalcin,

Figure 3-5. Amino acid sequences that bind NBIR3. Panning of a phage display library resulted in the identification a series of amino acid sequences that bind GST-NBIR3. The ratios on the right of the panel indicate the occurrence of that particular amino acid series within the clones sequenced from the fourth pan. The abbreviations for amino acids are as follows: P - Proline (Pro), A - Alanine (Ala), L - Leucine (Leu), I - Isoleucine (Ile), F - Phenylalanine (Phe), Y - Tyrosine (Tyr), W - Tryptophan (Trp), H - Histidine (His), R - Arginine (Arg), Q - Glutamine (Gln), N - Asparagine (Asn), E - Glutamic Acid (Glu), and S - Serine (Ser). Purification of GST-NBIR3, panning of the phage display library, amplification and sequencing were performed according to the Materials and Methods. Data shown is for the fourth round of panning the phage library.

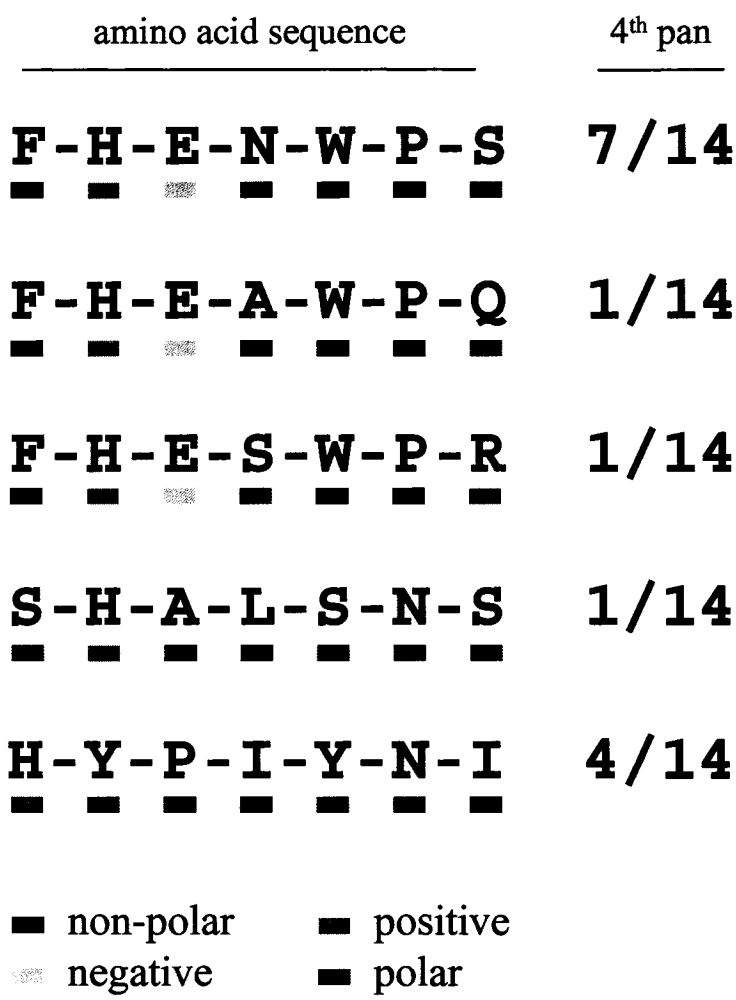
amino acid sequence
4th pan
F-H-E-N-W-P-S
7/14
F-H-E-A-W-P-Q
1/14
F-H-E-S-W-P-R
1/14
S-H-A-L-S-N-S
1/14
H-Y-P-I-Y-N-I
4/14
non-polar
positive
negative
polar

Table 3-1. Known human proteins containing all or a portion of the FHEXWP NBIR3-binding consensus sequence.

Accession #	Protein name	Sequence	Starts at aa	Size (aa #)
NP_000395	galactosidase, beta 1	FHEPWP	88	677
Q9UPN3	Microtubule-actin crosslinking factor 1, isoforms 1/2/3 (Actin cross-linking family protein 7) (Macrophin 1) (Trabeculin-alpha) (620 kDa actin-binding protein) (ABP620)	FHEAW	4598	5430
NP_258261	ATP-binding cassette, sub-family C, member 10; multidrug resistance-associated protein 7	FHEAW	355	1464
NP_056993	neuroblastoma-amplified protein NAG	HEAWPE	1618	2371
NP_057340	N-acetylglucosamine-1-phosphodiester alpha-N-acetylglucosaminidase (NAGPA)	HESWP	61	515
BAA13103.1	Y6 encoding protein	ENWPS	198	290
AAB19187.1	truncated pancreatic polypeptide receptor PP2	ENWPS	198	290
NP_060050.1	TRABID protein; TRAF-binding domain protein	ENWPS	16	708
NP_060555	Importin 9	EAWPQ	142	1041
AAQ98858	transducer of regulated CREB protein 3 (TORC3)	ESWPR	134	619

there was no positive control for a NAIP binding protein. Previous experiments using GST-XIAP with HA-Smac demonstrated that the technique was successfully employed but could not determine if GST-NBIR3 was functioning properly. A pull-down in parallel with either TAK1 or hippocalcin would help confirm whether or not there is an interaction between TRABID and NBIR3.

In summary, NBIR3 has now been shown to inhibit caspase-9, making it a member of the third BIR domain group of XIAP, c-IAP1 and c-IAP-2 in their ability to suppress the activity of this enzyme (Bratton *et al.*, 2001; Deveraux *et al.*, 1998). It is interesting to note that NBIR3 was found to bind a Smac-based peptide in a concentration-dependent manner and with similar characteristics to XBIR3, yet an interaction with the mature Smac protein could not be demonstrated. This result suggests that NAIP might be better than XIAP in protecting against an apoptotic death involving caspase-9 as Smac would not be able to antagonize its activity. As most experimental data collected by our group and others do not show this, other explanations need to be explored, such as additional binding proteins and self-association, as well as other methods of testing the interaction between NBIR3 and Smac. In the hunt for a unique IBM for NBIR3 through phage display, a potential binding sequence was determined to be FHEXWP. Although there was no detectable interaction between NBIR3 and TRABID, the first protein containing this sequence to be tested, it does not eliminate the possibility that the others could bind NBIR3 or that processing might be required for the interaction to take place. While the search for additional binding proteins continues, further exploration of the similarities and differences among the IAPs will aid endeavors into therapeutic intervention and the suppression of unwanted apoptosis.

Figure 3-6. Pull-down experiment with HA-TRABID. Western blot showing TRABID-transfected cell lysates used in a pull-down experiment with GST-tagged constructs. 1 mg of lysate was incubated with 10 μg of fusion protein bound to glutathione sepharose beads. The proteins that remained associated to the beads following a series of washes were separated on a 4-15% gel and transferred to PVDF. The Western blot was then probed with anti-HA. The following lanes indicate pull-downs with GST fusion protein and TRABID-transfected cell lysates (1) N123; (2) NBIR3L; (3) NBIR3S; and (4) GST. Cell lysates showing (5) no transfection or (6) over-expression of HA-TRABID. (7) MW marker. The following lanes indicate pull-downs with GST fusion protein and untransfected cell lysates: (8) N123; (9) NBIR3L (10) NBIR3S (11) GST. Production of GST-fusion proteins, transfection of cells, pull-down experiments, PAGE and Western blotting were all performed as described in Materials and Methods.

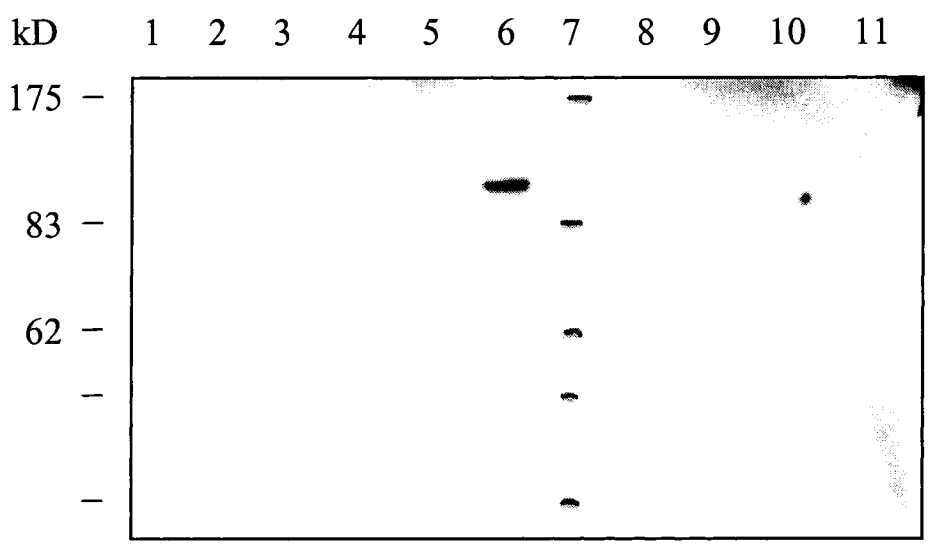
kD
1
2
3
4
5
6
7
8
9
10
11
175
83
62

DISCUSSION, CHAPTER THREE

Caspase-9 was inhibited by NBIR3. As XIAP, cIAP-1 and cIAP-2 have been shown to bind and inhibit this enzyme it was logical to assume that the third BIR of NAIP would as well. It is now established that polypeptides incorporating the second BIR domain and the immediate NH_2 linker region for these four IAP can inhibit caspase-3 and -7. Our group is in the process of establishing inhibition constants for NBIR3 and testing the suppression of caspase-9 with NAIP constructs of varying length. This inhibition curve marks the initial stage of studying the interaction between NAIP and caspase-9.

In the present study XBIR3 interaction with a Smac-based peptide was 2×10^{-8} M. This was approximately 100 times stronger than the interaction of XBIR3 with the processed Smac protein but 100 times weaker than linker_XBIR2-3 region, as determined by a recently published report (Huang *et al.*, 2003); the K_D appeared to vary with the amino acids of XIAP tested.

Binding between Smac and the BIR domains of NAIP was shown for the first time with the present study. NBIR3 (231-392) bound a Smac-based peptide with a K_D of 5×10^{-8} M for NBIR3 while NBIR2 (154-255) bound the same peptide with a K_D of 1.4×10^{-7} M. Surprisingly, it was not possible to demonstrate co-immunoprecipitation between GST-NBIR3 and processed Smac (present study) or when both proteins were expressed in eukaryotes (Davoodi *et al.*, 2004). The lack of association between NBIR3 and the processed Smac protein seems to indicate the binding is not as strong as with the peptide. Additional studies using SPR to compare and contrast the peptide and protein binding characteristics with each of the IAPs would be useful.

Table 3-2. SPR Biosensor measurements of a Smac-based peptide and Smac[1] interactions with GST-NAIP and -XIAP fusion proteins.

Chip	Analyte (GST fusions)	k_{on} (1/Ms)	k_{off} (1/s)	K_D (M)
AVPIAQKSEP -biotin	NBIR2 (154-255)	8.5×10^{4}	1.2×10^{-2}	1.4×10^{-7}
	NBIR3 (231-392)	6.3×10^{4}	3.3×10^{-3}	5.2×10^{-8}
	XBIR3 (238-356)	1.0×10^{5}	2.5×10^{-3}	2.4×10^{-8}
Smac[1]	linker_XBIR2 (124-240)	7.4×10^{5}	0.531	7.2×10^{-7}
	XBIR1 (1-135)			NB
	XBIR2 (156-240)	ND	ND	9.7×10^{-7}
	XBIR3 (252-356)	5.5×10^{4}	0.237	4.4×10^{-6}
	linker_XBIR2-3 (124-356)	7.0×10^{6}	2.2×10^{-3}	3.2×10^{-10}
	linker (124-158)			NB

[1] Values determined by the Wu laboratory (Huang *et al.*, 2003). NB, no binding; ND, not determined

As an initial step to finding unique partners of NAIP, recombinant GST-NBIR3 was isolated from the bacterial cultures and used to screen a phage display library. The majority of peptides that NBIR3 bound in the 4th round of panning contained a consensus sequence with 5 out of 7 amino acids conserved (FHEXWP). In the analysis of the BLAST-generated list of proteins in the human genome that contain these amino acids (Table 3-1 and Appendix A), no obvious family of proteins was identified nor any of the proteins NAIP or other IAPs was known to bind. Even though there were proteins that contained more of the NBIR3-binding consensus sequence, TRABID was chosen as the initial full-length candidate to test for binding because of its involvement in TNFα signaling. Although binding was not shown by a pull-down study, it does not rule out the other candidates in the list as possible binding partners for NAIP. Through the employment of other tools such as transient transfections for both proteins in an eukaryote system or confocal microscopy further testing could be verified.

The modulation of NAIP as an anti-apoptotic protein may prove useful for the suppression of apoptosis in neurodegenerative diseases. Furthermore, this inhibition of apoptosis can be conferred in some systems by NBIR3 alone. The discovery of IBMs has highlighted the possibility that not only cellular proteins but also oligopeptides based on these proteins can be used as modulators of IAP activities. Thus, it is possible that both the oligopeptides identified by phage display in this study and proteins containing these sequences may affect suppression of apoptosis mediated by NAIP. In the hunt for therapeutic targets, the identification of partners containing this binding motif becomes of clear interest. Whether these binding partners actually lead to a useful therapeutic target for intervention in neurodegenerative diseases will be determined later, but expanding the

overall knowledge of the signaling pathways for the IAPs will be valuable to the scientific community.

In order to bring this chapter to publication, it would be valuable to use surface plasmon resonance to test additional NAIP constructs binding to caspases-7 and -9 and to IAP antagonists. As other investigators have found that both the second and third BIR domains of XIAP are required for antagonism by Smac (Huang *et al.*, 2003) it would be useful to look at equivalent regions for NAIP. Both GST-fusion and mammalian expression constructs of the following regions of NAIP should to be generated if they do not already exist (see also Figure 3-7):

1) NBIR1
2) NBIR2
3) NBIR3
4) NBIR123
5) NBIR12
6) NBIR23
7) NBIR1-Linker A
8) N-Linker A - BIR2
9) N-Linker A - BIR23
10) NBIR2-linker B

Using SPR, the isolated GST-fusion proteins corresponding to the above-mentioned regions of NAIP would then be tested for binding with caspase-7, caspase-9 and Smac. As reconstituted *in vitro* caspase-9 activity assays did not demonstrate a Smac-mediated antagonism of GST-NAIP fusion proteins it could prove beneficial to utilize an intact cell caspase activity assay system similar to (Wilkinson *et al.*, 2004). Cells should be transfected with constructs expressing NAIP, Smac and/or with a control DNA. Following incubation, the cells should be challenged with Bax to determine cell survival, caspase-3 processing and caspase-3 activity. It will be interesting to determine whether or

not in this cellular system NBIR3 can be antagonized by Smac. It is anticipated based on the SPR study, that an interaction should occur (Figure 3-3) but based on the pull-down studies (Figure 3-4) and published results from our laboratory (Davoodi *et al.*, 2004), there may be an interaction but not be antagonism.

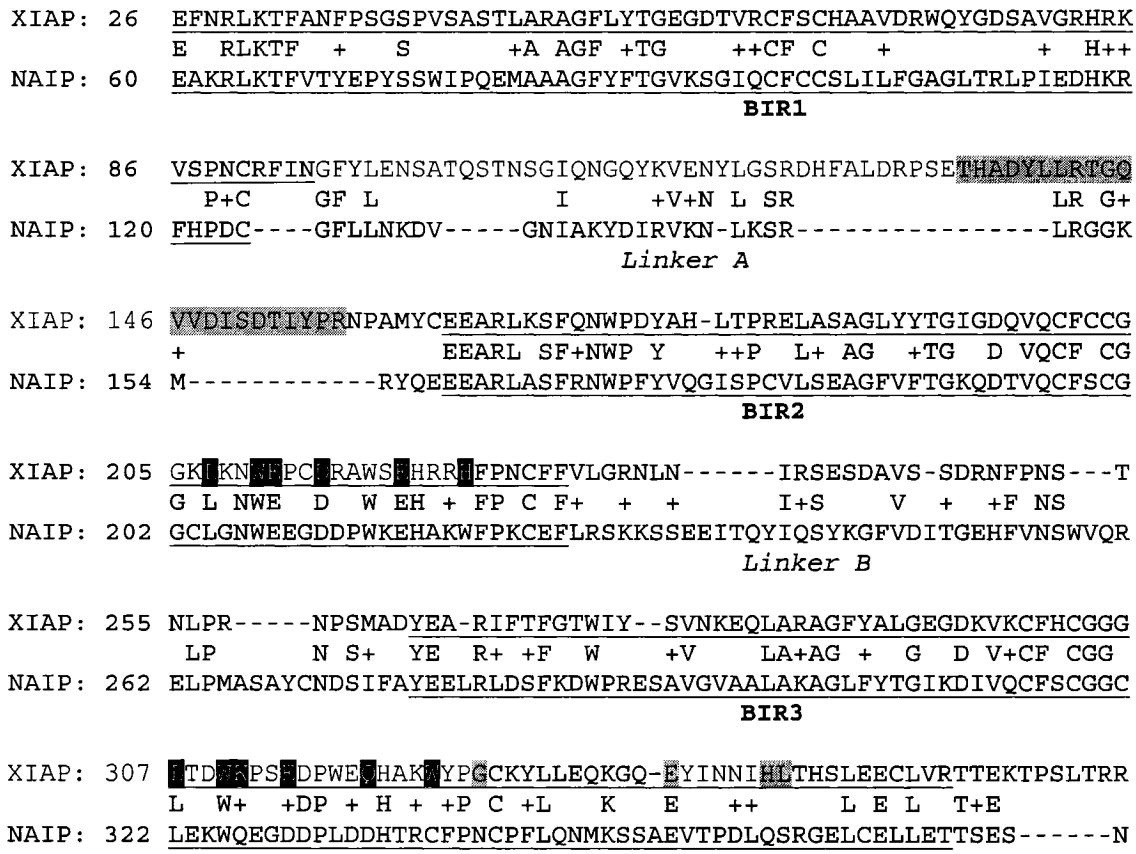

Figure 3-7. Alignment of BIR1 to BIR3 motifs from XIAP and NAIP. Identical residues are shown between the two sequences. XIAP residues making inhibitory interactions with either caspase -3/-7 or caspase-9 are shaded *gray*. Residues within XIAP BIR3 that directly interact with Smac (and the equivalent residues within BIR2 that are predicted to contribute to Smac binding) are *white* with a *black* background.

FINAL DISCUSSION

Although it was the first human IAP to be discovered, the complete biochemical characterization of NAIP has remained elusive. Difficulties with aggregation, solubility and its larger size (Davoodi *et al.*, 2004; Maier *et al.*, 2002) make it more challenging to study than other IAP family members, such as XIAP. While the suppression of apoptosis has been established for truncated portions of NAIP (reviewed in Liston *et al.*, 2003), cytoprotection mediated by the full-length human protein was not reported until this study, demonstrating the need for further studies of this member of the IAP family.

In the first part of this project, stable cells were established with an inducible construct for the selective overexpression of NAIP to assess the suppression of apoptosis provided by the full-length protein and to explore relevant cytoprotective mechanisms. The combined effects of trophic factors and adenoviral-mediated *NAIPΔE14/17* overexpression were used to determine if sufficiently divergent signaling pathways allow for an additive or synergistic suppression of apoptosis.

In the second part, the signaling pathways controlling *Naip* expression in neuronal cells were investigated. Following high-throughput screening analyses that identified compounds resulting in the up-regulation of murine *Naip1* transcription levels in a neuroblastoma cell line, sodium butyrate was chosen as an inducer. Using inhibition of specific kinases known to be affected by sodium butyrate and monitoring the transcript level of *Naip1*, signaling pathways involved in the sodium butyrate induced up-regulation of *Naip1* have been outlined.

In the third section, the mechanisms through which NBIR3 may mediate the suppression of apoptosis, such as through the inhibition of caspase-9; possible antagonists of NBIR3, such as Smac; and potential novel binding partners, were investigated. As it is known that NBIR3 mediates cytoprotection yet is less effective at inhibiting caspase-3/7 activity than NBIR2, it is now recognized that NBIR3 can inhibit caspase-9, similar to the third BIR domain of XIAP (Davoodi *et al.*, 2004). Through phage display library screening, pull-down studies and surface plasmon resonance analyses, potential binding partners of NBIR3 were identified.

By increasing our awareness of signaling pathways through which *NAIP* transcription is up-regulated and through which this protein mediates suppression of apoptosis, our understanding of its biochemical characteristics has been enhanced by this study and could lead to therapeutic interventions for diseases in which apoptosis is dysregulated.

Our laboratory previously determined a 40% increase in survival of HeLa cells transiently transfected with a construct expressing NBIR3, or all three BIR domains of NAIP, and then exposed to etoposide (Maier *et al.*, 2002). In the present study, through the use of transient transfection of HeLa cells, it was shown that cells overexpressing a full-length human NAIP construct displayed a 24% survival increase over those cells expressing the control vector. The lower survival rate mediated by the full-length construct, when compared to NBIR3, was likely due to a self-association event (Davoodi *et al.*, 2004). The development of cell lines stably expressing the full-length protein proceeded for the examination of NAIP cytoprotective role.

After successful demonstration of increased expression of full-length NAIP as determined by quantitative PCR and Western blots, the stable cells were subjected to apoptotic stress. In contrast to what was seen when HeLa cells were transiently transfected with a construct expressing full-length NAIP, the NAIP stable HeLa cell lines did not offer increased protection against etoposide or the other apoptotic triggers tested. As the transient transfection of full-length NAIP was shown to suppress apoptosis, in contrast to stable cell lines, the length of time for the overexpression of NAIP is key to understanding why cytoprotective effects could no longer be demonstrated. This phenomenon is not fully understood but can be caused by genetic mutations leading to the development of sublines due to repairs, or a lack of repairs, during cellular check points (Breivik, 2001).

Cells surviving the selection process were no longer able to suppress apoptosis due to a mutation within *NAIP* itself or within a critical component. Our collaborators found previous attempts to develop cell lines with a stable overexpression of *NAIP* resulted in mutations affecting the carboxyl terminus (J. Ikeda, unpublished observation). Other groups attempting to develop stable XIAP cell lines also discovered a loss in cytoprotection and attributed it to a compensatory mechanism to counter the continuous expression of an IAP (Colin Duckett, personal communication). The alteration in NAIP activity, therefore, is indicative of cells countering a potential neoplasmic threat by either mutating *NAIP* itself or increasing the level of a tumour suppressor, such as XAF. What actual mutations occurred in these cell lines should be explored further to elucidate the transition that has occurred.

Suppression of apoptosis was also studied following adenoviral-mediated expression of *NAIPΔE14/17* combined with trophic factors. It is interesting to note that the 80% cytoprotection offered by pretreatment with adeno-*NAIPΔE14/17* alone could not be augmented by the addition of BDNF, CNTF or NGF. Overall, there was no additive or synergistic protection with the trophic factors and NAIPΔE14/17, suggesting either NAIP levels were too high, at an MOI of 200, for a subtle effect to be observed or that similar signaling pathways were engaged. The latter explanation confirms results obtained by collaborators.

Although signaling pathways induced by NAIP have not yet been fully investigated our collaborators found motor neuron degeneration following axotomy of the sciatic nerve in 3-day-old rats can be prevented through adenoviral mediated *NAIPΔE14/17*, *c-IAP1* and *c-IAP2* expression (Perrelet *et al.*, 2000). The effect observed with these proteins was similar to that obtained with CNTF or BDNF. Of the neurotrophic factors used in this present study, BDNF and NGF bind to the Trk receptors to initiate signaling cascades through the phosphorylation of tyrosine residues and the docking of adapter proteins. The intracellular signaling cascades activated include the phosphatidylinositol-3-kinase/Akt kinase pathway, phospholipase Cγ and the Ras kinase pathway (Dawbarn & Allen, 2003). CNTF, however, uses the CNTFRα receptor coupled to LIF and gp130 for signaling through the JAK/STAT pathways. Convergence of *NAIPΔE14/17* and trophic factor suppression of apoptosis signaling pathways needs to be studied further to identify the common pathways involved in apoptosis suppression.

In another study it was found that after sciatic nerve axotomy there was a notable loss in NAIP protein expression and that this decrease was blocked by GDNF but not

BDNF or CNTF treatment (Perrelet *et al.*, 2002). Infection with adenoviral mediated antisense-*NAIP*, antisense-*XIAP,* or the XIAP binding protein, *XAF1,* induced a comparable decrease in motor neuron survival in GDNF-treated rats, but not in BDNF- or CNTF-treated rats. Increased survival of the motor neurons was noted in the presence of adeno-*NAIPΔE14/17* or the trophic factors, while co-infection of antisense-*NAIP* blocked the protective effect of adeno-*NAIPΔE14/17*. The results from this laboratory indicated that NAIPΔE14/17 and XIAP were essential for the GDNF-mediated rescue of axotomized motor neurons and that the intracellular survival mechanisms activated by GDNF and the neurotrophins were different (Perrelet *et al.*, 2002). Further exploration of these differences between the pathways could lead to a therapeutic target, increasing the efficacy of combined trophic factor and IAP interventions. The demonstration of the protective role of NAIP in a number of pathology models and the possibility of modulating NAIP expression points to use of pharmacological agents for therapeutic purposes. Defining the signaling pathways controlling NAIP up-regulation is an essential first step in the identification of possible therapeutic intervention points.

Similarities among the agents used to up-regulate murine *Naip1* in neuro-2a cell line indicated that G-coupled proteins play an important role in signal transduction for this gene. In fact, after sodium butyrate was chosen as an inducer of *Naip*, the receptors for this short chained fatty acid was shown to be GPR41 and GPR43 (Brown *et al.*, 2003; Le Poul *et al.*, 2003; Nilsson *et al.*, 2003; Senga *et al.*, 2003). In the present study, using inhibition of specific kinases known to be affected by NaB and monitoring the transcript level of *Naip1*, it was demonstrated that NaB-induced *Naip* up-regulation in neuro-2a cells was not dependent upon ERK1/2, p38 or PKA. Treatment with the broad-

based kinase inhibitor H-7, however, did result in a complete attenuation of NaB-induced *Naip* up-regulation. The H-7-sensitive kinase(s) was/were critical for *Naip* gene expression as this inhibitor was able to decrease the level of *Naip* transcript below that of the control cells. As a critical role for PKA was ruled out for NaB-mediated induction of *Naip*, the H-7 results implicate either PKC or PKG, although it cannot be ruled out that H-7 mediates a more fundamental repression of this gene. The involvement of PKC and/or PKG in NaB-induced *Naip* up-regulation needs to be verified independently with either inhibitors or dominant negative isoforms.

The examination of kinase expression changes following exposure of the cells to NaB treatment revealed an increase in the inhibitor of NF-κB kinase alpha (IKKα). This is significant given XIAP has been shown to be a strong stimulator of NF-κB (Hofer-Warbinek *et al.*, 2000) and, in a positive feedback loop, can be up-regulated by NF-κB (Stehlik *et al.*, 1998b). The inhibitory subunits (IκBα, IκBβ and IκBε) prevent NF-κB translocation to the nucleus and thus the activation of NF-κB requires the phosphorylation and dissociation of IκB, mediated by IKK-α and IKK-β. It has been demonstrated that XIAP and/or TAK1 can stimulate IKKβ kinase activity (Sanna *et al.*, 2002) and that TAK1 interacts with NIK, a kinase upstream of both IKKs (Hofer-Warbinek *et al.*, 2000). An interaction between NAIP and TAK1 has been demonstrated (Sanna *et al.*, 2002), consequently the *Naip* up-regulation either lies upstream of and contributes to NF-κB induction or it is downstream of NF-κB as this transcription factor was found to be important for the PMA-induced up-regulation of human *NAIP* in Jurkat cells (Busuttil *et al.*, 2002). The regulation of these components is cell-type specific and would have to be determined experimentally.

Extant scientific literature is represented in the following model (Figure D-1). NaB transmits through G protein couple receptors, leading to the activation of PDK1, PKC, Akt and NF-κB, among others. *Naip* was either induced through these phosphorylations or by the histone deacetylase inhibition activity of NaB. The former is likely as the broad spectrum kinase inhibitor H-7 decreased the basal levels of *Naip* and attenuated NaB-induced up-regulation of *Naip*. Other researchers have shown H-7 abolished the induction of $p21^{WAF1/CIP1}$ by NaB without changing the acetylation level of histone H3 and H4 (Kobayashi *et al.*, 2004). They concluded that the increase in the acetylation level induced by NaB appeared insufficient for NaB-induced transcription of the $p21^{WAF1/CIP1}$ gene. Interestingly, our laboratory has data to support matching protein expression patterns of $p21^{WAF1/CIP1}$ and NAIP in small intestine (Maier *et al.*, 2004).

Up-regulation of a gene is usually translated into increased protein levels and a cellular change that is mediated by these increased levels. With respect to NAIP, BIR3 mediates cytoprotection yet is less effective at inhibiting caspase-3/7 activity than BIR2 but more effective in the inhibition of caspase-9, similar to the third BIR domain of XIAP (Davoodi *et al.*, 2004). To further study the mechanisms through which NBIR3 may mediate the suppression of apoptosis, potential binding partners and antagonists of NBIR3 were investigated. Through phage display library screening, pull-down studies and surface plasmon resonance analyses, such partners were proposed.

Figure D-1. NaB-induced Naip up-regulation model. NaB binding to the GPC41/43 followed by signaling through PI3K, PDK1 and Akt can lead to the activation of p300, NF-κB and Naip1. See Appendix II for detailed description of the pathways involved.

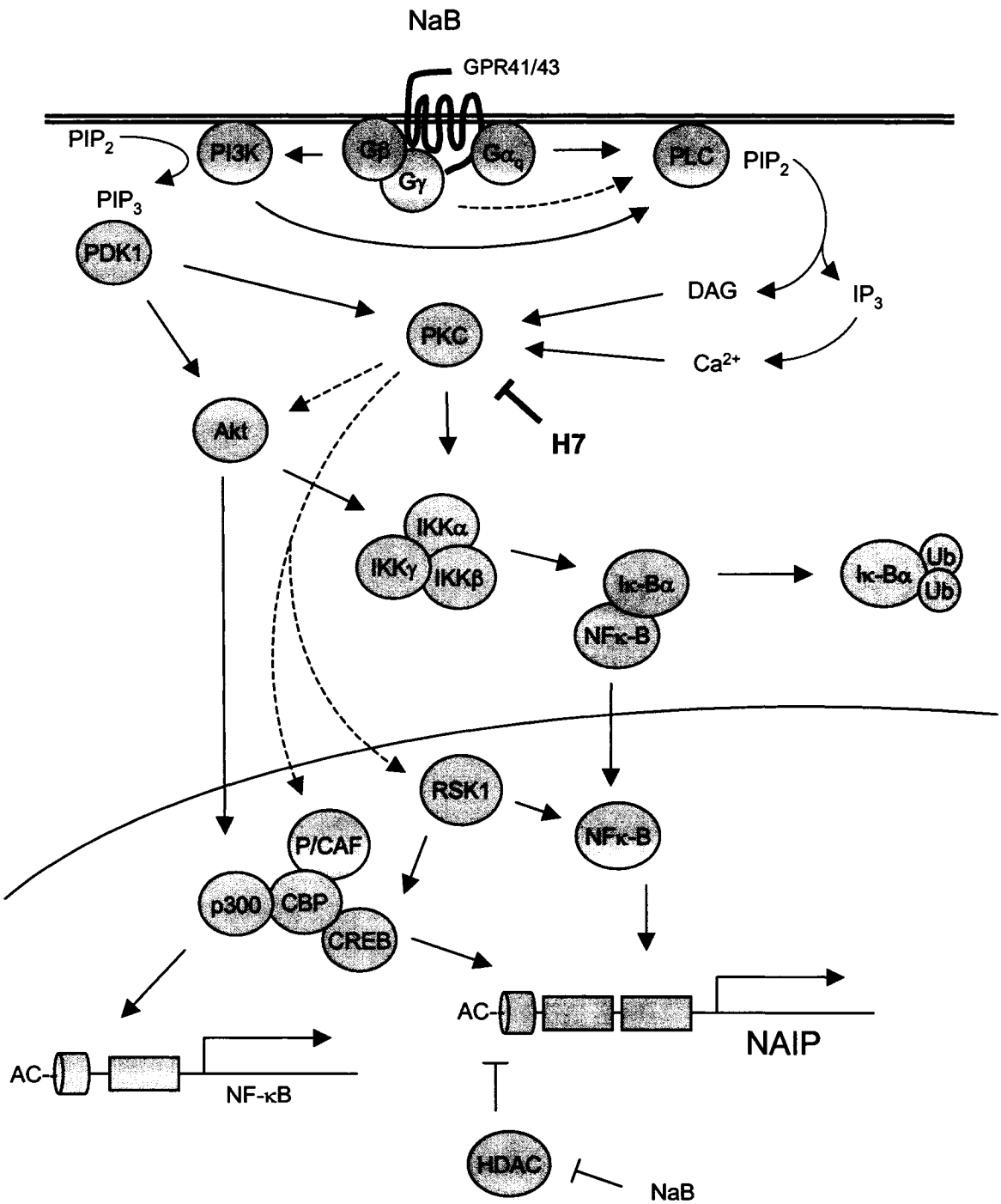
NaB
GPR41/43
PIP2
PI3K
Gβ
Gγ
Gαq
PLC
PIP2
PIP3
PDK1
DAG
IP3
PKC
Ca2+
Akt
H7
IKKα
IKKγ
IKKβ
Iκ-Bα
NFκ-B
Iκ-Bα
Ub
Ub
RSK1
NFκ-B
P/CAF
p300
CBP
CREB
AC
NAIP
AC
NF-κB
HDAC
NaB

As XIAP, cIAP-1 and cIAP-2 have been shown to bind and inhibit caspase-9 it was hypothesized that the third BIR of NAIP would as well. It is now established that polypeptides incorporating the second BIR domain and the immediate NH_2 linker region for these four IAP can inhibit caspase-3 and -7. The caspase-9 inhibition curve in the present study marks the initial stage of investigating the interaction between NBIR3 and this caspase before the enzymatic system was optimized. Our laboratory subsequently found that NBIR3 functions as a potent inhibitor of caspase-9 with an IC_{50} value of 33 nM (Davoodi *et al.*, 2004), similar to the IC_{50} value of 17 nM obtained for XBIR3 (Liu *et al.*, 2000).

A Smac-based peptide, which antagonized the XIAP-mediated inhibition of caspase-9, was shown to bind NBIR3 and XBIR3 with similar equilibrium dissociation constants. The use of SPR allowed for a clear demonstration of binding and allowed for the calculation of association and dissociation rates for the interactions. The XBIR3 interaction with a Smac-based peptide observed in the present study was found to be 2 x 10^{-8} M. This value was approximately 100 times stronger than the interaction of XBIR3 with the processed Smac protein but 100 times weaker than linker_XBIR2-3 region, as determined by a recently published report (Huang *et al.*, 2003). That data indicated that the linker region proximal to XBIR2 in combination with the second and third BIR domain of XIAP had the strongest K_D (3.2 x 10^{-10} M) for Smac binding As Smac can interact with XIAP in regions outside of the well-characterized tetrapeptide binding groove (Wu *et al.*, 2000), the K_D varied with the amino acids of XIAP tested. It was interesting to note that a construct containing the amino acids from 124-356 had a stronger binding coefficient than BIR3 (252-356) on its own. The intermediate

dissociation constant found in the present study is likely due the amino acids present in the XBIR3 construct used (238-356) and the use of a Smac-based peptide rather than the processed protein.

Binding between Smac and the BIR domains of NAIP was shown for the first time with the present study. NBIR3 (231-392) bound a Smac-based peptide with a K_D of 5 x 10^{-8} M for NBIR3 while NBIR2 (154-255) bound the same peptide with a K_D of 1 x 10^{-7} M. Similar results were obtained to those seen with XIAP, as XBIR3 bound more strongly to Smac than XBIR2 (Huang *et al.*, 2003). Surprisingly, it was not possible to demonstrate co-immunoprecipitation between GST-NBIR3 and processed Smac (present study) or when both proteins were expressed in eukaryotes (Davoodi *et al.*, 2004). The lack of association between NBIR3 and the processed Smac protein seems to indicate the binding is not as strong as it is with the peptide. This hypothesis should be tested further using the SPR technique.

As an initial step to finding unique partners of NAIP, recombinant GST-NBIR3 was isolated from bacterial cultures and used to screen a phage display library. The majority of peptides NBIR3 bound in the 4th round of panning contained a consensus sequence with 5 out of 7 amino acids conserved (FHEXWP). In the analysis of the BLAST-generated list of proteins in the human genome that contain these amino acids (Table 3-1 and Appendix A), no obvious family of proteins was identified nor were there any binding proteins known to interact with NAIP or other IAPs. Even though there were proteins that contained more of the NBIR3-binding consensus sequence, TRABID was chosen as the initial full-length candidate to test for binding because of its involvement in TNFα signaling. Although binding was not shown by a pull-down study, it does not rule

out the other candidates in the list as possible binding partners for NAIP. Through the employment of other tools, such as transient transfections of constructs expressing both proteins in an eukaryote system or confocal microscopy, interactions could be further studied.

The modulation of NAIP as an anti-apoptotic protein will prove useful for the suppression of apoptosis in neurodegenerative diseases. Furthermore, this inhibition of apoptosis can be conferred in some systems by NBIR3 alone. The discovery of IBMs has highlighted the possibility that not only cellular proteins but also oligopeptides based on these proteins can be used as modulators of IAP activities. Thus both the oligopeptides identified by phage display in this study and proteins containing these sequences may affect suppression of apoptosis mediated by NAIP. In the hunt for therapeutic targets, the identification of partners containing this binding motif is of clear interest.

FUTURE DIRECTIONS

The exploration of differences within the signaling pathways activated by NGF, BDNF, CNTF and GDNF point to the critical role of NAIP in GDNF-mediated cytoprotection. Combined NaB and GDNF treatment would likely prove useful as a possible additive or synergistic treatment. The up-regulation of Naip by combined cAMP and NaB treatment should be tested. In order to determine if PKA plays a critical role in the cAMP-induced up-regulation of Naip, an inhibitor such as Rp-AMP should be used.

In addition to the signaling pathways already outlined, NaB also mediates histone hyperacetylation near the gene so this affect on the up-regulation of *Naip* should be tested using other histone deacetylase inhibitors, such as trichostatin A. The actelyation levels need to be noted in the presence and absence of kinase inhibitors and phosphatases. As the specificity of AG90 has been called into question by others (Sandberg *et al.*, 2004), a dominant negative mutant of JAK2 should also be tested. An analysis of *Naip1* and *Naip5* transcript levels in mouse macrophages following LPS treatment and AG490 should be conducted. As there are many isoforms of PKC, a range of inhibitors for this kinase would have to tested. As PKCδ was shown to be involved with *cIAP2* up-regulation, to establish whether this isoform mediates NaB-induced *Naip* up-regulation the inhibitor rottlerin should be used (Wang *et al.*, 2003). As H-7 can inhibit PKG in addition to PKC, a more specific inhibitor, such as KT5823, would determine if the former kinase is involved (Ha *et al.*, 2003). For NF-κB, dominant negative adenoviral delivery to the neuro-2a cells would test the involvement of this transcription factor.

NaB-mediated changes in Naip should be monitored following the inhibition of PI3K by wortmannin or LY294002.

Continuing the examination of NBIR3 and NBIR2 interactions with the Smac, the processed protein should be tested for binding by the SPR technique. As the linker region preceeding BIR2, when present in a construct expressing both BIR2 and BIR3, was found to be important for the XIAP and Smac interactions, similar regions within NAIP should be tested to examine the critical region that lowers the K_D to nM concentrations.

CONCLUSION

BDNF, CNTF and NGF trophic factors use similar signaling pathways to NAIP in the suppression of apoptosis as the combined treatment does not result in an additive or synergistic effect.

The inhibition of Jak2 by AG490 mediates an up-regulation of *Naip1*. An H-7-sensitive kinase plays a fundamental role in the expression of *Naip* as this inhibitor can down-regulate basal *Naip* levels, in addition to the attenuation of NaB-induced up-regulation. Many of the pharmacological inducers tested signal through G-protein coupled receptors so these may play an important role in the up-regulation of *Naip*.

The BIR domains of NAIP have similar roles to those of XIAP as it has been demonstrated that both NBIR2 and NBIR3 can bind a Smac-based peptide and that NBIR3 can inhibit caspase-9.

REFERENCES

Airaksinen M. S., and Saarma M. (2002). The GDNF family: signalling, biological functions and therapeutic value. *Nat Rev Neurosci* **3:** 383-94.

Akiyama T., Ishida J., Nakagawa S., Ogawara H., Watanabe S., Itoh N., Shibuya M., and Fukami Y. (1987). Genistein, a specific inhibitor of tyrosine-specific protein kinases. *J Biol Chem* **262:** 5592-5.

Altschul S. F., Madden T. L., Schaffer A. A., Zhang J., Zhang Z., Miller W., and Lipman D. J. (1997). Gapped BLAST and PSI-BLAST: a new generation of protein database search programs. *Nucleic Acids Res* **25:** 3389-402.

Ambrosini G., Adida C., and Altieri D. C. (1997). A novel anti-apoptosis gene, survivin, expressed in cancer and lymphoma. *Nature Medicine* **3:** 917-21.

Aravind L., Dixit V. M., and Koonin E. V. (1999). The domains of death: evolution of the apoptosis machinery. *Trends Biochem Sci* **24:** 47-53.

Bankir L., Ahloulay M., Devreotes P. N., and Parent C. A. (2002). Extracellular cAMP inhibits proximal reabsorption: are plasma membrane cAMP receptors involved? *Am J Physiol Renal Physiol* **282:** F376-92.

Birkey Reffey S., Wurthner J. U., Parks W. T., Roberts A. B., and Duckett C. S. (2001). X-linked inhibitor of apoptosis protein functions as a cofactor in transforming growth factor-beta signaling. *J Biol Chem* **276:** 26542-9.

Birnbaum M. J., Clem R. J., and Miller L. K. (1994). An apoptosis-inhibiting gene from a nuclear polyhedrosis virus encoding a polypeptide with Cys/His sequence motifs. *J Virol* **68:** 2521-8.

Boatright K. M., and Salvesen G. S. (2003). Mechanisms of caspase activation. *Curr Opin Cell Biol* **15:** 725-31.

Bratton S. B., Walker G., Srinivasula S. M., Sun X. M., Butterworth M., Alnemri E. S., and Cohen G. M. (2001). Recruitment, activation and retention of caspases-9 and -3 by Apaf-1 apoptosome and associated XIAP complexes. *Embo J* **20:** 998-1009.

Breivik J. (2001). Don't stop for repairs in a war zone: Darwinian evolution unites genes and environment in cancer development. *Proc Natl Acad Sci U S A* **98:** 5379-81.

Brown A. J., Goldsworthy S. M., Barnes A. A., Eilert M. M., Tcheang L., Daniels D., Muir A. I., Wigglesworth M. J., Kinghorn I., Fraser N. J., Pike N. B., Strum J. C., Steplewski K. M., Murdock P. R., Holder J. C., Marshall F. H., Szekeres P. G., Wilson S., Ignar D. M., Foord S. M., Wise A., and Dowell S. J. (2003). The Orphan G protein-coupled receptors GPR41 and GPR43 are activated by propionate and other short chain carboxylic acids. *J Biol Chem* **278:** 11312-9.

Burns T. F., Bernhard E. J., and El-Deiry W. S. (2001). Tissue specific expression of p53 target genes suggests a key role for KILLER/DR5 in p53-dependent apoptosis in vivo. *Oncogene* **20:** 4601-12.

Busuttil V., Bottero V., Frelin C., Imbert V., Ricci J. E., Auberger P., and Peyron J. F. (2002). Blocking NF-kappaB activation in Jurkat leukemic T cells converts the survival agent and tumor promoter PMA into an apoptotic effector. *Oncogene* **21:** 3213-24.

Cerretti D. P., Kozlosky C. J., Mosley B., Nelson N., Van Ness K., Greenstreet T. A., March C. J., Kronheim S. R., Druck T., Cannizzaro L. A., and et al. (1992).

Molecular cloning of the interleukin-1 beta converting enzyme. *Science* **256:** 97-100.

Chai J., Shiozaki E., Srinivasula S. M., Wu Q., Datta P., Alnemri E. S., Shi Y., and Dataa P. (2001). Structural basis of caspase-7 inhibition by XIAP. *Cell* **104:** 769-80.

Chaly N., Bladon T., Setterfield G., Little J. E., Kaplan J. G., and Brown D. L. (1984). Changes in distribution of nuclear matrix antigens during the mitotic cell cycle. *J Cell Biol* **99:** 661-71.

Chang J. G., Hsieh-Li H. M., Jong Y. J., Wang N. M., Tsai C. H., and Li H. (2001). Treatment of spinal muscular atrophy by sodium butyrate. *Proc Natl Acad Sci U S A* **98:** 9808-13.

Chantalat L., Skoufias D. A., Kleman J. P., Jung B., Dideberg O., and Margolis R. L. (2000). Crystal structure of human survivin reveals a bow tie-shaped dimer with two unusual alpha-helical extensions. *Mol Cell* **6:** 183-9.

Chen Q., Baird S. D., Mahadevan M., Besner-Johnston A., Farahani R., Xuan J., Kang X., Lefebvre C., Ikeda J. E., Korneluk R. G., and MacKenzie A. E. (1998). Sequence of a 131-kb region of 5q13.1 containing the spinal muscular atrophy candidate genes SMN and NAIP. *Genomics* **48:** 121-7.

Chen Z., Naito M., Hori S., Mashima T., Yamori T., and Tsuruo T. (1999). A human IAP-family gene, apollon, expressed in human brain cancer cells. *Biochem Biophys Res Commun* **264:** 847-54.

Chin K. V., Yang W. L., Ravatn R., Kita T., Reitman E., Vettori D., Cvijic M. E., Shin M., and Iacono L. (2002). Reinventing the wheel of cyclic AMP: novel mechanisms of cAMP signaling. *Ann N Y Acad Sci* **968:** 49-64.

Chu S., and Ferro T. J. (2005). Sp1: regulation of gene expression by phosphorylation. *Gene* **348:** 1-11.

Conkright M. D., Canettieri G., Screaton R., Guzman E., Miraglia L., Hogenesch J. B., and Montminy M. (2003). TORCs: transducers of regulated CREB activity. *Mol Cell* **12:** 413-23.

Cory S., and Adams J. M. (2002). The Bcl2 family: regulators of the cellular life-or-death switch. *Nat Rev Cancer* **2:** 647-56.

Crocker S. J., Wigle N., Liston P., Thompson C. S., Lee C. J., Xu D., Roy S., Nicholson D. W., Park D. S., MacKenzie A., Korneluk R. G., and Robertson G. S. (2001). NAIP protects the nigrostriatal dopamine pathway in an intrastriatal 6-OHDA rat model of Parkinson's disease. *Eur J Neurosci* **14:** 391-400.

Crook N. E., Clem R. J., and Miller L. K. (1993). An apoptosis-inhibiting baculovirus gene with a zinc finger-like motif. *Journal of Virology* **67:** 2168-74.

Cui X., Imaizumi T., Yoshida H., Tanji K., Matsumiya T., and Satoh K. (2000). Lipopolysaccharide induces the expression of cellular inhibitor of apoptosis protein-2 in human macrophages. *Biochim Biophys Acta* **1524:** 178-182.

Davie J. R. (2003). Inhibition of histone deacetylase activity by butyrate. *J Nutr* **133:** 2485S-2493S.

Davoodi J., Lin L., Kelly J., Liston P., and MacKenzie A. E. (2004). Neuronal apoptosis-inhibitory protein does not interact with Smac and requires ATP to bind caspase-9. *J Biol Chem* **279:** 40622-8.

Dawbarn D., and Allen S. J. (2003). Neurotrophins and neurodegeneration. *Neuropathol Appl Neurobiol* **29:** 211-30.

Deb D. K., Sassano A., Lekmine F., Majchrzak B., Verma A., Kambhampati S., Uddin S., Rahman A., Fish E. N., and Platanias L. C. (2003). Activation of protein kinase C delta by IFN-gamma. *J Immunol* **171:** 267-73.

Degterev A., Boyce M., and Yuan J. (2003). A decade of caspases. *Oncogene* **22:** 8543-67.

Deveraux Q. L., Roy N., Stennicke H. R., Van Arsdale T., Zhou Q., Srinivasula S. M., Alnemri E. S., Salvesen G. S., and Reed J. C. (1998). IAPs block apoptotic events induced by caspase-8 and cytochrome c by direct inhibition of distinct caspases. *Embo Journal* **17:** 2215-23.

Deveraux Q. L., Takahashi R., Salvesen G. S., and Reed J. C. (1997). X-linked IAP is a direct inhibitor of cell-death proteases. *Nature* **388:** 300-4.

DiDonato C. J., Chen X. N., Noya D., Korenberg J. R., Nadeau J. H., and Simard L. R. (1997). Cloning, characterization, and copy number of the murine survival motor neuron gene: homolog of the spinal muscular atrophy-determining gene. *Genome Research* **7:** 339-52.

Diez E., Lee S. H., Gauthier S., Yaraghi Z., Tremblay M., Vidal S., and Gros P. (2003). Birc1e is the gene within the Lgn1 locus associated with resistance to Legionella pneumophila. *Nat Genet* **33:** 55-60.

Diez E., Yaraghi Z., MacKenzie A., and Gros P. (2000). The neuronal apoptosis inhibitory protein (Naip) is expressed in macrophages and is modulated after phagocytosis and during intracellular infection with Legionella pneumophila. *J Immunol* **164:** 1470-7.

Digby M. R., Kimpton W. G., York J. J., Connick T. E., and Lowenthal J. W. (1996). ITA, a vertebrate homologue of IAP that is expressed in T lymphocytes. *Dna and Cell Biology* **15:** 981-8.

Doyle B. T., O'Neill A. J., Newsholme P., Fitzpatrick J. M., and Watson R. W. (2002). The loss of IAP expression during HL-60 cell differentiation is caspase-independent. *J Leukoc Biol* **71:** 247-54.

Du C., Fang M., Li Y., Li L., and Wang X. (2000). Smac, a mitochondrial protein that promotes cytochrome c-dependent caspase activation by eliminating IAP inhibition. *Cell* **102:** 33-42.

Duckett C. S., Nava V. E., Gedrich R. W., Clem R. J., Van Dongen J. L., Gilfillan M. C., Shiels H., Hardwick J. M., and Thompson C. B. (1996). A conserved family of cellular genes related to the baculovirus iap gene and encoding apoptosis inhibitors. *Embo Journal* **15:** 2685-94.

Ehrhard P. B., Ganter U., Schmutz B., Bauer J., and Otten U. (1993). Expression of low-affinity NGF receptor and trkB mRNA in human SH-SY5Y neuroblastoma cells. *FEBS Lett* **330:** 287-92.

Encinas M., Tansey M. G., Tsui-Pierchala B. A., Comella J. X., Milbrandt J., and Johnson E. M., Jr. (2001). c-Src is required for glial cell line-derived neurotrophic factor (GDNF) family ligand-mediated neuronal survival via a phosphatidylinositol-3 kinase (PI-3K)-dependent pathway. *J Neurosci* **21:** 1464-72.

Endrizzi M. G., Hadinoto V., Growney J. D., Miller W., and Dietrich W. F. (2000). Genomic sequence analysis of the mouse Naip gene array. *Genome Res* **10:** 1095-102.

Evans P. C., Taylor E. R., Coadwell J., Heyninck K., Beyaert R., and Kilshaw P. J. (2001). Isolation and characterization of two novel A20-like proteins. *Biochem J* **357:** 617-23.

Farahani R., Fong W. G., Korneluk R. G., and MacKenzie A. E. (1997). Genomic organization and primary characterization of miap-3: the murine homologue of human X-linked IAP. *Genomics* **42:** 514-8.

Fink S. L., and Cookson B. T. (2005). Apoptosis, pyroptosis, and necrosis: mechanistic description of dead and dying eukaryotic cells. *Infect Immun* **73:** 1907-16.

Fong W. G., Liston P., Rajcan-Separovic E., St Jean M., Craig C., and Korneluk R. G. (2000). Expression and genetic analysis of XIAP-associated factor 1 (XAF1) in cancer cell lines. *Genomics* **70:** 113-22.

Franklin M. C., Kadkhodayan S., Ackerly H., Alexandru D., Distefano M. D., Elliott L. O., Flygare J. A., Mausisa G., Okawa D. C., Ong D., Vucic D., Deshayes K., and Fairbrother W. J. (2003). Structure and function analysis of peptide antagonists of melanoma inhibitor of apoptosis (ML-IAP). *Biochemistry* **42:** 8223-31.

Friedlander R. M. (2003). Apoptosis and caspases in neurodegenerative diseases. *N Engl J Med* **348:** 1365-75.

Gendron N. H., and MacKenzie A. E. (1999). Spinal muscular atrophy: molecular pathophysiology. *Current Opinion in Neurology* **12:** 137-142.

Gerhardt E., Kugler S., Leist M., Beier C., Berliocchi L., Volbracht C., Weller M., Bahr M., Nicotera P., and Schulz J. B. (2001). Cascade of caspase activation in potassium-deprived cerebellar granule neurons: targets for treatment with peptide and protein inhibitors of apoptosis. *Mol Cell Neurosci* **17:** 717-31.

Gotz R., Karch C., Digby M. R., Troppmair J., Rapp U. R., and Sendtner M. (2000). The neuronal apoptosis inhibitory protein suppresses neuronal differentiation and apoptosis in PC12 cells. *Hum Mol Genet* **9:** 2479-89.

Growney J. D., Scharf J. M., Kunkel L. M., and Dietrich W. F. (2000). Evolutionary divergence of the mouse and human Lgn1/SMA repeat structures. *Genomics* **64:** 62-81.

Ha K. S., Kim K. M., Kwon Y. G., Bai S. K., Nam W. D., Yoo Y. M., Kim P. K., Chung H. T., Billiar T. R., and Kim Y. M. (2003). Nitric oxide prevents 6-hydroxydopamine-induced apoptosis in PC12 cells through cGMP-dependent PI3 kinase/Akt activation. *Faseb J* **17:** 1036-47.

Hacker G., Hawkins C. J., Smith K. G., and Vaux D. L. (1996). Effects of viral inhibitors of apoptosis in models of mammalian cell death. *Behring Institute Mitteilungen*: 118-26.

Hauser H. P., Bardroff M., Pyrowolakis G., and Jentsch S. (1998). A giant ubiquitin-conjugating enzyme related to IAP apoptosis inhibitors. *Journal of Cell Biology* **141:** 1415-22.

Hawkins C. J., Uren A. G., Hacker G., Medcalf R. L., and Vaux D. L. (1996). Inhibition of interleukin 1 beta-converting enzyme-mediated apoptosis of mammalian cells by baculovirus IAP. *Proceedings of the National Academy of Sciences of the United States of America* **93:** 13786-90.

Hay B. A., Wassarman D. A., and Rubin G. M. (1995). Drosophila homologs of baculovirus inhibitor of apoptosis proteins function to block cell death. *Cell* **83:** 1253-62.

Hegde R., Srinivasula S. M., Zhang Z., Wassell R., Mukattash R., Cilenti L., DuBois G., Lazebnik Y., Zervos A. S., Fernandes-Alnemri T., and Alnemri E. S. (2002). Identification of Omi/HtrA2 as a mitochondrial apoptotic serine protease that disrupts inhibitor of apoptosis protein-caspase interaction. *J Biol Chem* **277:** 432-8.

Hinds M. G., Norton R. S., Vaux D. L., and Day C. L. (1999). Solution structure of a baculoviral inhibitor of apoptosis (IAP) repeat. *Nature Structural Biology* **6:** 648-51.

Hinek A. (1996). Biological roles of the non-integrin elastin/laminin receptor. *Biol Chem* **377:** 471-80.

Hofer-Warbinek R., Schmid J. A., Stehlik C., Binder B. R., Lipp J., and de Martin R. (2000). Activation of NF-kappa B by XIAP, the X chromosome-linked inhibitor of apoptosis, in endothelial cells involves TAK1. *J Biol Chem* **275:** 22064-8.

Holcik M., Thompson C. S., Yaraghi Z., Lefebvre C. A., MacKenzie A. E., and Korneluk R. G. (2000). The hippocampal neurons of neuronal apoptosis inhibitory protein 1 (NAIP1)-deleted mice display increased vulnerability to kainic acid-induced injury. *Proc Natl Acad Sci U S A* **97:** 2286-90.

Hopper E., Belinsky M. G., Zeng H., Tosolini A., Testa J. R., and Kruh G. D. (2001). Analysis of the structure and expression pattern of MRP7 (ABCC10), a new member of the MRP subfamily. *Cancer Lett* **162:** 181-91.

Huang S., Scharf J. M., Growney J. D., Endrizzi M. G., and Dietrich W. F. (1999). The mouse Naip gene cluster on Chromosome 13 encodes several distinct functional transcripts. *Mamm Genome* **10:** 1032-5.

Huang Y., Park Y. C., Rich R. L., Segal D., Myszka D. G., and Wu H. (2001). Structural basis of caspase inhibition by XIAP: differential roles of the linker versus the BIR domain. *Cell* **104:** 781-90.

Huang Y., Rich R. L., Myszka D. G., and Wu H. (2003). Requirement of both the second and third BIR domains for the relief of X-linked inhibitor of apoptosis protein (XIAP)-mediated caspase inhibition by Smac. *J Biol Chem* **278:** 49517-22.

Hubbard S. R., and Till J. H. (2000). Protein tyrosine kinase structure and function. *Annu Rev Biochem* **69:** 373-98.

Hunter A. M., Kottachchi D., Lewis J., Duckett C. S., Korneluk R. G., and Liston P. (2003). A novel ubiquitin fusion system bypasses the mitochondria and generates biologically active Smac/DIABLO. *J Biol Chem* **278:** 7494-9.

Hutchison J. S., Derrane R. E., Johnston D. L., Gendron N., Barnes D., Fliss H., King W. J., Rasquinha I., MacManus J., Robertson G. S., and MacKenzie A. E. (2001). Neuronal apoptosis inhibitory protein expression after traumatic brain injury in the mouse. *J Neurotrauma* **18:** 1333-47.

Ingram-Crooks J., Holcik M., Drmanic S., and MacKenzie A. E. (2002). Distinct expression of neuronal apoptosis inhibitory protein (NAIP) during murine development. *Neuroreport* **13:** 397-402.

Inohara N., and Nunez G. (2001). The NOD: a signaling module that regulates apoptosis and host defense against pathogens. *Oncogene* **20:** 6473-81.

Ip N. Y. (1998). The neurotrophins and neuropoietic cytokines: two families of growth factors acting on neural and hematopoietic cells. *Ann N Y Acad Sci* **840:** 97-106.

Jacobson K. A., Moro S., Manthey J. A., West P. L., and Ji X. D. (2002). Interactions of flavones and other phytochemicals with adenosine receptors. *Adv Exp Med Biol* **505:** 163-71.

Jacobson M. D., Weil M., and Raff M. C. (1997). Programmed cell death in animal development. *Cell* **88:** 347-54.

Jakel S., Mingot J. M., Schwarzmaier P., Hartmann E., and Gorlich D. (2002). Importins fulfil a dual function as nuclear import receptors and cytoplasmic chaperones for exposed basic domains. *Embo J* **21:** 377-86.

Johnson G. L., and Lapadat R. (2002). Mitogen-activated protein kinase pathways mediated by ERK, JNK, and p38 protein kinases. *Science* **298:** 1911-2.

Johnson R. M., McNeeley P. A., DeMoor K., Stewart G. R., Glaeser B. S., and Pitchford S. (1994). Recombinant human ciliary neurotrophic factor stimulates the metabolic activity of SH-SY5Y cells as measured by a cytosensor microphysiometer. *Brain Res* **646:** 327-31.

Jones G., Jones D., Zhou L., Steller H., and Chu Y. (2000). Deterin, a new inhibitor of apoptosis from Drosophila melanogaster. *J Biol Chem* **275:** 22157-65.

Ka H., and Hunt J. S. (2003). Temporal and spatial patterns of expression of inhibitors of apoptosis in human placentas. *Am J Pathol* **163:** 413-22.

Karin M., Cao Y., Greten F. R., and Li Z. W. (2002). NF-kappaB in cancer: from innocent bystander to major culprit. *Nat Rev Cancer* **2:** 301-10.

Kasof G. M., and Gomes B. C. (2001). Livin, a novel inhibitor of apoptosis protein family member. *J Biol Chem* **276:** 3238-46.

Kawabata H., Kawahara K., Kanekura T., Araya N., Daitoku H., Hatta M., Miura N., Fukamizu A., Kanzaki T., Maruyama I., and Nakajima T. (2002). Possible role of transcriptional coactivator P/CAF and nuclear acetylation in calcium-induced keratinocyte differentiation. *J Biol Chem* **277:** 8099-105.

Kerr J. F., Wyllie A. H., and Currie A. R. (1972). Apoptosis: a basic biological phenomenon with wide-ranging implications in tissue kinetics. *Br J Cancer* **26:** 239-57.

Kiela P. R., Hines E. R., Collins J. F., and Ghishan F. K. (2001). Regulation of the rat NHE3 gene promoter by sodium butyrate. *Am J Physiol Gastrointest Liver Physiol* **281:** G947-56.

Kobayashi H., Tan E. M., and Fleming S. E. (2004). Acetylation of histones associated with the p21WAF1/CIP1 gene by butyrate is not sufficient for p21WAF1/CIP1 gene transcription in human colorectal adenocarcinoma cells. *Int J Cancer* **109:** 207-13.

Kobe B., and Kajava A. V. (2001). The leucine-rich repeat as a protein recognition motif. *Curr Opin Struct Biol* **11:** 725-32.

Koonin E. V., and Aravind L. (2000). The NACHT family - a new group of predicted NTPases implicated in apoptosis and MHC transcription activation. *Trends Biochem Sci* **25:** 223-4.

Kornfeld R., Bao M., Brewer K., Noll C., and Canfield W. (1999). Molecular cloning and functional expression of two splice forms of human N-acetylglucosamine-1-phosphodiester alpha-N-acetylglucosaminidase. *J Biol Chem* **274:** 32778-85.

Kovarik P., Stoiber D., Novy M., and Decker T. (1998). Stat1 combines signals derived from IFN-gamma and LPS receptors during macrophage activation. *Embo J* **17:** 3660-8.

Kozak M. (1984). Compilation and analysis of sequences upstream from the translational start site in eukaryotic mRNAs. *Nucleic Acids Res* **12:** 857-72.

Laemmli U. K. (1970). Cleavage of structural proteins during the assembly of the head of bacteriophage T4. *Nature* **227:** 680-5.

Lagace M., Xuan J. Y., Young S. S., McRoberts C., Maier J., Rajcan-Separovic E., and Korneluk R. G. (2001). Genomic organization of the X-linked inhibitor of apoptosis and identification of a novel testis-specific transcript. *Genomics* **77:** 181-8.

Lavens S. E., Peachell P. T., and Warner J. A. (1992). Role of tyrosine kinases in IgE-mediated signal transduction in human lung mast cells and basophils. *Am J Respir Cell Mol Biol* **7:** 637-44.

Le Poul E., Loison C., Struyf S., Springael J. Y., Lannoy V., Decobecq M. E., Brezillon S., Dupriez V., Vassart G., Van Damme J., Parmentier M., and Detheux M. (2003). Functional characterization of human receptors for short chain fatty acids and their role in polymorphonuclear cell activation. *J Biol Chem* **278:** 25481-9.

Li F., Ambrosini G., Chu E. Y., Plescia J., Tognin S., Marchisio P. C., and Altieri D. C. (1998). Control of apoptosis and mitotic spindle checkpoint by survivin. *Nature* **396:** 580-4.

Lin J. H., Deng G., Huang Q., and Morser J. (2000). KIAP, a novel member of the inhibitor of apoptosis protein family. *Biochem Biophys Res Commun* **279:** 820-31.

Lindholm D., Mercer E. A., Yu L. Y., Chen Y., Kukkonen J., Korhonen L., and Arumae U. (2002). Neuronal apoptosis inhibitory protein: structural requirements for hippocalcin binding and effects on survival of NGF-dependent sympathetic neurons. *Biochim Biophys Acta* **1600:** 138-47.

Linford N. J., Yang Y., Cook D. G., and Dorsa D. M. (2001). Neuronal apoptosis resulting from high doses of the isoflavone genistein: role for calcium and p42/44 mitogen-activated protein kinase. *J Pharmacol Exp Ther* **299:** 67-75.

Liston P., Fong W. G., Kelly N. L., Toji S., Miyazaki T., Conte D., Tamai K., Craig C. G., McBurney M. W., and Korneluk R. G. (2001). Identification of XAF1 as an antagonist of XIAP anti-Caspase activity. *Nat Cell Biol* **3:** 128-33.

Liston P., Fong W. G., and Korneluk R. G. (2003). The inhibitors of apoptosis: there is more to life than Bcl2. *Oncogene* **22:** 8568-80.

Liston P., Lefebvre C., Fong W. G., Xuan J. Y., and Korneluk R. G. (1997). Genomic characterization of the mouse inhibitor of apoptosis protein 1 and 2 genes. *Genomics* **46:** 495-503.

Liston P., Roy N., Tamai K., Lefebvre C., Baird S., Cherton-Horvat G., Farahani R., McLean M., Ikeda J. E., MacKenzie A., and Korneluk R. G. (1996). Suppression of apoptosis in mammalian cells by NAIP and a related family of IAP genes. *Nature* **379:** 349-53.

Liu Z., Sun C., Olejniczak E. T., Meadows R. P., Betz S. F., Oost T., Herrmann J., Wu J. C., and Fesik S. W. (2000). Structural basis for binding of Smac/DIABLO to the XIAP BIR3 domain. *Nature* **408:** 1004-8.

Lomaga M. A., Yeh W. C., Sarosi I., Duncan G. S., Furlonger C., Ho A., Morony S., Capparelli C., Van G., Kaufman S., van der Heiden A., Itie A., Wakeham A., Khoo W., Sasaki T., Cao Z., Penninger J. M., Paige C. J., Lacey D. L., Dunstan C. R., Boyle W. J., Goeddel D. V., and Mak T. W. (1999). TRAF6 deficiency results in osteopetrosis and defective interleukin-1, CD40, and LPS signaling. *Genes Dev* **13:** 1015-24.

MacKenzie C. R., Hirama T., Lee K. K., Altman E., and Young N. M. (1997). Quantitative analysis of bacterial toxin affinity and specificity for glycolipid receptors by surface plasmon resonance. *J Biol Chem* **272:** 5533-8.

Magun R., Gagnon A., Yaraghi Z., and Sorisky A. (1998). Expression and regulation of neuronal apoptosis inhibitory protein during adipocyte differentiation. *Diabetes* **47:** 1948-52.

Maier J. K., Coffill C. R., Pelletier L., Franks D. J., MacKenzie A. E., and Gendron N. H. (2004). The distribution of neuronal apoptosis inhibitory protein in human tissues suggests a role in cellular differentiation. *In preparation.*

Maier J. K., Lahoua Z., Gendron N. H., Fetni R., Johnston A., Davoodi J., Rasper D., Roy S., Slack R. S., Nicholson D. W., and MacKenzie A. E. (2002). The neuronal apoptosis inhibitory protein is a direct inhibitor of caspases 3 and 7. *J Neurosci* **22:** 2035-43.

Majdan M., and Miller F. D. (1999). Neuronal life and death decisions functional antagonism between the Trk and p75 neurotrophin receptors. *Int J Dev Neurosci* **17:** 153-61.

Majello B., De Luca P., Hagen G., Suske G., and Lania L. (1994). Different members of the Sp1 multigene family exert opposite transcriptional regulation of the long terminal repeat of HIV-1. *Nucleic Acids Res* **22:** 4914-21.

Marinissen M. J., and Gutkind J. S. (2001). G-protein-coupled receptors and signaling networks: emerging paradigms. *Trends Pharmacol Sci* **22:** 368-76.

Markovits J., Linassier C., Fosse P., Couprie J., Pierre J., Jacquemin-Sablon A., Saucier J. M., Le Pecq J. B., and Larsen A. K. (1989). Inhibitory effects of the tyrosine kinase inhibitor genistein on mammalian DNA topoisomerase II. *Cancer Res* **49:** 5111-7.

Martins L. M., Iaccarino I., Tenev T., Gschmeissner S., Totty N. F., Lemoine N. R., Savopoulos J., Gray C. W., Creasy C. L., Dingwall C., and Downward J. (2002). The serine protease Omi/HtrA2 regulates apoptosis by binding XIAP through a reaper-like motif. *J Biol Chem* **277:** 439-44.

Matsumoto K., Nakayama T., Sakai H., Tanemura K., Osuga H., Sato E., and Ikeda J. E. (1999). Neuronal apoptosis inhibitory protein (NAIP) may enhance the survival of granulosa cells thus indirectly affecting oocyte survival. *Molecular Reproduction and Development* **54:** 103-11.

Matsumoto M., Nomura T., Momose K., Ikeda Y., Kondou Y., Akiho H., Togami J., Kimura Y., Okada M., and Yamaguchi T. (1996). Inactivation of a novel neuropeptide Y/peptide YY receptor gene in primate species. *J Biol Chem* **271:** 27217-20.

Mayo M. W., Denlinger C. E., Broad R. M., Yeung F., Reilly E. T., Shi Y., and Jones D. R. (2003). Ineffectiveness of histone deacetylase inhibitors to induce apoptosis

involves the transcriptional activation of NF-kappa B through the Akt pathway. *J Biol Chem* **278:** 18980-9.

Mercer E. A., Korhonen L., Skoglosa Y., Olsson P. A., Kukkonen J. P., and Lindholm D. (2000). NAIP interacts with hippocalcin and protects neurons against calcium-induced cell death through caspase-3-dependent and -independent pathways. *Embo J* **19:** 3597-607.

Miller L. K. (1999). An exegesis of IAPs: salvation and surprises from BIR motifs. *Trends Cell Biol* **9:** 323-8.

Mora A., Komander D., van Aalten D. M., and Alessi D. R. (2004). PDK1, the master regulator of AGC kinase signal transduction. *Semin Cell Dev Biol* **15:** 161-70.

Morreau H., Galjart N. J., Gillemans N., Willemsen R., van der Horst G. T., and d'Azzo A. (1989). Alternative splicing of beta-galactosidase mRNA generates the classic lysosomal enzyme and a beta-galactosidase-related protein. *J Biol Chem* **264:** 20655-63.

Muchmore S. W., Chen J., Jakob C., Zakula D., Matayoshi E. D., Wu W., Zhang H., Li F., Ng S. C., and Altieri D. C. (2000). Crystal structure and mutagenic analysis of the inhibitor-of-apoptosis protein survivin. *Mol Cell* **6:** 173-82.

Neves S. R., Ram P. T., and Iyengar R. (2002). G protein pathways. *Science* **296:** 1636-9.

Newton A. C. (1997). Regulation of protein kinase C. *Curr Opin Cell Biol* **9:** 161-7.

Nicholson D. W. (1999). Caspase structure, proteolytic substrates, and function during apoptotic cell death. *Cell Death Differ* **6:** 1028-42.

Nilsson N. E., Kotarsky K., Owman C., and Olde B. (2003). Identification of a free fatty acid receptor, FFA2R, expressed on leukocytes and activated by short-chain fatty acids. *Biochem Biophys Res Commun* **303:** 1047-52.

Notarbartolo M., Cervello M., Dusonchet L., and D'Alessandro N. (2002). NAIP-DeltaEx10-11: a novel splice variant of the apoptosis inhibitor NAIP differently expressed in drug-sensitive and multidrug-resistant HL60 leukemia cells. *Leuk Res* **26:** 857-62.

Okugawa S., Ota Y., Kitazawa T., Nakayama K., Yanagimoto S., Tsukada K., Kawada M., and Kimura S. (2003). Janus kinase 2 is involved in lipopolysaccharide-induced activation of macrophages. *Am J Physiol Cell Physiol* **285:** C399-408.

Ono-Saito N., Niki I., and Hidaka H. (1999). H-series protein kinase inhibitors and potential clinical applications. *Pharmacol Ther* **82:** 123-31.

Oppenheim R. W. (1989). The neurotrophic theory and naturally occurring motoneuron death. *Trends Neurosci* **12:** 252-5.

Pari G., Berrada F., Verge G., Karpati G., and Nalbantoglu J. (2000). Immunolocalization of NAIP in the human brain and spinal cord. *Neuroreport* **11:** 9-14.

Perera L. P., and Waldmann T. A. (1998). Activation of human monocytes induces differential resistance to apoptosis with rapid down regulation of caspase-8/FLICE. *Proc Natl Acad Sci U S A* **95:** 14308-13.

Perrelet D., Ferri A., Liston P., Muzzin P., Korneluk R. G., and Kato A. C. (2002). IAPs are essential for GDNF-mediated neuroprotective effects in injured motor neurons in vivo. *Nat Cell Biol* **4:** 175-9.

Perrelet D., Ferri A., MacKenzie A. E., Smith G. M., Korneluk R. G., Liston P., Sagot Y., Terrado J., Monnier D., and Kato A. C. (2000). IAP family proteins delay motoneuron cell death in vivo. *Eur J Neurosci* **12:** 2059-67.

Pommier Y., Sordet O., Antony S., Hayward R. L., and Kohn K. W. (2004). Apoptosis defects and chemotherapy resistance: molecular interaction maps and networks. *Oncogene* **23:** 2934-49.

Richter B. W., Mir S. S., Eiben L. J., Lewis J., Reffey S. B., Frattini A., Tian L., Frank S., Youle R. J., Nelson D. L., Notarangelo L. D., Vezzoni P., Fearnhead H. O., and Duckett C. S. (2001). Molecular cloning of ILP-2, a novel member of the inhibitor of apoptosis protein family. *Mol Cell Biol* **21:** 4292-301.

Riedl S. J., Renatus M., Schwarzenbacher R., Zhou Q., Sun C., Fesik S. W., Liddington R. C., and Salvesen G. S. (2001). Structural basis for the inhibition of caspase-3 by XIAP. *Cell* **104:** 791-800.

Rothe M., Pan M. G., Henzel W. J., Ayres T. M., and Goeddel D. V. (1995). The TNFR2-TRAF signaling complex contains two novel proteins related to baculoviral inhibitor of apoptosis proteins. *Cell* **83:** 1243-52.

Roy C. R., and Tilney L. G. (2002). The road less traveled: transport of Legionella to the endoplasmic reticulum. *J Cell Biol* **158:** 415-9.

Roy N., Deveraux Q. L., Takahashi R., Salvesen G. S., and Reed J. C. (1997). The c-IAP-1 and c-IAP-2 proteins are direct inhibitors of specific caspases. *Embo Journal* **16:** 6914-25.

Roy N., Mahadevan M. S., McLean M., Shutler G., Yaraghi Z., Farahani R., Baird S., Besner-Johnston A., Lefebvre C., Kang X., and et al. (1995). The gene for neuronal apoptosis inhibitory protein is partially deleted in individuals with spinal muscular atrophy. *Cell* **80:** 167-78.

Salvesen G. S., and Abrams J. M. (2004). Caspase activation - stepping on the gas or releasing the brakes? Lessons from humans and flies. *Oncogene* **23:** 2774-84.

Salvesen G. S., and Duckett C. S. (2002). IAP proteins: blocking the road to death's door. *Nat Rev Mol Cell Biol* **3:** 401-10.

Sandberg E. M., Ma X., VonDerLinden D., Godeny M. D., and Sayeski P. P. (2004). Jak2 tyrosine kinase mediates angiotensin II-dependent inactivation of ERK2 via induction of mitogen-activated protein kinase phosphatase 1. *J Biol Chem* **279:** 1956-67.

Sanna M. G., Correia Jd Jda S., Ducrey O., Lee J., Nomoto K., Schrantz N., Deveraux Q. L., and Ulevitch R. J. (2002). IAP Suppression of Apoptosis Involves Distinct Mechanisms: the TAK1/JNK1 Signaling Cascade and Caspase Inhibition. *Mol Cell Biol* **22:** 1754-66.

Sariola H., and Saarma M. (2003). Novel functions and signalling pathways for GDNF. *J Cell Sci* **116:** 3855-62.

Scharf J. M., Damron D., Frisella A., Bruno S., Beggs A. H., Kunkel L. M., and Dietrich W. F. (1996). The mouse region syntenic for human spinal muscular atrophy lies within the Lgn1 critical interval and contains multiple copies of Naip exon 5. *Genomics* **38:** 405-17.

Scheid M. P., and Woodgett J. R. (2003). Unravelling the activation mechanisms of protein kinase B/Akt. *FEBS Lett* **546:** 108-12.

Schuck P. (1997). Reliable determination of binding affinity and kinetics using surface plasmon resonance biosensors. *Curr Opin Biotechnol* **8:** 498-502.

Schug J., and Overton G. C. (1998). "TESS: Transcription Element Search Software on the WWW," http://www.cbil.upenn.edu/tess

Senga T., Iwamoto S., Yoshida T., Yokota T., Adachi K., Azuma E., Hamaguchi M., and Iwamoto T. (2003). LSSIG is a novel murine leukocyte-specific GPCR that is induced by the activation of STAT3. *Blood* **101:** 1185-7.

Shaywitz A. J., and Greenberg M. E. (1999). CREB: a stimulus-induced transcription factor activated by a diverse array of extracellular signals. *Annu Rev Biochem* **68:** 821-61.

Shin S., Sung B. J., Cho Y. S., Kim H. J., Ha N. C., Hwang J. I., Chung C. W., Jung Y. K., and Oh B. H. (2001). An anti-apoptotic protein human survivin is a direct inhibitor of caspase-3 and -7. *Biochemistry* **40:** 1117-23.

Shin S. W., Lee M. Y., Kwon G. Y., Park J. W., Yoo M., Kim S. K., Oh T. H., and Choe B. K. (2003). Cloning and characterization of rat neuronal apoptosis inhibitory protein cDNA. *Neurochem Int* **42:** 481-91.

Shiozaki E. N., Chai J., Rigotti D. J., Riedl S. J., Li P., Srinivasula S. M., Alnemri E. S., Fairman R., and Shi Y. (2003). Mechanism of XIAP-Mediated Inhibition of Caspase-9. *Mol Cell* **11:** 519-27.

Simic G., Seso-Simic D., Lucassen P. J., Islam A., Krsnik Z., Cviko A., Jelasic D., Barisic N., Winblad B., Kostovic I., and Kruslin B. (2000). Ultrastructural analysis and TUNEL demonstrate motor neuron apoptosis in Werdnig-Hoffmann disease. *Journal of Neuropathology and Experimental Neurology* **59:** 398-407.

Simons M., Beinroth S., Gleichmann M., Liston P., Korneluk R. G., MacKenzie A. E., Bahr M., Klockgether T., Robertson G. S., Weller M., and Schulz J. B. (1999). Adenovirus-mediated gene transfer of inhibitors of apoptosis protein delays apoptosis in cerebellar granule neurons. *Journal of Neurochemistry* **72:** 292-301.

Srinivasula S. M., Hegde R., Saleh A., Datta P., Shiozaki E., Chai J., Lee R. A., Robbins P. D., Fernandes-Alnemri T., Shi Y., and Alnemri E. S. (2001). A conserved XIAP-interaction motif in caspase-9 and Smac/DIABLO regulates caspase activity and apoptosis. *Nature* **410:** 112-6.

Stehlik C., de Martin R., Binder B. R., and Lipp J. (1998a). Cytokine induced expression of porcine inhibitor of apoptosis protein (iap) family member is regulated by NF-kappa B. *Biochemical and Biophysical Research Communications* **243:** 827-32.

Stehlik C., de Martin R., Kumabashiri I., Schmid J. A., Binder B. R., and Lipp J. (1998b). Nuclear factor (NF)-kappaB-regulated X-chromosome-linked iap gene expression protects endothelial cells from tumor necrosis factor alpha-induced apoptosis. *Journal of Experimental Medicine* **188:** 211-6.

Strom A. C., and Weis K. (2001). Importin-beta-like nuclear transport receptors. *Genome Biol* **2:** REVIEWS3008.

Sun C., Cai M., Gunasekera A. H., Meadows R. P., Wang H., Chen J., Zhang H., Wu W., Xu N., Ng S. C., and Fesik S. W. (1999). NMR structure and mutagenesis of the inhibitor-of-apoptosis protein XIAP. *Nature* **401:** 818-22.

Sun C., Cai M., Meadows R. P., Xu N., Gunasekera A. H., Herrmann J., Wu J. C., and Fesik S. W. (2000). NMR structure and mutagenesis of the third Bir domain of the inhibitor of apoptosis protein XIAP. *J Biol Chem* **275:** 33777-81.

Sun D., Leung C. L., and Liem R. K. (2001). Characterization of the microtubule binding domain of microtubule actin crosslinking factor (MACF): identification of a novel group of microtubule associated proteins. *J Cell Sci* **114:** 161-172.

Suzuki Y., Imai Y., Nakayama H., Takahashi K., Takio K., and Takahashi R. (2001a). A serine protease, HtrA2, is released from the mitochondria and interacts with XIAP, inducing cell death. *Mol Cell* **8:** 613-21.

Suzuki Y., Nakabayashi Y., Nakata K., Reed J. C., and Takahashi R. (2001b). X-linked inhibitor of apoptosis protein (XIAP) inhibits caspase-3 and -7 in distinct modes. *J Biol Chem* **276:** 27058-63.

Takahashi R., Deveraux Q., Tamm I., Welsh K., Assa-Munt N., Salvesen G. S., and Reed J. C. (1998). A single BIR domain of XIAP sufficient for inhibiting caspases. *Journal of Biological Chemistry* **273:** 7787-90.

Tamm I., Trepel M., Cardo-Vila M., Sun Y., Welsh K., Cabezas E., Swatterthwait A., Arap W., Reed J. C., and Pasqualini R. (2003). Peptides targeting caspase inhibitors. *J Biol Chem* **21:** 21.

Thornberry N. A., Bull H. G., Calaycay J. R., Chapman K. T., Howard A. D., Kostura M. J., Miller D. K., Molineaux S. M., Weidner J. R., Aunins J., and et al. (1992). A novel heterodimeric cysteine protease is required for interleukin-1 beta processing in monocytes. *Nature* **356:** 768-74.

Tinel A., and Tschopp J. (2004). The PIDDosome, a protein complex implicated in activation of caspase-2 in response to genotoxic stress. *Science* **304:** 843-6.

Troy C. M., and Salvesen G. S. (2002). Caspases on the brain. *J Neurosci Res* **69:** 145-50.

Tschopp J., Martinon F., and Burns K. (2003). NALPs: a novel protein family involved in inflammation. *Nat Rev Mol Cell Biol* **4:** 95-104.

Uren A. G., Coulson E. J., and Vaux D. L. (1998). Conservation of baculovirus inhibitor of apoptosis repeat proteins (BIRPs) in viruses, nematodes, vertebrates and yeasts. *Trends in Biological Sciences* **23:** 159-162.

Uren A. G., Pakusch M., Hawkins C. J., Puls K. L., and Vaux D. L. (1996). Cloning and expression of apoptosis inhibitory protein homologs that function to inhibit apoptosis and/or bind tumor necrosis factor receptor-associated factors. *Proceedings of the National Academy of Sciences of the United States of America* **93:** 4974-8.

van Loo G., van Gurp M., Depuydt B., Srinivasula S. M., Rodriguez I., Alnemri E. S., Gevaert K., Vandekerckhove J., Declercq W., and Vandenabeele P. (2002). The serine protease Omi/HtrA2 is released from mitochondria during apoptosis. Omi interacts with caspase-inhibitor XIAP and induces enhanced caspase activity. *Cell Death Differ* **9:** 20-6.

Verdecia M. A., Huang H., Dutil E., Kaiser D. A., Hunter T., and Noel J. P. (2000). Structure of the human anti-apoptotic protein survivin reveals a dimeric arrangement. *Nature Structural Biology* **7:** 602-8.

Verhagen A. M., Ekert P. G., Pakusch M., Silke J., Connolly L. M., Reid G. E., Moritz R. L., Simpson R. J., and Vaux D. L. (2000). Identification of DIABLO, a mammalian protein that promotes apoptosis by binding to and antagonizing IAP proteins. *Cell* **102:** 43-53.

Verhagen A. M., Silke J., Ekert P. G., Pakusch M., Kaufmann H., Connolly L. M., Day C. L., Tikoo A., Burke R., Wrobel C., Moritz R. L., Simpson R. J., and Vaux D. L. (2002). HtrA2 promotes cell death through its serine protease activity and its ability to antagonize inhibitor of apoptosis proteins. *J Biol Chem* **277:** 445-54.

Verhagen A. M., and Vaux D. L. (2002). Cell death regulation by the mammalian IAP antagonist Diablo/Smac. *Apoptosis* **7:** 163-6.

Vucic D., Stennicke H. R., Pisabarro M. T., Salvesen G. S., and Dixit V. M. (2000). ML-IAP, a novel inhibitor of apoptosis that is preferentially expressed in human melanomas. *Curr Biol* **10:** 1359-66.

Wang Q., Wang X., and Evers B. M. (2003). Induction of cIAP-2 in human colon cancer cells through PKC delta/NF-kappa B. *J Biol Chem* **278:** 51091-9.

Watarai M., Derre I., Kirby J., Growney J. D., Dietrich W. F., and Isberg R. R. (2001). Legionella pneumophila is internalized by a macropinocytotic uptake pathway controlled by the Dot/Icm system and the mouse Lgn1 locus. *J Exp Med* **194:** 1081-96.

Way K. J., Chou E., and King G. L. (2000). Identification of PKC-isoform-specific biological actions using pharmacological approaches. *Trends Pharmacol Sci* **21:** 181-7.

Weinrauch Y., and Zychlinsky A. (1999). The induction of apoptosis by bacterial pathogens. *Annu Rev Microbiol* **53:** 155-87.

Wilkinson J. C., Wilkinson A. S., Scott F. L., Csomos R. A., Salvesen G. S., and Duckett C. S. (2004). Neutralization of Smac/Diablo by inhibitors of apoptosis (IAPs). A caspase-independent mechanism for apoptotic inhibition. *J Biol Chem* **279:** 51082-90.

Wimmer K., Zhu X. X., Lamb B. J., Kuick R., Ambros P. F., Kovar H., Thoraval D., Motyka S., Alberts J. R., and Hanash S. M. (1999). Co-amplification of a novel gene, NAG, with the N-myc gene in neuroblastoma. *Oncogene* **18:** 233-8.

Wright E. K., Goodart S. A., Growney J. D., Hadinoto V., Endrizzi M. G., Long E. M., Sadigh K., Abney A. L., Bernstein-Hanley I., and Dietrich W. F. (2003). Naip5 affects host susceptibility to the intracellular pathogen Legionella pneumophila. *Curr Biol* **13:** 27-36.

Wu G., Chai J., Suber T. L., Wu J. W., Du C., Wang X., and Shi Y. (2000). Structural basis of IAP recognition by Smac/DIABLO. *Nature* **408:** 1008-12.

Wu H., and Arron J. R. (2003). TRAF6, a molecular bridge spanning adaptive immunity, innate immunity and osteoimmunology. *Bioessays* **25:** 1096-105.

Xu D. G., Crocker S. J., Doucet J. P., St-Jean M., Tamai K., Hakim A. M., Ikeda J. E., Liston P., Thompson C. S., Korneluk R. G., MacKenzie A., and Robertson G. S. (1997a). Elevation of neuronal expression of NAIP reduces ischemic damage in the rat hippocampus. *Nature Medicine* **3:** 997-1004.

Xu D. G., Korneluk R. G., Tamai K., Wigle N., Hakim A., Mackenzie A., and Robertson G. S. (1997b). Distribution of neuronal apoptosis inhibitory protein-like immunoreactivity in the rat central nervous system. *Journal of Comparative Neurology* **382:** 247-59.

Xu M., Okada T., Sakai H., Miyamoto N., Yanagisawa Y., MacKenzie A. E., Hadano S., and Ikeda J. E. (2002). Functional human NAIP promoter transcription regulatory elements for the NAIP and PsiNAIP genes(1). *Biochim Biophys Acta* **1574:** 35-50.

Yamaguchi K., Nagai S., Ninomiya-Tsuji J., Nishita M., Tamai K., Irie K., Ueno N., Nishida E., Shibuya H., and Matsumoto K. (1999). XIAP, a cellular member of

the inhibitor of apoptosis protein family, links the receptors to TAB1-TAK1 in the BMP signaling pathway. *Embo Journal* **18:** 179-87.

Yamamoto K., Sakai H., Hadano S., Gondo Y., and Ikeda J. E. (1999). Identification of two distinct transcripts for the neuronal apoptosis inhibitory protein gene. *Biochem Biophys Res Commun* **264:** 998-1006.

Yang J., Kawai Y., Hanson R. W., and Arinze I. J. (2001). Sodium butyrate induces transcription from the G alpha(i2) gene promoter through multiple Sp1 sites in the promoter and by activating the MEK-ERK signal transduction pathway. *J Biol Chem* **276:** 25742-52.

Yaraghi Z., Korneluk R. G., and MacKenzie A. (1998). Cloning and characterization of the multiple murine homologues of NAIP (neuronal apoptosis inhibitory protein). *Genomics* **51:** 107-13.

Yaseen N. R., and Blobel G. (1999). Two distinct classes of Ran-binding sites on the nucleoporin Nup-358. *Proc Natl Acad Sci U S A* **96:** 5516-21.

Ye R. D. (2001). Regulation of nuclear factor kappaB activation by G-protein-coupled receptors. *J Leukoc Biol* **70:** 839-48.

You M., Ku P. T., Hrdlickova R., and Bose H. R. J. (1997). ch-IAP1, a member of the inhibitor-of-apoptosis protein family, is a mediator of the antiapoptotic activity of the v-Rel oncoprotein. *Molecular and Cellular Biology* **17:** 7328-41.

Yuan J., Shaham S., Ledoux S., Ellis H. M., and Horvitz H. R. (1993). The C. elegans cell death gene ced-3 encodes a protein similar to mammalian interleukin-1 beta-converting enzyme. *Cell* **75:** 641-52.

Yuk J. S., and Ha K. S. (2005). Proteomic applications of surface plasmon resonance biosensors: analysis of protein arrays. *Exp Mol Med* **37:** 1-10.

APPENDIX I
Proteins containing FHEXWP

The protein that contained the greatest similarity to the consensus sequence was β1-galactosidase (GLB1) as it was found to have the amino acids FHEPWP located within its N-terminus. The *GLB1* gene gives rise to two alternatively spliced mRNAs: a major transcript of 2.5 kb, which encodes the classic lysosomal form of the enzyme of 677 amino acids, and a minor transcript of 2.0 kb that encodes a β-galactosidase-related protein of 546 amino acids with no enzymatic activity, a different subcellular localization (Morreau *et al.*, 1989) and was found to be identical to the elastin-binding protein (EBP) (Hinek, 1996). Interestingly, the FHEPWP sequence is contained within the 131 amino acids missing from the latter protein.

The largest candidate found to have the NBIR3 binding sequence was the microtubule-actin crosslinking factor 1 (MACF1), a member of the spectraplakin family of cytoskeletal crosslinking proteins that possesses actin and microtubule binding domains (Sun *et al.*, 2001). This 5430 amino acid protein has a FHEAW sequence located near the C-terminus at position 4598 within one of the spectrin-like regions, domains that can also be found in dystrophin and other spectrin family proteins. Within the N-terminus of the ATP-binding cassette, sub-family C, member 10 (ABCC10) or the multidrug resistance-associated protein 7 (MRP7), the FHEAW sequence was located one-quarter of the way along its 1464 primary amino acid length. The MRP subfamily of ABC proteins has both membrane spanning domains and nucleotide binding folds, which allow them to act as plasma membrane transporters that function to reduce intracellular drug concentrations (Hopper *et al.*, 2001). Interestingly, NAIP also contains an ATP

binding cassette and is part of the NACHT (Koonin & Aravind, 2000) and NOD (Inohara & Nunez, 2001) families implicated in apoptosis and immune response.

Not much is known about the protein produced by the neuroblastoma-amplified gene (NAG) but its transcript levels were raised in 63% of neuroblastoma cell lines and 70% of neuroblastoma tumors tested with N-myc gene amplification (Wimmer *et al.*, 1999). HEAWPE was found at position 1618 of its 2371 amino acids within this obscure protein. Conversely, N-acetylglucosamine-1-phosphodiester alpha-N-acetylglucosaminidase is known to catalyze the second step in the synthesis of the mannose 6-phosphate recognition signal on lysosomal enzymes (Kornfeld *et al.*, 1999). NAGPA was found to have HESWP located at the 61st position of its 515 amino acids, which would place the NBIR3 binding sequence inside the Golgi as this enzyme is believed to be a type I membrane-spanning protein with the NH_2 terminus in the lumen of the Golgi and the COOH terminus in the cytosol (Kornfeld *et al.*, 1999).

The neuropeptide Y (NPY), peptide YY (PYY), and pancreatic polypeptide (PP) are 36-amino acid peptides that act through receptors on neurons and peripheral cells. Although there are functional orthologues in rabbit and mouse, the human Y6 encoding protein apparently lost its receptor function and became inactivated by a frameshift mutation during early in primate evolution (Matsumoto *et al.*, 1996). The authors suggested that this gene might have a novel function in humans, despite its inactivation, as transcripts were abundantly detected in the heart and skeletal muscle. The Y6 encoding protein and the truncated pancreatic polypeptide receptor PP2 have a 100% identity after amino acid 173 with an ENWPS sequence that occurs at position 198 of the 290 amino acid proteins. Additionally, this sequence is conserved in the mouse and rabbit

orthologues at position 198 of their 371 amino acids. Another potential NAIP binding partner, TORC3 has ESWPR located at the 134th position of its 619 amino acids. Transducers of regulated CREB (TORC) proteins are potent inducers of cAMP-responsive genes and are able to function cooperatively with cAMP to regulate CREB activity. These proteins are able to enhance CRE-dependent transcription via a phosphorylation-independent interaction with the bZIP DNA binding/dimerization domain of CREB (Conkright *et al.*, 2003).

Macromolecular transport between the nucleus and cytoplasm proceeds through nuclear pore complexes (NPCs) and is normally receptor mediated. The importins fulfill a dual function as nuclear import receptors and cytoplasmic chaperones for exposed basic domains (Jakel *et al.*, 2002). Work mainly on importin β has demonstrated that these receptors bind RanGTP via the amino-terminal domain and cargo via the carboxy-terminal domain. To permit shuttling through the NPCs, transport receptors also contain one or multiple binding domains for components of the NPCs, called nucleoporins, which are primarily located in an amino-terminal/central region of importin β (Strom & Weis, 2001). One of the potential NBIR3 binding partners, Importin 9 has an EAWPQ sequence at position 142 of its 1041 amino acids, and thus by extrapolation, close to the RanGTP and nucleoporin binding regions. The nucleoporins form a large complex of proteins that span the nuclear membrane and have filamentous projections into both the nucleus and cytoplasm. Nup-358 is a 358 kD nucleoporin that contains both importin-binding domains and a zinc finger region that is also a RanGDP-binding site (Yaseen & Blobel, 1999). Similarity to these zinc fingers was discovered in one of the other NBIR3 potential binding partners, the TRAF binding domain (TRABID) protein. TRABID is a 708 amino

acid protein with ENWPS at 16th amino acid and in the middle of one of the zinc finger nucleoporin-like sequences. (Evans *et al.*, 2001).

APPENDIX II
Signaling pathways

Receptors for NaB and other short chained fatty acids (SCFAs) were recently identified in humans as G protein-coupled receptors GPR41 and GPR43 (Brown *et al.*, 2003; Le Poul *et al.*, 2003; Nilsson *et al.*, 2003) and as the leukemia inhibitory factor (LIF) or interleukin-6 (IL-6) up-regulator of the leukocyte-specific STAT-induced GPCR (LSSIG), which is the murine orthologue to the human GPR43 (Senga *et al.*, 2003). This class of receptors has tissue-specific expression patterns so it has yet to be determined whether NaB is functioning through the murine GPR41 and/or GPR43 receptors in the neuro-2a cell line or through another receptor that has yet to be identified.

With this class of receptors, transmission of an extracellular signal to the interior of the cell is mediated through the extracellular binding of a ligand to a seven transmembrane receptor coupled to the cytoplasmic face of the cell by a heterotrimeric G-protein (composed of an α, β and γ subunit) (reviewed in Marinissen & Gutkind, 2001). The conformational change of the receptor induced by the ligand leads to the exchange of GDP for GTP on the Gα subunit and dissociation of Gα-GTP from the G$\beta\gamma$ dimer. The dissociated subunits then mediate physiological actions by interacting with numerous effectors, including protein kinases, phospholipases, phosphodiesterases and ion channels. The G-protein signal is terminated by the hydrolysis of GTP on the Gα subunit, allowing Gα-GDP to sequester free G$\beta\gamma$ (Marinissen & Gutkind, 2001).

To determine which of the 17 identified Gα subunits were involved in SCFA signaling, researchers examined yeast strains containing hGPR43 and different yeast/mammalian Gα chimeras and found GPR43 may activate the G_i, G_q, and G_{12}

(Brown *et al.*, 2003). After confirmation of G_i activity in *Xenopus* oocytes researchers investigated the activation of G_q in a mammalian system through the transient transfection of hGPR43 in HEK293 cells, introduction of a calcium-sensitive fluorescent dye, and measuring intracellular calcium ion concentrations ($[Ca^{2+}]_i$) by FLIPR. Pertussis toxin (PTX), a specific inhibitor of $G_{i/o}$ family proteins, had no significant effect on either the magnitude or the half-effective concentration (EC_{50}) of the $[Ca^{2+}]_i$ response to acetate in HEK293 cells expressing GPR43, which indicated that hGPR43 may activate G_q in addition to G_i family proteins (Brown *et al.*, 2003). Dual coupling through the $G_{i/o}$ and G_q subunits for GPR43 was also confirmed by other investigators (Le Poul *et al.*, 2003).

In the G_q pathway, phosphatidylinositol 4,5-bisphosphate (PIP_2) is catalyzed by phosphoinositide-specific phospholipase C (PLC) activation to generate the two second messengers inositol-1,4,5-trisphosphate (IP_3) and diacylglycerol (DAG) (reviewed in Neves *et al.*, 2002). IP_3 triggers the release of calcium from intracellular stores, and DAG recruits phosphokinase C (PKC) to the membrane and activates it (Neves *et al.*, 2002). The family of PKC serine-threonine kinases includes three major categories. The first are conventional PKC isotypes PKCα, PKCβ, and PKCγ, which require an increase in intracellular calcium and are responsive to phorbol ester induction (reviewed in Newton, 1997). The second category is the group of novel PKCs, which include PKCδ, PKCε, PKCθ, PKCη, and PKCμ and is activated by phorbol esters but does not require an increase in intracellular calcium for the induction of their kinase domain. The last category includes the atypical isoforms, PKCζ and PKCλ, which are calcium insensitive and not activated by the phorbol esters (Newton, 1997).

The $G\alpha_i$ pathway was originally identified through the inhibition of adenyl cyclase (reviewed in Neves *et al.*, 2002). Once released from $G\alpha_i$-GTP, the $G\beta\gamma$ subunits can regulate PLC, K^+ channels, adenylyl cyclase, and phosphatidylinositol 3-kinase (PI3K). G_q can also activate PI3K and the phosphorylation of PIP_2 at the D3 position of the inositol ring to generate the phosphatidylinositol 3,4,5-trisphosphate (PIP_3) second messenger (reviewed in Mora *et al.*, 2004; Ye, 2001). Many of the diverse effects triggered through the activation of PI3K and generation of PIP_3 are mediated by the 3-phosphoinositide-dependent protein kinase-1 (PDK1) and the activation of a subgroup of the AGC family of protein kinases.

PDK1 and the three isoforms of protein kinase B (PKBα, PKBβ and PKBγ, also known as Akt1, Akt2 and Akt3) possess a Pleckstrin homology (PH) domain, through which they can interact with each other and bind PIP_3 or PIP_2. The binding of Akt to PIP_3 induces a conformational change that greatly enhances the rate at which the Thr308 in the T-loop can be phosphorylated by PDK1 (Scheid & Woodgett, 2003). In fact, PDK1 is the major T-loop kinase of other PI3K-regulated AGC kinases, such as, p70 ribosomal S6 kinase (S6K), serum- and glucocorticoid-induced protein kinase (SGK) and atypical isoforms of PKC (reviewed in Mora *et al.*, 2004).

Although Akt is activated by, and dependent upon, multisite phosphorylation, it remains unclear which kinase is responsible for the phosphorylation of the Ser473 residue located C-terminal to the catalytic domain in a region termed the hydrophobic motif. Once activated, however, Akt phosphorylates and modulates the function of a number of regulatory proteins, which can result in the inhibition of apoptosis, promotion of cell division or stimulation of glucose uptake and storage. In a recently published article,

p300 was shown to be phosphorylated by Akt following NaB treatment (Mayo *et al.*, 2003). This important adapter protein can then bind other scaffolding proteins, such as the CREB (cAMP response element binding protein)-binding protein (CBP) and p300/CBP associated factor (P/CAF), which can be activated through phosphorylation and lead to histone acetylation (Kawabata *et al.*, 2002). S6K controls a number of different steps of protein synthesis, required for cell growth and storage of amino acids. The roles played by PKC isoforms activated downstream of PI3K are less well defined (Mora *et al.*, 2004).

Through the use of inhibitors of PKC, investigators have demonstrated that G-protein-mediated nuclear factor of κB (NF-κB) activation can be attenuated by blocking various isoforms of this kinase (reviewed in Ye, 2001). NF-κB is a family of closely related dimeric transcription factors that bind to the κB sites (reviewed in Karin *et al.*, 2002; Pommier *et al.*, 2004). They are the cellular homolog of the retroviral oncogene v-REL, consisting of five proteins: p50/p105 (NF-κB1), p52/p100 (NF-κB2), c-Rel, RelB and RelA (p65), which function as homo- or heterodimers (the p65/RelA and p50 heterodimer being the most prevalent). In most resting cells, NF-κB is retained in the cytoplasm bound to the inhibitory proteins IkB's (IkBα, IkBβ, IkBε, p105 and p100). As IκB binding obscures the NF-κB nuclear localization signal (NLS) and thus blocks the entry of NF-κB into the nucleus, phosphorylation and degradation of the inhibitory IκB is required for the activation of this transcription factor. The phosphorylation of IκB is mediated by the IκB kinases (IKK), consisting of IKKα, IKKβ, and IKKγ/NEMO, which results in the ubiquitination and degradation of IκB by the proteasome. Once translocated to the nucleus, the NF-κB complexes bind to a set of related DNA target sites,

collectively called κB sites and stimulate the expression of genes suppressing apoptosis, promoting cell growth, stimulating immune responses and functioning in negative feedback (Karin *et al.*, 2002; Pommier *et al.*, 2004).

In the present study, the broad spectrum inhibitor H-7 was shown to down-regulate the basal levels of *Naip* in addition to the attenuation of NaB-induced up-regulation of *Naip.* This isoquinoline derivative, 1-(5-isoquinolinesulfonyl)-2-methylpiperazine (H-7) has been reported as an inhibitor of PKA, PKC and PKG with a K_i value within the low micromolar range (reviewed in Ono-Saito *et al.*, 1999). The inhibition of PKC by H-7 has been shown to be competitive with respect to ATP, but not to phospholipid or Ca^{2+}, which means that only certain isoforms of this kinase are involved.

APPENDIX III
Innate Immunity

Not only has the mechanism of *Legionella* resistance remained elusive, it has yet to be established which region of Naip5 may be involved in susceptibility determination. Analysis of the primary amino acid sequence of NAIP has identified a variety of potential protein kinase C, tyrosine kinase, casein kinase II and cAMP/cGMP-dependent protein kinase phosphorylation sites; myristoylation sites; glycosylation sites; lipid attachment sites and an ATP/GTP-binding site. Similarity with other proteins that act as nucleotide phosphatases (NTPases) has resulted in a new family called NACHT that is named after NAIP, MHC class II transcription activator (CIITA), yeast incompatibility locus protein (HET-E) and mammalian telomerase-associated protein (TP1) (Koonin & Aravind, 2000). The alignment of the NACHT proteins identified seven distinct motifs, including the ATP/GTPase-specific loop, the Mg^{2+}-binding site (Walker A and B motifs, respectively) and five more specific regions. The NACHT NTPases have a sister group of another family of ATPases, the AP-ATPases, which include Apaf-1, CED-4 from *C. elegans*, numerous plant proteins involved in stress and disease response and a group of predicted ATPases from *Actinomycetes* that are implicated in transcriptional regulation. The AP-ATPases have repeated protein-protein interaction modules located C-terminally of the NTPase domain so when comparing the presence of leucine rich regions in CARD4 and some of the plant pathogen-resistance proteins, these authors were the first to assign leucine rich repeats (LRR) to the C-terminus of NAIP (Aravind *et al.*, 1999; Koonin & Aravind, 2000). In subsequent analysis of this region, however, it appears that although there are a number of leucine residues, there do not appear to be any consensus

sequences for known LRRs (Andrey V. Kajava, personal communication and Kobe & Kajava, 2001).

The NACHT family was recently designated the CATERPILLER gene family (CARD, transcription enhancer, R (purine)-binding, pyrin, lots of LRRs) (reviewed in Tschopp *et al.*, 2003). The NOD subfamily was identified through structural homology with Apaf-1. The AP-ATPases are similar to the Nods, a growing family of proteins containing a nucleotide-binding oligomerization (NOD) that are involved in the regulation of apoptosis and immune responses (Inohara & Nunez, 2001). The NOD module is homologous to the ATP-binding cassette (ABC) found in a large number of proteins with diverse biological function. Many NOD-containing proteins are organized and function in a similar manner: the centrally located NOD domain mediates self-association, triggering induced proximity of proteins bound by the amino-terminal domain (reviewed in Inohara & Nunez, 2001; Tschopp *et al.*, 2003). Both NOD1 and NOD2 seem to mediate responsiveness to LPS as NF-κB activation induced by cytoplasmic LPS is blocked by a dominant-negative version of NOD1. The role of Naip in *Legionella* resistance has yet to be determined but it is intriguing to consider that, similar to the other NOD proteins, it might be involved in binding intracellular LPS.

Curriculum Vitae

Academic Qualifications.

2006 Ph.D. Faculty of Medicine, Department of Biochemistry, Children's Hospital of Eastern Ontario Research Institute (CHEO RI), University of Ottawa (UO), Ottawa, Ontario, Canada.

1998 M.Sc. Faculty of Medicine, Department of Biochemistry, University of Ottawa Heart Institute, Ottawa, Ontario, Canada.

1994 B.Sc. (Honours Certificate) Combined Chemistry and Biochemistry, Mount Saint Vincent University (MSVU) and Dalhousie University, Halifax, Nova Scotia (NS), Canada.

1992 B.Sc. (with Distinction) Chemistry, MSVU, Halifax, N.S.

1990-91 Canada World Youth. International development and cultural exchange programme. Volunteer community service work in British Columbia, Canada and Jamaica.

1988 High School Diploma (First Class Honours), Hants West High, Newport, NS.

Scholarships, Honours and Awards.

2000-01 Fonds de la recherche en santé du Québec (FRSQ). Graduate studentship for a Ph.D. student pursuing health related research.

2000 Teaching Assistant of the Year. Faculty of Science, Department of Biochemistry, UO.

1998-00 Canadian Genetic Diseases Network and the Children's Hospital of Eastern Ontario. Graduate studentship for the potential alleviation of childhood diseases with a genetic component.

1988-92 MSVU Diamond Jubilee Presidential Scholarship. Full academic scholarship in recognition of academic excellence.

1988-92 MSVU Dean's List. Recognition of academic excellence.

1990 Sister Mary Evelyn award. Recognition of excellence in Chemistry, MSVU.

1988-90 Canada Scholarship for Science and Engineering students. Recognition of academic excellence in the sciences.

1988 Hon. H. E. Kendall Chapter IODE award for academic excellence and extracurricular activities.

1988 Nova Scotia Teachers' Union Scholarship for academic excellence.

1987 Nova Scotia Lieutenant Governor's Medal for outstanding leadership skills and academic excellence.

Professional Societies.

1995-99 Canadian Federation of Biological Sciences (CFBS)
1991-94 Canadian Society for Chemistry (CSC)
1991-94 Chemical Institute of Canada (CIC)

University Committees.

2001 Honourary lifetime membership in the Canadian Union of Public Employees (CUPE), Local 2626 (for Teaching and Research Assistants), UO.

1999-00 External Vice-President of CUPE, Local 2626, UO.

1999-00 and 1994-97
Executive member, Biochemistry Graduate Students' Association, UO.

1999-00 and 1994-96
Student representative to the Biochemistry Graduate Studies Committee, UO.

1997-99 Chair of the Mobilization and Communication Committee of CUPE, Local 2626, UO.

1997-99 Biochemistry steward for CUPE, Local 2626, UO.

1997-99 One of the founding executive members, CUPE, Local 2626, UO.

1993-94 Principal organizer for the 19th Annual CSC/CIC Atlantic Student Chemistry Conference, MSVU.

1991-93	Member, Advisory Committee to the President for Environmental Issues, MSVU.
1991-93	President, Student Environmental Group, MSVU
1989-90	Science Representative, Students' Council, MSVU.
1989-92	Executive Member, Science Society, MSVU.
1988-89	Assistant Photopool Director, Students' Council, MSVU.

Teaching and Related Work Experience.

2000-01	Supervision of fourth year undergraduate B.Sc. student, CHEO RI, UO.
1999	Panelist for Teaching Assistantship Orientation Workshops, University of Ottawa Centre for University Teaching, UO.
1998-00	Supervision of undergraduate B.Sc. summer students, CHEO RI, UO.
1998-00	Teaching Assistant, Molecular Biology Lab Course, UO.
1995-97	Supervision of fourth year undergraduate B.Sc. students, Heart Institute, UO.
1995-97	Teaching Assistant, Physical Biochemistry Lab Course, UO.
1992-94	Teaching Assistant, Introduction to Biochemistry Lab Course, MSVU.
1992-94	Student Research Assistant in Biochemistry, Dalhousie University. Characterization of Lipoprotein(a) in the European hedgehog.
1993	Summer Student Research Assistant, Université de Limoges, Limoges, France. Identification of apo(a) isoforms in the European hedgehog.
1991-92	Student Research Assistant in Biology, MSVU and the National Research Council (Institute of Marine Bioscience), Halifax, NS. Production, purification and structure elucidation of a novel antibiotic.

Abstracts and Posters.

1 . C. R. Coffill, N. H. Gendron and A. E. MacKenzie. (2003). Keystone Symposium: Molecular Mechanisms of Apoptosis Meeting. Stable cell lines that selectively express full-length Neuronal Apoptosis Inhibitory Protein (NAIP) are not protected from cell death.

2. N. A. Arbour, C. R. Coffill, D. G. Barnes, and A. E. MacKenzie. (2001). Canadian Genetic Diseases Network Annual Scientific Meeting. Neuronal Apoptosis Inhibitory Protein (NAIP) Expression and its Effects on Cell Cycle Progression.

3. C. R. Coffill, N. H. Gendron, Q. Chen, J.-E. Ikeda and A. E. MacKenzie. (2000). International Human Genome Meeting and the Canadian Genetic Diseases Network Annual Scientific Meeting. Cytoprotective studies through the development of stable cell lines that selectively expressed Neuronal Apoptosis Inhibitory Protein (NAIP).

4. C. R. Coffill, Y. Lu, D. G. Barnes, G. Cherton-Horvat, C. G. Craig, J. Ikeda and A. E. MacKenzie. (1999). Canadian Genetic Diseases Network Annual Scientific Meeting. Pretreatment with adeno-NAIP and trophic factors increases the survival of SHSY-5Y cells exposed to doxorubicin.

5. J. Schultz, A. Gambarotta, N. Couture, C. Coffill and T. Neville. (1996). American Heart Association. Mild hyperlipidemia in chow-fed human and mouse hepatic lipase transgenic mice.

6. C. Coffill, J. Doull and S. Ayer. (1992) APICS Biology Conference. Purification of the Antibiotic Jenomycin from Cultures of *Streptomyces venezuelae.*

7. C. Coffill, J. Doull and S. Ayer. (1992) CIC Atlantic Student Chemistry Conference. Purification and Structural Determination of the Antibiotic, Jadomycin B from Cultures of *Streptomyces venezuelae.*

Conference Presentations.

1. C. Coffill, D. Hutt and D. Sparks. (1997). Canadian Lipoprotein Conference. The apolipoprotein composition of HDL affects the hydrolytic activity of hepatic lipase.

2. C. Coffill, T. Neville and D. Sparks. (1997). Canadian Lipoprotein Conference. The neutral lipid composition of HDL affects the conformation of apoA-I and the charge of LpA-I.

3. C. Coffill, T. Ramsamy and D. Sparks. (1996). Canadian Lipoprotein Conference. The neutral lipid composition of HDL affects the hydrolytic activity of hepatic lipase.

4. C. Coffill and D. Sparks. (1995). Canadian Lipoprotein Conference. Hepatic lipase and HDL remodelling.

5. C. Coffill, M. Laplaud and P. Dolphin. (1994). CIC Atlantic Student Chemistry Conference. Characterization of Lp(a) isolated from the European hedgehog.

Publications.

1. J. K. X. Maier, C. R. Coffill, L. Pelletier, D. J. Franks, A. E. MacKenzie and N. H. Gendron. (2005). The Distribution of Neuronal Apoptosis Inhibitory Protein in Human Tissues Suggests a Role in Cellular Differentiation. *In preparation.*

2. S. Braschi, C. R. Coffill, T. A. Neville, D. M. Hutt and D. L. Sparks. (2001) Effect of acylglyceride content on the structure and function of reconstituted high density lipoprotein particles. *J Lipid Res.* **42:** 79-87.

3. S. Braschi, N. Couture, A. Gambarotta, B. Gauthier, C. Coffill, D. Sparks, N. Maeda, and J. Schultz. (1998). Hepatic lipase affects both HDL and apoB-containing lipoprotein levels in the mouse. *Biochim. Biophys. Acta.* **1392:** 276-90.

4. C. R. Coffill, T. A. Ramsamy, D. M. Hutt, J. R. Schultz and D. L. Sparks. (1997). Diacylglycerol is the preferred substrate in high density lipoproteins for human hepatic lipase. *J. Lipid Res.* **38:** 2224-2231.